A comparative isotopic study of the biogeochemical cycle of carbon in modern redox-stratified lakes

Robin Havas[a,*], Christophe Thomazo[a,b], Miguel Iniesto[c], Didier Jézéquel[d], David Moreira[c], Rosaluz Tavera[e], Jeanne Caumartin[f], Elodie Muller[f], Purificación López-García[c], Karim Benzerara[f]

[a] Biogéosciences, CNRS, Université de Bourgogne Franche-Comté, 21000 Dijon, France

[b] Institut Universitaire de France, 75005 Paris, France

[c] Ecologie Systématique Evolution, CNRS, Université Paris-Saclay, AgroParisTech, 91190 Gif-sur-Yvette, France

[d] IPGP, CNRS, Université de Paris, 75005 Paris, and UMR CARRTEL, INRAE & USMB, France

[e] Departamento de Ecología y Recursos Naturales, Universidad Nacional Autónoma de México, México

[f] Sorbonne Université, Muséum National d'Histoire Naturelle, CNRS, Institut de Minéralogie, de Physique des Matériaux et de Cosmochimie (IMPMC), 75005 Paris, France.

[*] *Correspondence to*: Robin Havas (robin.havas@gmail.com)

Keywords: Carbon cycle; DIC; POC; isotopic fractionation; Precambrian analogs

Deleted: : the hidden role of DOC

Formatted: Strikethrough

Deleted: 21 000

Formatted: Left, Line spacing: single

Deleted: ; DOC

Abstract. The carbon cycle is central to the evolution of biogeochemical processes at the surface of the Earth. Understanding the interplay between the C cycle and physico-chemical and biological conditions in ancient times is challenging because of major differences between the modern and the ancient Earth. Notably, the atmosphere was less oxidizing and the oceans were redox-stratified. Here, we characterized and compared the C cycles in four redox-stratified alkaline lakes from Mexico based on the concentrations and isotopic compositions of dissolved inorganic and particulate organic C (DIC and POC). Measurements were performed in both the water columns and surficial bottom sediments with the assessment of their physico-chemical parameters (conductivity, temperature, O_2, Chl. a, turbidity,). The four lakes exhibit a range of DIC concentrations from 7 to 35 mM, following a gradient of alkalinity/salinity. The DIC and sedimentary carbonates isotopic compositions ($\delta^{13}C_{DIC}$, $\delta^{13}C_{Carb}$) also varied correlatively with alkalinity increasing from -4.1 to +2.0 ‰ and -1.5 to +4.7 ‰, respectively. The porewaters $\delta^{13}C_{DIC}$ reaches up to ~10 ‰ in the sediment of one of the lakes. The $\delta^{13}C_{POC}$ varies from -29.0 to -23.5 ‰ in both the water columns and sediments of the four lakes. The depth profiles of $\delta^{13}C_{POC}$, [POC] and C:N of organic matter shows very similar variations among three of the lakes located in the same area. From the inter-comparison of these datasets in four different systems, we identify the impact of external abiotic factors such as the hydrological regime and inorganic C sources which control the alkalinity, carbonate isotopic signatures, and stratification of some of the physico-chemical parameters. We identify the presence of oxygenic photosynthesis and aerobic respiration metabolisms in the four lakes as well as of methanogenesis in the one with extreme porewater $\delta^{13}C_{DIC}$. Anoxygenic photosynthesis and/or chemoautotrophy are also recognized in two of the lakes, but their POC and DIC signatures can be equivocal. Finally, we find that geochemical signatures of OC in the surficial sediments do not always record the same part of the stratified water column and can be altered by early diagenesis, whereas recently deposited carbonates are more consistently recording the lakes oxycline isotopic compositions. Overall, this work highlights how the integration of datasets from multiple environments facilitates our understanding of the processes affecting the C cycle in redox-stratified systems, while showing the versatility of these processes and how they are recorded in the sedimentary archives.

Deleted: In

Deleted: ocean, which has been

Deleted: through most of the Earth's history, the dissolved organic carbon (DOC) reservoir holds a critical role in these processes because of its large size and involvement in many biogeochemical reactions. However, it is rarely measured and examined in modern stratified analogs and yet commonly invoked in past C cycle studies.

Deleted: of

Deleted: crater

Deleted: . For this purpose, we analyzed

Deleted: DOC together with

Deleted: In parallel we measured physico-chemical parameters of

Deleted: .

Deleted: have high DOC

Deleted: (

Deleted: ~ 15 to 160 times the amount

Deleted: POC, averaging 2 ± 4 mM; 1SD, n=28) with an important variability between and within the lakes

Deleted: All lakes exhibit prominent DOC peaks (up to 21 mM), found in the oxic and/or anoxic zones. $\delta^{13}C_{DOC}$ signatures also span a broad range of values from -29.3 to -8.7 ‰ (with as much as 12.5 ‰ variation within a single lake), while

Deleted: and $\delta^{13}C_{DIC}$ varied

Deleted: and -4.1 to +2.0 ‰, respectively. The DOC peaks in

Deleted: associated isotopic variability seem mostly related to

Deleted: and/or anoxygenic primary productivity through the release of excess fixed C in three of the lakes (Atexcac, La Preciosa and La Alberca de los Espinos). By contrast, the variability of [DOC] and $\delta^{13}C_{DOC}$ in Lake Alchichica could

Deleted: mainly explained

Deleted: partial degradation and accumulation in anoxic waters.

Deleted: DOC records metabolic reactions that would not have been clearly detected if only DIC and POC reservoirs had been analyzed. For example, DOC analyses evidence an active DIC-uptake and use of a DIC-concentrating mechanism by part of the photosynthetic plankton. Despite the prominent role of DOC in the

Deleted: lakes, variations of [DOC]/$\delta^{13}C_{DOC}$

Deleted: associated reactions

Deleted: not reflected

Deleted: organic carbon record, hence calling for special care when considering sediments as reliable

Deleted: of metabolic activities in stratified water columns. Overall, this study brings to light the need of further investigating the role of DOC in the C cycles of modern stratified analogs.

Formatted: Font:Bold

1. INTRODUCTION

The carbon cycle and biogeochemical conditions prevailing at the surface of the Earth are intimately bound through biological (*e.g.* photosynthesis) and geological processes (*e.g.* volcanic degassing, silicate weathering). Accordingly, the analysis of carbon isotopes in the rock record has been used to reconstruct the evolution of the biosphere and oxygenation of the Earth's (*e.g.* Hayes et al., 1989; Karhu and Holland, 1996; Schidlowski, 2001; Bekker et al., 2008). However, because the oceans have been redox-stratified throughout most of the Earth's history (Lyons et al., 2014; Havig et al., 2015; Satkoski et al., 2015), processes affecting the C cycle were likely different from those occurring in most modern, well oxygenated environments. Indeed, while biological processes evolved through time, dominant chemical reactions occurring in a reducing *vs* oxidizing world were likely not the same. These changing conditions could impact the C cycle at diverse scales, starting from the diversity and relative abundance of microbial carbon and energy metabolism (*e.g.* Wang et al., 2016; Iñiguez et al., 2020; Hurley et al., 2021), to larger ecological interactions (*e.g.* Jiao et al., 2010; Close and Henderson, 2020; Klawonn et al., 2021) and global C dynamics (*e.g.* Ridgwell and Arndt, 2015; Ussiri and Lal, 2017). Nonetheless, some modern stratified analogs (anoxic at depth) of early oceans exist, and need to be characterized in order to better understand the C cycle in ancient redox-stratified systems and how it was recorded by the sedimentary archives (*e.g.* Lehmann et al., 2004; Posth et al., 2017; Fulton et al., 2018). To this end, a number of recent studies investigated the C cycle of modern stratified water columns (*e.g.* Crowe et al., 2011; Kuntz et al., 2015; Camacho et al., 2017; Posth et al., 2017; Schiff et al., 2017; Havig et al., 2018; Cadeau et al., 2020; Saini et al., 2021; Petrash et al., 2022), with the clear advantage that many of their bio-geo-physico-chemical parameters could be directly measured, together with the main C reservoirs. However, these investigations of the C cycle in Precambrian analogues usually focus on a single environment instead of integrating views from several systems (*e.g.* Camacho et al., 2017; Schiff et al., 2017).

Here, we propose to describe the C cycle of four modern redox-stratified alkaline crater lakes, located in the trans-Mexican volcanic belt (Ferrari et al., 2012). For this purpose, we measured the concentrations and isotopic compositions of dissolved inorganic carbon (DIC) and particulate organic carbon (POC) throughout the stratified water column of the lakes. In parallel, depth profiles of several physico-chemical parameters as well as trace and major elements concentrations were measured, allowing to pinpoint the main biogeochemical reactions occurring in the water columns and connect them with specific C isotopes signatures. Last, sedimentary organic carbon and carbonates as well as porewater DIC from surficial sediments (~ 10 cm) at the bottom of the lakes were characterized in order to further constrain the main geochemical reactions taking place in the lower water columns and infer on possible exchanges between the sediment and water column reservoirs.

The four lakes share similar geological and climatic contexts but have distinct solution chemistries (Zeyen et al., 2021) – as well as distinct planktonic communities (Iniesto et al., 2022). Overall, their inter-comparison via the same methodology allows to assess the effects of specific physico-chemical and biological parameters on the C cycle. Moreover, they all correspond to closed lakes in endorheic basins (Alcocer, 2021; Zeyen et al., 2021). This facilitates the identification of external environmental constraints (*e.g.* evaporation, C sources) and allows to discuss their influence on processes occurring within the water columns. Accordingly, we start by constraining the main DIC sources and external controls on the alkalinity of the lakes. Then, we describe the influence played by the inter-lake alkalinity gradient on the lakes stratification and inorganic C cycle, and how it is recorded in the

Deleted: ... [1]

Formatted: Outline numbered + Level: 1 + Numbering Style: 1, 2, 3, ... + Start at: 1 + Alignment: Left + Aligned at: 0.25" + Indent at: 0.5"

Deleted:

Deleted: combined

Deleted: and have evolved together throughout the Earth's history.

Deleted: from

Formatted: Font:Italic

Deleted: Because

Deleted: This impacts

Deleted: (e.g. Paneth and O'Leary, 1985; Hessen and Anderson, 2008; Wang et al., 2016; Iñiguez et al., 2020), to larger ecological interactions (e.g.

Formatted: Font:Italic

Formatted: Font:Italic

Formatted: Font:Italic

Deleted:

Moved down [1]: Here, we propose to describe the C cycle of four modern redox-stratified alkaline crater lakes, located in the trans-Mexican volcanic belt (Ferrari et al., 2012).

Deleted: They relate to similar geological contexts and climates but have distinct solution chemistries – aligning along an alkalinity/salinity gradient (Zeyen et al., 2021) – as well as distinct planktonic communities (Iniesto et al., in press). Moreover, they harbor various types of microbialites (Gérard et al., 2013; Saghaï et al., 2016; Iniesto et al., 2021a, 2021b; Zeyen et al., 2021). We measured the concentrations and isotopic compositions of C-containing phases throughout the stratified water column of the lakes, including DOC, dissolved inorganic carbon (DIC) and particulate organic carbon (POC). In parallel, depth profiles of several physico-chemical parameters as well as trace and major elements concentrations were measured allowing to pinpoint the main occurring biogeochemical reactions and connect them with specific C isotopes signatures. Last, surficial sediments (~ 10 cm) at the bottom of the lakes were also characterized in order to further constrain the main geochemical reactions taking place in the lower water columns and infer possible exchanges between the sediment and water column reservoirs.

Formatted: Font:Italic

Moved (insertion) [1]

Deleted: Here, the inter-comparison via the same methodology of four redox-stratified lakes of the same type (tropical alkaline volcanic crater-lakes) but with distinct solution chemistries and microbial diversities (Zeyen et al., 2021; Iniesto et al., in press), allows to assess the effects of specific physico-chemical and biological parameters on the C cycle. Thus, we present the main biogeochemical reactions occurring in the water columns (e.g. oxygenic/anoxygenic photosynthesis or methanogenesis) and how they are recorded (or not) in surficial sediments. Then, we shed a new light on the microbial cycling of DOC and how the analysis of its isotopes can provide deeper insights into microbial processes and overall C cycle dynamics in stratified water columns. Finally, we discuss the possible implications ... [2]

surficial sediments. Then, combining POC and DIC data, we present the sources of organic C to the lakes by describing the main autotrophic reactions occurring in the water columns (*e.g.* oxygenic and anoxygenic photosynthesis). Finally, we discuss the fate of POC, being recycled (*e.g.* via methanogenesis) or deposited in the sediments and focus on how these reactions are recorded (or not) in surficial sediments.

2. SETTING / CONTEXT

2.1. Geology

The four lakes studied here are volcanic maars formed after phreatic, magmatic and phreatomagmatic explosions, in relation with volcanic activity in the Trans-Mexican-Volcanic Belt (TMVB, Fig. 1). TMVB originates from the subduction of the Rivera and Cocos plates beneath the North America plate, resulting in a long and wide (~1000 and 90-230 km, respectively) Neogene volcanic arc spreading across central Mexico (Ferrari et al., 2012). The TMVB harbors a large variety of monogenetic scoria cones and phreatomagmatic vents (maars and tuff-cones) as well as stratovolcanoes, calderas and domes (Carrasco-Núñez et al., 2007; Ferrari et al., 2012; Siebe et al., 2014). Maar crater formation usually occurs when ascending magmas meet water-saturated substrates, leading to successive explosions and excavation of older units (Lorenz, 1986; Carrasco-Núñez et al., 2007; Siebe et al., 2012; Chako Tchamabé et al., 2020).

Three of the studied lakes (Alchichica, Atexcac and La Preciosa) are located in a restricted area (~ 50 km²) of the Serdan-Oriental Basin (SOB) in the easternmost part of the TMVB (Fig. 1). The SOB is a closed intra-montane basin at high altitude (~2300 m), surrounded by the Los Humeros caldera in the north and the Cofre de Perote-Citlatépel volcanic range in the east. The basement is mainly composed of folded and faulted Cretaceous limestones and shales, covered by andesitic to basaltic lava flows (Carrasco-Núñez et al., 2007; Armienta et al., 2008; Chako Tchamabé et al., 2020). The formations of Alchichica and Atexcac craters were dated back to ~ 6-13 ± 5-6 and 330 ± 80 ka, respectively (Table 1; Carrasco-Núñez et al., 2007; Chako Tchamabé et al., 2020). The age of lake La Preciosa is not known. The fourth lake, La Alberca de los Espinos, is located at the margin of the Zacapu tectonic lacustrine basin in the Michoacán-Guanajuato Volcanic Field (MGVF) in the western-central part of the TMVB (Fig. 1). It lies at about 1985 m, mainly on andesitic basement rocks and was dated at ~25 ± 2 ka (Siebe et al., 2012, 2014).

2.2. Climate and limnology

Due to their geographical proximity, lakes from the SOB experience a similar temperate to semi-arid climate (Armienta et al., 2008; Sigala et al., 2017). The present climate of the SOB is dominated by dry conditions as reflected by higher evaporation than precipitation fluxes in Lake Alchichica (~ 1686 *vs* 392 mm/year; Alcocer, 2021). In Alchichica, Atexcac and La Preciosa, this trend is reflected by a drop in their water level evidenced by the emersion of microbialite deposits in these lakes (Fig. S1; Zeyen et al., 2021). This evaporation-dominated climate strongly contributes to the achievement of relatively high lake salinities from 1.2 to 7.9 psu, ranging from sub- to hyposaline. In comparison, La Alberca's climate is temperate to semi-humid and it is a freshwater lake (0.6 psu, Rendon-Lopez, 2008; Sigala et al., 2017).

Formatted: Outline numbered + Level: 1 + Numbering Style: 1, 2, 3, … + Start at: 1 + Alignment: Left + Aligned at: 0.25" + Indent at: 0.5"

Formatted: Outline numbered + Level: 2 + Numbering Style: 1, 2, 3, … + Start at: 1 + Alignment: Left + Aligned at: 0" + Indent at: 0.25"

Deleted: downward within

Deleted: years

Deleted:

Moved down [2]: Figure 1. Geographical location and photographs of the studied crater lakes. (a) Geological map from Ferrari et al. (2012) representing the location of the four studied lakes in the trans-Mexican volcanic belt (TMVB). (b), (c) Close up © Google Earth views of lake Alberca de los Espinos and the Serdan-Oriental Basin (SOB), respectively. (d-g) Pictures of the four studied lakes (d from © Google Image ['enamoratedemexicowebsite'], e from © Google Earth street view, and g from © 'Agencia Es Imagen').

Formatted: Font:Times New Roman, 10.5 pt

Formatted: Left, None, Outline numbered + Level: 2 + Numbering Style: 1, 2, 3, … + Start at: 1 + Alignment: Left + Aligned at: 0" + Indent at: 0.25"

Deleted: from each other

Deleted: with

Deleted: fluxes higher

Deleted: for example

Deleted: (~

Deleted: an

Deleted:

The four lakes are warm monomictic, *i.e.*, they are stratified throughout most of the year (~ 9 months) and mix once a year when the thermal stratification breaks down in the cold winter (Armienta et al., 2008). They are all "closed lakes" located in an "endorheic" basin (Alcocer, 2021; Zeyen et al., 2021), *i.e.* they have no inflow, outflow nor a connection to other basins through surficial waters such as streams. Overall, water input is only supplied by precipitations and groundwater inflow as evidenced and quantified for Lake Alchichica (Alcocer, 2021 and references therein).

Finally, the four lakes are alkaline (pH ~ 9) but distribute over a gradient of chemical compositions (including alkalinity, salinity and Mg/Ca ratio), interpreted as reflecting varying concentration stages of an initial alkaline dilute water (Table 1; Zeyen et al., 2021). Variations in concentrations stages may be due to different climates (mostly between La Alberca and lakes from the SOB) and more generally, different hydrological regimes. Microbialite deposits are found in all four lakes (Gérard et al., 2013; Saghaï et al., 2016; Iniesto et al., 2021a, 2021b; Zeyen et al., 2021), with an increasing abundance from lower to higher alkaline conditions (Zeyen et al., 2021).

3. METHOD

3.1. Sample Collection

The sediment core from Lake La Preciosa was collected in May 2016. All other samples were collected in May 2019. The depth profiles of several physico-chemical parameters were measured in the water columns of the four lakes using an YSI Exo 2 multi-parameter probe: temperature, pH, ORP (oxidation reduction potential), conductivity, O_2, chlorophyll a, phycocyanin, and turbidity. Precisions for these measurements were 0.01 °C, 0.1 pH unit, 20 mV, 0.001 mS/cm, 0.1 mg/L, 0.01 µg/L, 0.01 µg/L and 2% FTU unit, respectively. The ORP signal was not calibrated before each profile and is thus used to discuss relative variations over a depth profile. Measurements of the aforementioned parameters allowed to pinpoint depths of interest for further chemical and isotopic analyses, notably around the redoxcline of the lakes. Water samples were collected with a Niskin bottle. Particulate matter was collected on pre-combusted (2 h at 490°C) and weighted glass fiber filters (Whatman GF/F, 0.7 µm) and analyzed for particulate organic carbon (POC), major and trace elements. Between 1.5 and 5 L of lake water were filtered before the GF/F filters got clogged. Then, processed solution was filtered again at 0.22 µm with Filtropur S filters (that were pre-rinsed with the lake water filtered at 0.7 µm) for analyses of dissolved inorganic carbon (DIC), major, minor and trace ions.

Sediment cores were collected using a 90 mm Uwitec corer close to the deepest point of each lake's water column (Table 1), where anoxic conditions prevail almost all year long. Cores measured between 20 and 85 cm in length. Slices of about 2-3 cm were cut under anoxic conditions, using a glove bag filled with N_2 (anoxia were monitored using a WTW3630 equipped with a FDO O_2 optode). Interstitial porewater was drained out of the core slices using Rhizons in the glove bag. Sediments were transported back to the laboratory within aluminized foils (Protpack, UK). Sediments were then fully dried in a laboratory anoxic N_2-filled glove box.

Formatted: Font:Italic
Deleted: (Alcocer, 2021; Zeyen et al., 2021)
Deleted: meaning that
Deleted: ,
Deleted:)
Deleted: , evolving due to different climates (mostly between Alberca and lakes from the SOB) and more generally, different hydrological regimes. Microbialite deposits are found in all four lakes with an increasing abundance from lower to higher alkaline conditions (Zeyen et al., 2021).
Moved down [3]: Table 1.
Formatted: Font:10.5 pt
Formatted: Outline numbered + Level: 1 + Numbering Style: 1, 2, 3, … + Start at: 1 + Alignment: Left + Aligned at: 0.25" + Indent at: 0.5"
Deleted: General information of the studied lakes. Abbreviations: TMVB: Trans-Mexican volcanic belt; MGVF: Michoaćan-Guanajuato volcanic field; masl:
Moved down [4]: meters above sea level. *NB*: Sampling in May 2019 except for La Preciosa's sediments, sampled in May 2016.
Formatted: Font:10.5 pt
Deleted: Lake … [3]
Moved down [5]: Alchichica … [4]
Formatted: English (US)
Formatted Table
Deleted: Lake … [5]
Moved down [6]: Alchichica … [6]
Formatted Table
Formatted: Font:6 pt, English (US)
Formatted: Font:6 pt
Formatted … [7]
Deleted: ,
Deleted: FNU
Deleted: semi-
Deleted: was
Deleted: report
Deleted: chemoclines
Deleted: For analyses of dissolved inorganic and organ … [8]
Deleted: ashed
Deleted: at
Deleted: bottom
Deleted: where the
Deleted: was at its deepest
Deleted:) and
Deleted: .
Deleted: pore water
Deleted: .

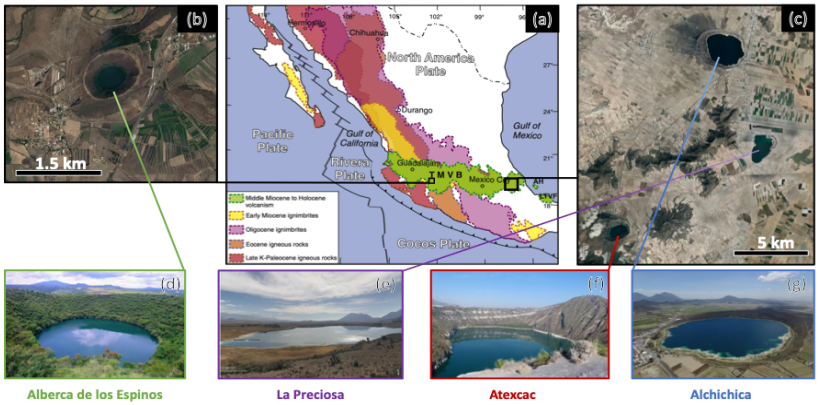

Figure 1. Geographical location and photographs of the studied crater lakes. (a) Geological map from Ferrari et al. (2012) representing the location of the four studied lakes in the trans-Mexican volcanic belt (TMVB). (b), (c) Close up © Google Earth views of lake Alberca de los Espinos and the Serdan-Oriental Basin (SOB), respectively. (d-g) Pictures of the four studied lakes (d from © Google Image ['enamoratedemexicowebsite'], e from © Google Earth street view, and g from © 'Agencia Es Imagen').

Lake	General location	Sampling location	Elevation (m.a.s.l.)
Alchichica	Serdan Oriental Basin, eastern TMVB	19°24'51.5" N; 097°24'09.9" W	2320
Atexcac	Serdan Oriental Basin, eastern TMVB	19°20'2.2'' N; 097°26'59.3'' W	2360
La Preciosa	Serdan Oriental Basin, eastern TMVB	19°22'18.1'' N; 097°23'14.4'' W	2330
La Alberca de los Espinos	Zacapu Basin, MGVF, central TMVB	19°54'23.9'' N; 101°46'07.8'' W	1985

Lake	Lake Basement	Age	Max Depth (m)	Alkalinity (mmol/L)	Salinity (psu)	pH
Alchichica	limestone, basalts	6-13 ± 5-6 ka	63	~35	7.9	9.22
Atexcac	limestone, andesites, basalts	330 ± 80 ka	39	~26	7.4	8.85
La Preciosa	limestone, basalts	Pleistocene	46	~13.5	1.15	9.01
La Alberca de los Espinos	andesite xenoliths	25 ± 2 ka	30	~7	0.6	9.14

Table 1. General information about the studied lakes. Abbreviations: TMVB: Trans-Mexican volcanic belt; MGVF: Michoaćan-Guanajuato volcanic field; m.a.s.l.: meters above sea level. *NB*: Sampling in May 2019 except for La Preciosa's sediments, sampled in May 2016.

Moved (insertion) [2]
Deleted:
Formatted: Font:Times New Roman, 10.5 pt
Moved (insertion) [5]
Formatted: Position:Horizontal: 1.13", Relative to: Page, Vertical: 0.04", Relative to: Paragraph, Horizontal: 0.13", Wrap Around
Formatted Table
Formatted: Position:Horizontal: 1.13", Relative to: Page, Vertical: 0.04", Relative to: Paragraph, Horizontal: 0.13", Wrap Around
Formatted: Position:Horizontal: 1.13", Relative to: Page, Vertical: 0.04", Relative to: Paragraph, Horizontal: 0.13", Wrap Around
Formatted: Position:Horizontal: 1.13", Relative to: Page, Vertical: 0.04", Relative to: Paragraph, Horizontal: 0.13", Wrap Around
Formatted: English (US)
Formatted: Font:6 pt, English (US)
Formatted: Space After: 12 pt, Line spacing: multiple 1.08 li
Moved (insertion) [6]
Formatted: Position:Horizontal: 1.13", Relative to: Page, Vertical: 0.26", Relative to: Paragraph, Horizontal: 0.13", Wrap Around
Formatted Table
Formatted: Position:Horizontal: 1.13", Relative to: Page, Vertical: 0.26", Relative to: Paragraph, Horizontal: 0.13", Wrap Around
Formatted: Position:Horizontal: 1.13", Relative to: Page, Vertical: 0.26", Relative to: Paragraph, Horizontal: 0.13", Wrap Around
Formatted: Position:Horizontal: 1.13", Relative to: Page, Vertical: 0.26", Relative to: Paragraph, Horizontal: 0.13", Wrap Around
Formatted: Font:6 pt
Moved (insertion) [3]
Formatted: Font:10.5 pt
Formatted: Justified
Moved (insertion) [4]
Formatted: Font:10.5 pt

3.2. Dissolved inorganic carbon (DIC) concentration and isotope measurements

Twelve milliliters of the 0.7-µm filtered lake water were filtered at 0.22-µm directly into hermetic Exetainer® tubes in order to avoid exchange between DIC and atmospheric CO_2. DIC concentrations and isotopic compositions were measured at the Institut de Physique du Globe de Paris (IPGP, France), using an Analytical Precision 2003 GC-IRMS, running under He-continuous flow, and following the protocol described by Assayag et al. (2006). In short, a given volume of the solution is taken out of the Exetainer® tube with a syringe, while the same volume of helium is introduced in order to maintain a stable pressure and atmospheric-CO_2-free conditions within the sample tubes. The collected sample is introduced in another Exetainer® tube that was pre-filled with a few drops of 100% phosphoric acid (H_3PO_4) and pre-flushed with He gas. Under acidic conditions, the DIC quantitatively converts to gaseous and aqueous CO_2, which equilibrates overnight within the He filled head space of the tube. Quantification and isotopic analyses of released gaseous CO_2 are then carried out by GC-IRMS using internal standards of known composition that were prepared and analyzed via the same protocol. Each measurement represents an average of four injections in the mass spectrometer. Chemical preparation and IRMS analysis were duplicated for all the samples. The $\delta^{13}C_{DIC}$ reproducibility calculated for the 65 samples was better than ±0.2 ‰, including internal and external reproducibility. Standard deviation for [DIC] was 0.6 ± 0.9 mmol/L on average.

Specific DIC speciation, *i.e.*, $CO_{2(aq)}$, HCO_3^- and CO_3^{2-} activities, was computed using Phreeqc with the full dissolved chemical composition of each sample as an input. It should be noted that these results are provided by calculations of theoretical chemical equilibria and do not necessarily take into account local kinetic effects, which, for example, could lead to local exhaustion of $CO_{2(aq)}$ where intense photosynthesis occurs.

3.3. Particulate organic carbon and nitrogen (POC / PON)

Particulate organic matter from the lake water columns was collected on GF/F filters, ground in a ball mill before and after decarbonation. Decarbonation was performed with 12N HCl vapors in a desiccator for 48 h. Aliquots of dry decarbonated samples (25 - 70 mg) were weighed in tin capsules. POC and PON contents and $\delta^{13}C_{POC}$ were determined at the Laboratoire Biogéosciences (Dijon, France) using a Vario MICRO cube elemental analyzer (Elementar, Hanau, Germany) coupled in continuous flow mode with an IsoPrime IRMS (Isoprime, Manchester, UK). USGS 40 and IAEA 600 certified materials were used for calibration and showed a reproducibility better than 0.15 ‰ for $\delta^{13}C$. External reproducibility based on triplicate analyses of samples (n=23) was 0.1 ‰ on average for $\delta^{13}C_{POC}$ (1SD). External reproducibilities of POC and PON concentrations were on average 0.001 and 0.005 mmol/L, respectively (*i.e.* 3 and 7 % of measured concentrations).

3.4. Geochemical characterizations of the sediments

Sedimentary organic carbon (SOC), sedimentary organic nitrogen (SON) and their isotopic compositions were measured on carbonate-free residues of the first 12 cm of the sediment cores, produced after overnight 1N HCl digestion. Plant debris (mainly found in La Alberca and Atexcac) were picked upon initial sediment grinding in an agate mortar and analyzed separately. Aliquots of dried decarbonated samples (~ 4-70 mg) were weighed in tin

Formatted: Outline numbered + Level: 2 + Numbering Style: 1, 2, 3, … + Start at: 1 + Alignment: Left + Aligned at: 0" + Indent at: 0.25"

Deleted: 22-µm-

Deleted: solutions

Deleted: placed in

Deleted: determined

Deleted: water sample

Deleted: mmoles

Formatted: Font:Italic

Deleted: Additionally, dating of the DIC was achieved by measuring its ^{14}C content and was performed by Beta Analytic laboratory, Miami, USA.

Deleted: . ... [9]

Formatted: Outline numbered + Level: 2 + Numbering Style: 1, 2, 3, … + Start at: 1 + Alignment: Left + Aligned at: 0" + Indent at: 0.25"

Deleted: lakes

Deleted: quartz

Deleted: Laboratory

Deleted: mmoles

Formatted: Font:Italic

Formatted: Outline numbered + Level: 2 + Numbering Style: 1, 2, 3, … + Start at: 1 + Alignment: Left + Aligned at: 0" + Indent at: 0.25"

Deleted: sediments

capsules. SOC and SON contents and $\delta^{13}C$ were determined at the Laboratoire Biogéosciences (Dijon) using a Vario MICRO cube elemental analyzer (Elementar GmbH, Hanau, Germany) coupled in continuous flow mode with an IsoPrime IRMS (Isoprime, Manchester, UK). USGS 40 and IAEA 600 certified materials were used for calibration and had a reproducibility better than 0.2 ‰ for $\delta^{13}C_{SOC}$. Sample analyses (n=67) were at least duplicated and showed an average external reproducibility of 0.1 ‰ for $\delta^{13}C$ (1SD). External reproducibilities for SOC and SON contents were 0.1 and 0.03 wt. %, respectively.

Carbon isotopic compositions of carbonates from the bottom sediments in La Alberca were analyzed at the Laboratoire Biogéosciences (Dijon) using a ThermoScientific™ Delta V Plus™ IRMS coupled with a Kiel VI carbonate preparation device. External reproducibility was assessed by multiple measurements of NBS19 standard and was better than ± 0.1 ‰ (2σ). Carbonate total concentration was determined by mass balance after decarbonatation for SOC analysis.

Mineralogical assemblages of sediments were determined on bulk powders by X-Ray diffraction (XRD) at the Laboratoire Biogéosciences (Dijon). Samples were ground in an agate mortar. Diffractograms were obtained with a Bruker D8 Endeavor diffractometer with CuKα radiation and LynxEye XE-T detector, under 40 kV and 25 mA intensity. Minerals identification were based on COD ("Crystallography Open Database") and BGMN databases. Estimation of their abundances were achieved using a Rietveld refinement analysis implemented in the Profex software.

Solid sulfide contents were determined on dry bulk sediments in Lake La Alberca after a wet chemical extraction using a boiling acidic Cr(II)-solution as detailed in Gröger et al. (2009).

3.5. Major and trace elements concentrations

Dissolved and particulate matter elemental compositions were measured at the Pôle Spectrométrie Océan (Plouzané, France) by inductively coupled plasma atomic-mass spectroscopy (ICP-AES, Horiba Jobin) for major elements and by high resolution-ICP-mass spectrometry using an Element XR (HR-ICP-MS, Thermo Fisher Scientific) for trace elements. Major element measurement reproducibility based on internal multi-elemental solution was better than 5%. Trace elements were analyzed by a standard-sample bracketing method and calibrated with a multi-elemental solution. Analytical precision for trace elements was generally better than 5%. Dissolved sulfate concentrations were analyzed by ion chromatography at the IPGP (Paris, France) with an uncertainty lower than 5%.

4. RESULTS

4.1. Lake Alchichica

The water column of Lake Alchichica showed a pronounced stratification compared to previous years at the same period (Fig. 2, Fig. S2; Lugo et al., 2000; Adame et al., 2008; Macek et al., 2020). The water temperature varied from about 20 °C at the surface to 15.5 °C at a 30 m depth and below. Dissolved O_2 was slightly oversaturated at the lake surface (112 % or 7.5 mg/L) and rapidly decreased to 0 mg/L between ~ 10 and 20 m depth, while the oxidation reduction potential (ORP) followed a similar trend but decreasing below 30 m. Conductivity hardly

Deleted: Laboratory

Deleted: Laboratory

Deleted: sulfides minerals concentrations

Formatted: Outline numbered + Level: 2 + Numbering Style: 1, 2, 3, … + Start at: 1 + Alignment: Left + Aligned at: 0" + Indent at: 0.25"

Deleted:

Deleted: sulfates/chloride and ammonium

Deleted: (NH_4^+)

Deleted: determined at the IPGP

Deleted: and by continuous flow colorimetric analysis, respectively,

Deleted:

Formatted: Font:+Theme Body (Calibri), 11 pt

Formatted: Outline numbered + Level: 1 + Numbering Style: 1, 2, 3, … + Start at: 1 + Alignment: Left + Aligned at: 0.25" + Indent at: 0.5"

Deleted:

Formatted: Outline numbered + Level: 2 + Numbering Style: 1, 2, 3, … + Start at: 1 + Alignment: Left + Aligned at: 0" + Indent at: 0.25"

Deleted: Conductivity slightly decreased from 13.8 to 13.7 mS/cm between the surface and 20 m in depth (salinity decreasing from 7.9 to 7.8 psu). Dissolved O_2 was saturated

Deleted: in

Deleted: . The

Deleted: signal was stable between 130 and 120 mV from the surface to

Deleted: and then

decreased from 13.8 to 13.7 mS/cm between ~8 and 20 m depth (salinity decreasing from 7.9 to 7.8 psu). Chlorophyll a averaged 2 µg/L, with a broad peak between ~ 7 and 29 m at around 4 µg/L (with a narrow maximum at 6 µg/L at 23 m) and then decreased to minimum values (0.5 µg/L) in the lower water column. pH remained constant at ~9.2 over the whole water column. Based on the temperature profiles, the epi-, meta- and hypolimnion layers of Lake Alchichica in May 2019 extended from 0-10, 10-20 and 20-63 m, respectively (Fig. 2).

Dissolved inorganic carbon (DIC) in the pelagic water column had concentrations comprised between 33 and 35 mM (Fig. 3; Table 2). The $\delta^{13}C_{DIC}$ decreased from 2 to ~ 1.5 ‰ between 5 and 60 m depth (Fig. 4; Table 2). Calculated pCO_2 was about three times higher than the atmospheric pCO_{2atm} (Table S1). Particulate organic carbon (POC) was much smaller with maximum and minimum concentrations of 0.1 mM at 30 m and ~0.02 mM in the bottom part of the water column, respectively. $\delta^{13}C_{POC}$ increased from -26.5 ‰ in the top 30 meters to -24.1 ‰ at 55 m depth. The C:N molar ratio of particulate organic matter (POM) showed a similar profile with values around 10.5 down to 30 m, progressively decreasing towards 5.9 at 55 m (Fig. 3; Table 2).

In the first 12 cm of the sediments, porewater DIC had a concentration (~ 35 mM) and a $\delta^{13}C_{DIC}$ (~ 0 ‰) similar to and slightly lower than the water column values, respectively. Solid carbonates were contained within several phases (aragonite, hydromagnesite, huntite and calcite) and had a bulk C isotopic composition around 4.6 ‰ (Table 3). Sedimentary organic matter had a $\delta^{13}C_{SOC}$ increasing from -25.7 to -24.5 ‰ and constant C:N molar ratio slightly higher than 10 (Figs. 3, 4; Table 3).

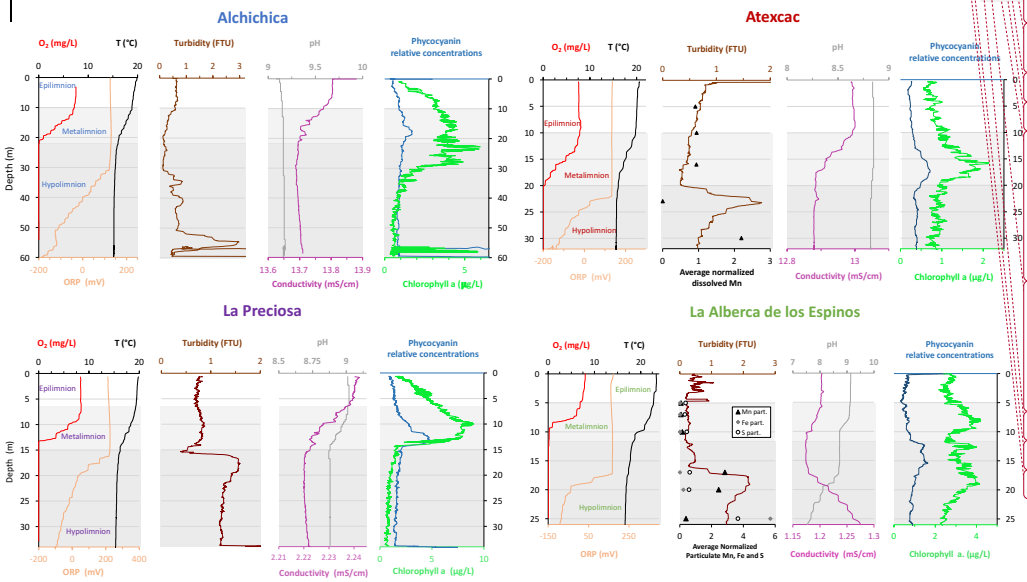

Figure 2. Physico-chemical parameters depth profiles of Alchichica, Atexcac, La Preciosa and Alberca de los Espinos in May 2019 including: dissolved oxygen concentration (mg/L), water temperature (°C), oxidation-reduction potential (ORP, mV), turbidity (Formazin Turbidity Unit), pH, conductivity (mS/cm), phycocyanin and chlorophyll a pigments (µg/L). Absolute values for phycocyanin concentrations were not determined; only relative variations are represented (with increasing concentrations to the right). Discrete concentration values of dissolved Mn in Atexcac and particulate Mn, Fe and S in La Alberca, normalized by their respective average were added. Epi-, meta- and hypo-limnion layers are represented for each lake according to temperature profiles.

Deleted: down to -270 mV at 60

Deleted: of

Deleted: .

Deleted: 6 µg/L

Deleted:

Deleted: Finally,

Deleted: these results

Deleted: 60

Formatted: None

Deleted: represented about 95% of all the carbon (DIC+DOC+POC)

Deleted: . Its concentration was almost constant

Deleted: 34.5

Deleted: mM throughout the whole water column except at 10 m where it significantly decreased to 33

Deleted: ,

Deleted: in

Deleted: 4). The analysis of DI^{14}C content at a depth of 35 m reached 39 % modern carbon (pMC), equivalent to an apparent age of ~ 7540 years before "present" (i.e. before 1950).

Deleted: represented about 0.13 % of the total carbon measured in the water column

Deleted: a concentration of 0.07 mM at a 5 m depth, increasing to a

Deleted: then decreasing to

Deleted: . The C:N

Deleted: 3). $\delta^{13}C_{POC}$ increased from -26.5 ‰ in the top 30 meters to -24.1 ‰ at 55 m in depth. Dissolved organic carbon (DOC) represented about 5% of total carbon, with concentrations around 0.5 mM throughout the water column except in the hypolimnion where it reached up to 5.4 mM. Its isotopic composition varied from -29.3 to -25.1 ‰, with maximum values found in the hypolimnion (Fig. 4). ... [10]

Deleted: S1). Dissolved Mn surprisingly showed the highest concentrations near the surface (~1.6 µM) before decreasing to ~0.4 µM between 20 and 55 m and increasing to 1 µM at 60 m. Similarly, dissolved Fe was higher at the lake surface (~0.3 µM) and progressively decreased near 0 at 50/55m (Fig. 5, Table S1).

Deleted: concentrations

Deleted: ratios

Deleted: S2

4.2. Lake Atexcac

Stratification of the Lake Atexcac water column was also very well defined (Fig. 2). Temperature was about 20.6 °C at the surface and rapidly decreased to 16 °C below 20 m. Conductivity had the same evolution with values around 13 mS/cm near the surface (salinity around 7.4 psu). Dissolved O_2 was also slightly oversaturated at the lake surface (115 % or 7.6 mg/L) and rapidly decreased to 0 mg/L between ~ 10 and 20 m, while ORP signal only decreased below 22 m depth. Chlorophyll a averaged 1 µg/L and showed a narrow peak centered at around 16 m, reaching ~2 µg/L. Turbidity showed a pronounced increase below 20 m, peaking at 23.3 m and returning to surface values at 26 m. Finally, pH remained around 8.85 throughout the water column. Based on the temperature profiles, the epi-, meta- and hypolimnion of Atexcac in May 2019 can be broadly defined as extending from 0-10, 10-20 and 20-39 m, respectively (Fig. 2).

The DIC concentration in the pelagic water column was around 26 mM except at 23 m where it decreased to 24.2 mM (Fig. 3, Table 2). Calculated pCO_2 was about five times higher than the atmospheric pCO_{2atm} (Table S1). The $\delta^{13}C_{DIC}$ was stable around 0.4 ‰ in the epi-/metalimnion but increased to 0.9 ‰ at 23 m and reached minimum values (0.2 ‰) at the bottom of the lake. POC had concentrations of 0.05 mM in the epi-/metalimnion, decreasing to 0.02 mM in the hypolimnion. The C:N molar ratio of POM showed the same depth profile decreasing from ~9.6 in the epi-/metalimnion to 6.6 in the hypolimnion (Fig. 3). $\delta^{13}C_{POC}$ showed minimum values in the epi-/metalimnion (-29.3 ‰ at 16 m) and increased to -26.5 ‰ in the hypolimnion.

Dissolved sulfate concentration was relatively stable at around 2.51 mM throughout the water column but increased to 2.64 mM at 23 m. Dissolved Mn concentration was constant at 1 µM down to 16 m before dropping to 0 at 23 m and increasing again to 2.35 µM at 30 m (Fig. 2; Table S2). This type of profile evolution was also found for other heavy elements such as Cu, Sr, Ba or Pb among others.

In the first 12 cm of the sediments, porewater DIC concentration varied between ~ 21 and 26 mM and $\delta^{13}C_{DIC}$ was around 0 ‰. Carbonates corresponded to aragonite and calcite and had a bulk C isotopic composition comprised between 2.1 and 2.6 ‰ (Table 3). Sedimentary organic matter had a $\delta^{13}C_{SOC}$ around -27 ‰ and a C:N molar ratio increasing from 8 to 10 (Figs. 3, 4; Table 3).

4.3. Lake La Preciosa

Lake La Preciosa was also stratified at the time of sample collection (Fig. 2). The temperature varied from about 20 °C to 16 °C. Conductivity had a similar evolution with values around 2.24 mS/cm near the surface (salinity around 1.15 psu). Dissolved O_2 was oversaturated at the lake surface (120 %, *i.e.*, 8.4 mg/L) and rapidly decreased to 0 between ~ 8 and 14 m, while the ORP decreased right below 16 m. Chlorophyll a concentration averaged 3 µg/L in Lake La Preciosa and recorded the highest peak compared to the other lakes (about 9 µg/L at 10 m) before decreasing to 0.7 µg/L below 15 m. Turbidity showed a large peak between 16 and 19 m. Finally, pH showed a small decrease from 9 to 8.8 between the surface and 15 m depth. Based on the temperature profiles, epi-, meta- and hypolimnion layers of La Preciosa in May 2019 can be broadly defined as extending from 0-6, 6-15 and 15-46 m, respectively (Fig. 2).

Deleted: .

Formatted: Outline numbered + Level: 2 + Numbering Style: 1, 2, 3, … + Start at: 1 + Alignment: Left + Aligned at: 0" + Indent at: 0.25"

Deleted: high (…bout 20.6 – 19.6 …°C) between 0…at the surface and 10 m in depth; it …apidly decreased and remained constant at …o 16 °C below 20 m. Conductivity had the same evolution with values around 13 mS/cm near the surface and decreasing to 12.9 mS/cm under 20 m (salinity decreasing from about …round 7.44 to 7.3… psu). Dissolved O_2 was saturated…lso slightly oversaturated at the lake surface (115 %, i.e.,… or 7.6 mg/L) and rapidly decreased to 0 mg/L between ~ 10 and 20 m. The… while ORP signal was almost constant (~ 134 mV) between the surface and 22 m in depth, before decreasing and reaching -175 mV at a 32 m depth.…nly decreased below 22 m depth. Chlorophyll a averaged 1 µg/L and showed a narrow peak centered at around 16 m, reaching ~2 µg/L, with similar values at the surface and bottom of the lake (0.8 µg/L).… Turbidity showed a pronounced increase below 20 m, peaking at 23.3 m and returning to surface values at 26 m. Finally, pH remained between 8.80 and…round 8.85 throughout the water column. Based on these results … [11]

Deleted: …he DIC represented about 84 % of all carbon present (DIC+DOC+POC) …oncentration in the pelagic water column. Its concentration remained …was around 26.5…mM from the surface down to 16 m in depth. Below 16 m, DIC decreased in the hypolimnion, and notably at 23 …xcept at 23 m where it reached a value of …ecreased to 24.2 …mM (Fig. 3, Table 2). Calculated pCO_2 was about five times higher than the atmospheric pCO_{2atm} (Table S1). The $\delta^{13}C_{DIC}$ was stable around 0.4 ‰ in the epi-/metalimnion. It markedly…but increased to 0.9 ‰ at 23 m and reached minimum values (0.2 ‰) at the bottom of the lake. POC represented about 0.13 % of the total carbon measured in the water column with …OC had concentrations of 0.05 mM in the epi- and …/metalimnion, decreasin … [12]

Deleted: TDP concentrations slightly decreased from ~0.25 µM to 0.19 µM at 16 m, then increased in the hypolimnion to ~ 0.45 µM (Fig. 5; Table S1). …issolved sulfate concentration was relatively stable at around 2.51 mM throughout the water column except at 23 m, where it…ut increased to 2.64 mM. Dissolved Cl concentration sli … [13]

Deleted: …n the first 12 cm of the sediments, porewater DIC concentration varied between ~ 21 and 26 mM and $\delta^{13}C_{DIC}$ was around 0 ‰. Carbonates corresponded to aragonite and calcite and had a bulk C isotopic composition comprised between 2.1 and 2.6 ‰ (Table 3). Sedimen … [14]

Formatted: Outline numbered + Level: 2 + Numbering Style: 1, 2, 3, … + Start at: 1 + Alignment: Left + Aligned at: 0" + Indent at: 0.25"

Deleted: at the surface …o 16 °C at 15 m… Conductivity had a similar evolution decreasing from…ith values around 2.24 to 2.22 …S/cm between…ear the surface and 15 m (salinity decreasing from…round 1.15 to 1.14 …su). Dissolved O_2 was saturated … [15]

Formatted: Font:Italic

Deleted: . The ORP signal was stable between 213 and 225 mV from… while the lake surface to 16 m and then …RP decreased down to -105 mV at a 35 m depth. right below 16 m. Chlorophyll a concentration averaged 3 µg/L in Lake La Preciosa water column …nd recorded the highest peak compared to the other lakes, increasing t … [16]

The DIC concentration was constant throughout the water column at 13.3 mM, with an exception at 12.5 m, where it decreased to 11.5 mM (Fig. 3, Table 2). Calculated pCO_2 at the surface represented about two times the atmospheric pCO_{2atm} (Table S1). The $\delta^{13}C_{DIC}$ decreased from about 0.5 ‰ to -0.36 ‰ between the surface and the hypolimnion. POC concentration decreased from ~0.06 mM in the epi-/metalimnion to 0.02 mM in the hypolimnion. Similarly, $(C:N)_{POM}$ decreased from ~11.2 in the epi-/metalimnion to 7.6 in the hypolimnion. $\delta^{13}C_{POC}$ increased downward from ~ -27 to ~25 ‰ to with a peak to -23.5 ‰ at 15 m.

In the first 10 cm of the sediments, $\delta^{13}C_{SOC}$ values increased downwards from ~ -25.5 to -23.2 ‰ and C:N molar ratio from 9.8 to 11 (Figs. 3, 4; Table 3). Carbonates corresponded to aragonite and calcite and had a bulk C isotopic composition averaging 2.6 ‰ (Table 3). Porewaters from the 2016 La Preciosa core were not retrieved.

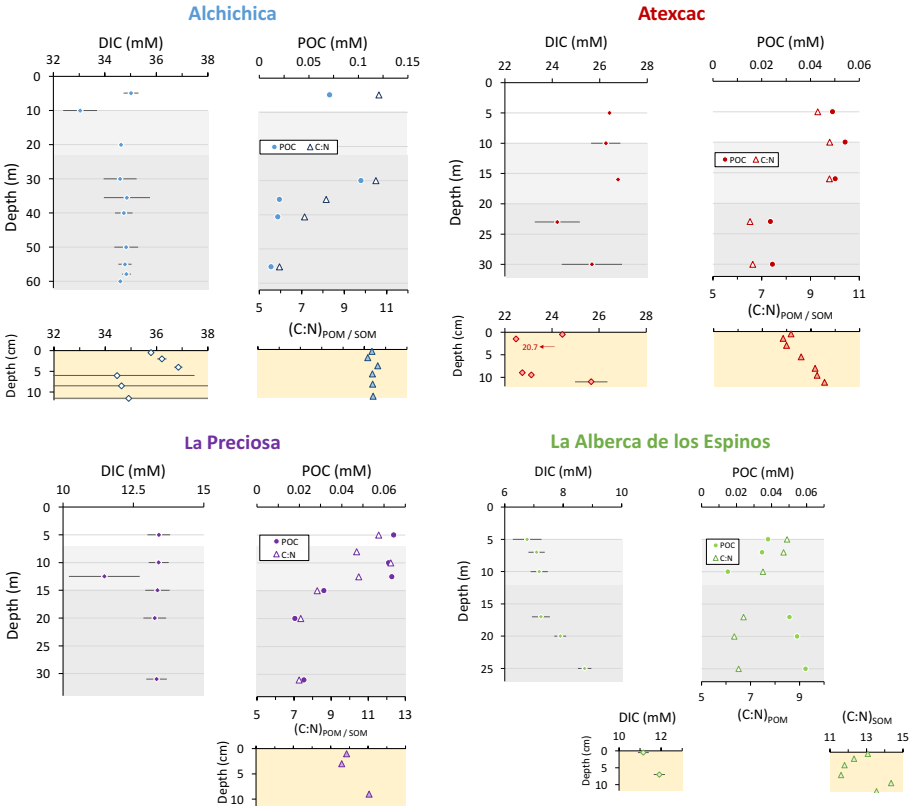

Figure 3. Concentrations in mmol/L (mM) of DIC, DOC, POC and sum of all three reservoirs, C:N molar ratios of POM as a function of depth in the water columns, as well as DIC concentrations in the surficial sediment porewaters and C:N molar ratios of sedimentary OM. Porewaters from La Preciosa's 2016 core were not retrieved.

4.4. Lake La Alberca de los Espinos

Stratification of the water column in La Alberca de los Espinos was also well defined (Fig. 2). Temperature was higher than in the other lakes (evolving from ~23 °C at the surface to 16.5 °C at depth). Dissolved O_2 was

Deleted: DIC represented about 97% of all carbon present (DIC+DOC+POC) in La Preciosa water column. Its

Deleted: DIC

Deleted: POC represented about 0.3% of the total carbon measured in the water column with a

Deleted: of

Deleted: - and

Deleted: , decreasing

Deleted: The

Deleted: ratio of

Formatted: Subscript

Deleted: showed a very similar depth profile with a value around

Deleted: decreasing

Deleted: decreased

Deleted: -26.4

Deleted: 27.4 ‰ between 5 and 10 m and peaked at

Deleted: before returning to value close to -25 ‰ downward. DOC represented about 3% of the total carbon, with a concentration around 0.5 mM throughout the water column except at 15 m where it peaked at 1.6 mM. $\delta^{13}C_{DOC}$ was mostly around -26 ‰ except between 10 and 12.5 m, where it reached up to -20 ‰. The total C concentration was relatively stable at ~13.8 mM, while $\delta^{13}C_{total}$ was centered around -1 ‰ with a decrease down to -2.8 ‰ at 12.5 m.

Deleted: TDP was stable at ~ 0.21 µM between 5 and 12.5 m and increased in the hypolimnion to 0.31 µM (Fig. 5, Table S1). Dissolved sulfate concentration slightly decreased from ~1.22 to 1.15 mM between the surface and 12.5 m and was stable at ~1.16 mM downward. The total S concentration remained stable throughout the water column at a value of ~1.19 mM. Dissolved Cl followed a similar profile with a value around 8.4 mM at the surface decreasing to ~7.8 mM below 12.5 m (Table S1). Dissolved Mn was around 1 µM at 5 m, decreased to 0.3 and 0.6 µM between 8 and 15 m and increased back to values above 1 µM below that. Dissolved Fe was above detection limit (~0.1 µM) at a 5 m depth (0.12 µM) only (Fig. 5; Table S1).

Deleted: ratios

Deleted: S2).

Deleted:

Formatted: Outline numbered + Level: 2 + Numbering Style: 1, 2, 3, … + Start at: 1 + Alignment: Left + Aligned at: 0" + Indent at: 0.25"

Deleted: around 23 °C between 0 and 5 m in depth; it rapidly decreased to 18.2 °C at 12 m and slowly decreased down to 16.5 °C at 26 m. Conductivity was at 1.20 mS/cm down to 6 m, and decreased to 1.17 mS/cm down to 16 m before increasing to 1.27 mS/cm at 26 m (salinity between 0.58 and 0.64 psu). Dissolved O_2 was saturated

oversaturated at the lake surface (118 %, *i.e.*, 7.9 mg/L) and rapidly decreased to 0 between ~ 5 and 12 m, while the ORP only decreased below 17 m depth. Conductivity decreased from 1.20 to 1.17 mS/cm at 16 m before increasing to 1.27 mS/cm at 26 m (salinity between 0.58 and 0.64 psu). La Alberca had relatively high chlorophyll a levels throughout the water column (3.1 µg/L on average) but showed at least three distinctive peaks, all reaching approximately 4 µg/L. They were found (i) between 6 and 9.5 m, (ii) at around 12.5 m and (iii) between 16 and 19 m. The turbidity profile showed a pronounced increase from 16 to 19 m. The pH showed relatively important variations from 9.15 at the lake surface to 8.75 between 6.5 and 10 m, further decreasing to 7.5 between 16 and 26 m. Based on the temperature profiles, epi-, meta- and hypolimnion layers of Lake La Alberca de los Espinos in May 2019 can be defined as extending from 0-5, 5-12 and 12-30 m, respectively (Fig. 2). Though we notice *via* the conductivity and pH profiles that different conditions prevail at the top and bottom of the hypolimnion.

The DIC concentration progressively increased from 6.8 mM at 5 m to 8.7 mM at 26 m. Calculated pCO_2 at the surface were near equilibrium with atmospheric pCO_{2atm} but strongly increased with depth, up to ~ 40 times pCO_{2atm} (Table S1). The $\delta^{13}C_{DIC}$ first decreased from about -2.5 ‰ to -4.1 ‰ at 10 m, and then increased back, up to -2 ‰ at 25 m. POC concentrations reached minimum values of 0.02 mM at 10 m but increased back to maximum

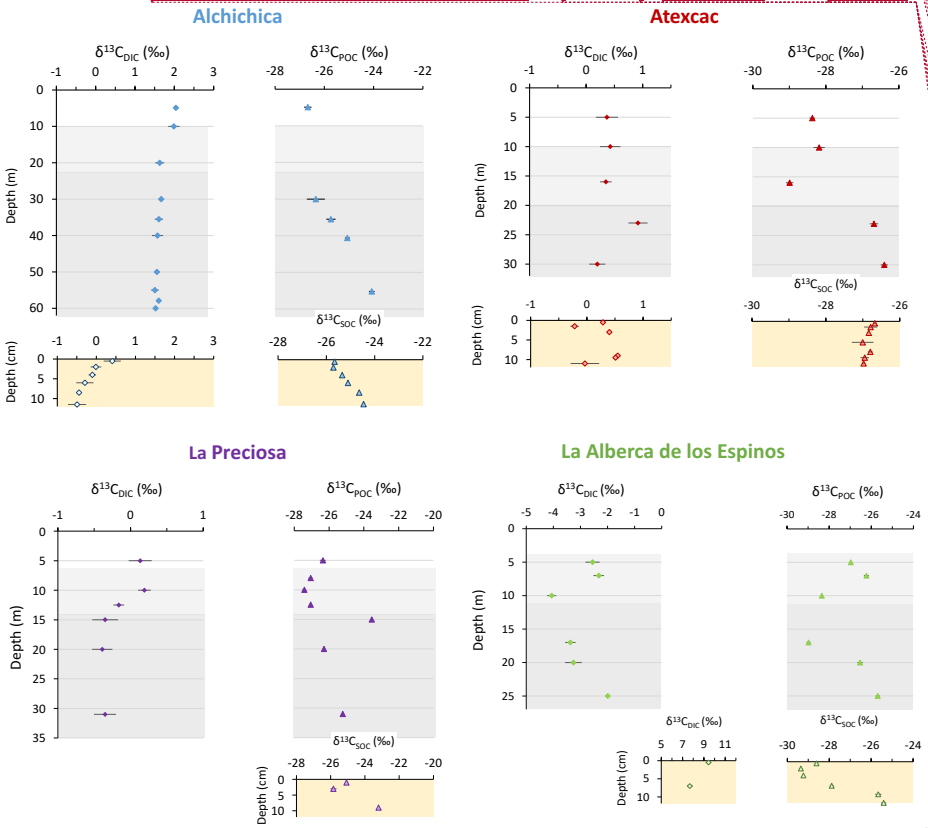

Figure 4. Isotopic compositions of DIC and POC reservoirs as a function of depth in the water columns as well as isotopic compositions of the porewater-DIC and solid organic carbon from the surficial sediments.

Deleted: . The ORP signal was mostly comprised between 160 and 170 mV between

Formatted: Font:Italic

Deleted: surface and

Deleted: before decreasing

Deleted: -65 mV

Deleted: 21 m and -92 mV

Deleted: .

Deleted:

Deleted:

Deleted: , and a slight decrease towards the sediment-water interface

Deleted:

Deleted: these results

Deleted: 2).

Deleted: DIC represented about 91 % of all carbon present (DIC+DOC+POC) in the water column. Its

Deleted: .2

Deleted: between 10 and 17

Deleted: It further

Deleted: 8.7 mM down to 26 m (Fig. 3,

Deleted: 2

Deleted: was

Deleted: 4 ‰ between the surface and 7 m in depth, decreased

Deleted: POC represented about 0.5 % of the total carbon measured in the water column with a concentration of 0.04 mM at the surface decreasing to

Deleted:

Deleted:

Deleted: and increasing

Deleted: 0.05 mM

values in the hypolimnion (~0.05 mM). The C:N molar ratio of POM progressively decreased from 8.5 at the surface to below 6.5 in the hypolimnion. The $\delta^{13}C_{POC}$ had minimum values at 10 and 17 m (-28.3 and -29 ‰, respectively). Above and below, $\delta^{13}C_{POC}$ was around -26.4 ‰.

Dissolved sulfates as measured by chromatography were only detectable at 5 m with a low concentration of 12 µM, while total dissolved S measured by ICP-AES showed values in the hypolimnion higher than in the upper layers (~ 10.3 *vs.* 7.4 µM, Table S2). Dissolved Mn concentrations decreased from 1.5 to 0.5 µM between 5 and 10 m, then increased to 2 µM at 25 m. Aqueous Fe was only detectable at 25 m with a concentration of 0.23 µM (Table S2). In parallel, particulate S concentrations increased with depth, with a marked increase from 0.1 to 0.6 µM between 20 and 25m. This was spatially correlated with a 25-fold increase in particulate Fe (from 0.2 to 5.97 µM). Particulate Mn showed a peak between 17 and 20 m around 1 µM, contrasting with values lower than 0.15 µM in the rest of the water column (Fig. 2, Table S3).

In the first centimeters of the sediments, porewater DIC concentration and $\delta^{13}C_{DIC}$ varied between ~ 11 and 12 mM and between +8 and +10 ‰, respectively (Figs. 3, 4). Surficial sedimentary carbonates corresponded to calcite and had a $\delta^{13}C$ around -1.5 ‰. Sedimentary organic matter had a $\delta^{13}C_{SOC}$ globally increasing from -29.4 to -25.5 ‰ and a C:N molar ratio varying between 11.6 and 14.3 (Figs. 3, 4; Table 3).

Lake	Sample	DIC	POC	$(C:N)_{POM}$	$\delta^{13}C_{DIC}$	$\delta^{13}C_{POC}$
		mmol/L		(molar)	‰	
Alchichica	AL 5m	35.0	0.07	10.6	2.0	-26.7
	AL 10m	33.0			2.0	
	AL 20m	34.6			1.6	
	AL 30m	34.6	0.10	10.5	1.7	-26.3
	AL 35m	34.9	0.02	8.1	1.6	-25.7
	AL 40m	34.7	0.02	7.1	1.6	-25.1
	AL 50m	34.8			1.6	
	AL 55m	34.8	0.01	5.9	1.5	-24.1
	AL 58m	34.8			1.6	
	AL 60m	34.6			1.5	
Atexcac	ATX 5m	26.4	0.05	9.3	0.4	-28.4
	ATX 10m	26.2	0.05	9.8	0.4	-28.2
	ATX 16m	26.8	0.05	9.8	0.3	-29.0
	ATX 23m	24.2	0.02	6.5	0.9	-26.7
	ATX 30m	25.7	0.02	6.6	0.2	-26.4
La Preciosa	LP 5m	13.4	0.06	11.6	0.1	-26.4
	LP 8m		0.07	10.4		-27.1
	LP 10m	13.4	0.06	12.2	0.2	-27.4
	LP 12.5m	11.5	0.06	10.5	-0.2	-27.1
	LP 15m	13.4	0.03	8.2	-0.3	-23.5
	LP 20m	13.3	0.02	7.4	-0.4	-26.3
	LP 31m	13.3	0.02	7.3	-0.4	-25.2
La Alberca de Los Espinos	Albesp 5m	6.8	0.04	8.5	-2.6	-27.0
	Albesp 7m	7.1	0.03	8.3	-2.3	-26.2
	Albesp 10m	7.2	0.02	7.5	-4.1	-28.3
	Albesp 17m	7.2	0.05	6.7	-3.4	-29.0
	Albesp 20m	7.9	0.05	6.3	-3.3	-26.5
	Albesp 25m	8.7	0.06	6.5	-2.0	-25.7

Table 2. Concentrations and isotopic compositions of dissolved inorganic carbon (DIC) and particulate organic carbon (POC) and C:N molar ratios of particulate organic matter (POM).

Deleted: .

Deleted: DOC represented about 8 % of the total carbon, with a concentration around 0.4 mM throughout the water column except at 7 and 17 m where DOC peaked to 1 and 1.7 mM, respectively (Fig. 3). Its isotopic composition was mostly comprised between -27 and -25 ‰ except at 7 m where it reached -15 ‰ (Fig. 4). Total C concentration increased downward from about 7 to 9 mM (Fig. 3). $\delta^{13}C_{total}$ decreased from -3.9 to -7.9 ‰ between 5 and 17 m and then increased up to -3.2 ‰ at 25 m (Fig. 4).

Formatted: Font:+Theme Body (Calibri), 11 pt

Deleted: Total dissolved phosphorus increased from 2.9 to 27.4 µM between 5 and 25 m (Fig. 5, Table S1).

Deleted:

Formatted: Font:Italic

Deleted: S1). Dissolved Cl slightly decreased from 4.25 to 4 mM between 5 and 10 m, before increasing back to 4.2 mM at 25 m.

Deleted: Fig. 5,

Deleted: S1

Deleted:

Deleted:

Deleted: 06

Deleted: above 10 m and lower than 0.15 below 20 m

Deleted:

Deleted: .

Deleted: S2). Surficial sedimentary carbonates had a $\delta^{13}C_{CaCO3}$ around -1.5 ‰.

Formatted: Font:Bold, Underline

Deleted: Figure 5. Concentrations of dissolved nutrients in micromoles.L^{-1} in the water columns of the four lakes as a function of depth. TDP and TDS stands for 'total dissolved P' and S', respectively, and were measured by ICP-AES. Fe and Mn were measured by ICP-MS. Nitrogen species were measured by colorimetry. ... [17]

5. DISCUSSION

5.1. Inorganic Carbon: origins and implications of the alkalinity/DIC gradient

5.1.1. Sources of DIC and origin of the alkalinity inter-lake gradient

Salinity and DIC gradually increase from Lake La Alberca de los Espinos (~0.6 psu and 7 mM) to Alchichica (~7.9 psu and 35 mM), while lakes La Preciosa and Atexcac have intermediate values of 1.15 and 7.44 psu and 13 and 26 mM, respectively (Table 1 and 2). This matches a gradient of alkalinity (with values of ~ 8, 15, 32 and 47 meq/L, Fig. S3a) previously described for these lakes (Zeyen et al., 2021), consistently with the fact that alkalinity is mostly composed of HCO_3^- and CO_3^{2-} ions in most natural waters. This alkalinity gradient may result from different concentration stages of an initial dilute alkaline water (Zeyen et al., 2021), those different concentration stages being ultimately controlled by the different hydrological regimes of the lakes. First, the weathering of Cretaceous limestone in the SOB (with a $\delta^{13}C$ of approximately 0 ± 1 ‰; Gonzales-Partida et al., 1993; Armstrong-Altrin et al., 2011) together with basaltic/andesitic bedrock (Armienta et al., 2008; Carrasco-Núñez et al., 2007; Lelli et al., 2021) favors the inflow of more alkaline and DIC-concentrated groundwaters than in Lake La Alberca which lies on a essentially basaltic basement (Rendon-Lopez, 2008; Siebe et al., 2014; Zeyen et al., 2021). Second, the SOB area presently experiences higher evaporation than precipitation rates (Alcocer, 2021), probably playing an important role in concentrating solutes and decreasing the water level in lakes Atexcac, Alchichica and La Preciosa (Anderson and Stedmon, 2007; Zeyen et al., 2021). Consistently, substantial "sub-fossil" microbialite deposits emerge above the current water level in lakes Alchichica and Atexcac, evidencing some significant lake level decrease (by up to 15 m in Lake Atexcac, *i.e.* ~40% of today's lake maximum depth; and by about 4 m in Alchichica). Scattered but well emerged patches of microbialites are also found in Lake La Preciosa (suggesting a water level decrease by up to ~5-6 m). By contrast, emerged microbialites are barely observed in Lake La Alberca de los Espinos (Fig. S1).

Additional local parameters, such as varying groundwater paths and fluxes (Furian et al., 2013; Mercedes-Martín et al., 2019; Milesi et al., 2020; Zeyen et al., 2021), most likely play a role in explaining part of the variations in DIC concentration between lakes. For example, Lake La Preciosa's water composition significantly differs from that of lakes Alchichica and Atexcac, despite a similar geological context and climate (all located within 50 km^2, Fig. 1). This could be explained by the fact that groundwaters in the SOB area become more saline as they flow towards the center of the basin and through the crater lakes (Silva Aguilera, 2019; Alcocer, 2021). Since groundwaters flow through La Preciosa first, they are more concentrated as they enter Alchichica than when they enter La Preciosa (Silva Aguilera, 2019; Alcocer, 2021; Lelli et al., 2021). Moreover, distinct regimes of volcanic CO_2 degassing into these crater lakes may also contribute to variations of the C mass balance and $\delta^{13}C_{DIC}$ values between the four lakes. Near the lakes from the SOB area, geothermal fluids derived from meteoric waters interacting with deep volcanic fluids as well as the calcareous basement rocks were evidenced (Peiffer et al., 2018; Lelli et al., 2021). In the water column of Lake La Alberca, the $\delta^{13}C_{total}$ averages -4.8 ‰ (Havas et al., submitted). This is very similar to signatures of mantle-CO_2 (Javoy et al., 1986; Mason et al., 2017) which could buffer the overall C isotopic composition of this lake. A contribution from mantle CO_2 degassing in La Alberca may partially explain the striking increases of P_{CO2} and [DIC] and decrease of pH observed at depth (Table S1; Figs. 2 and 3).

Formatted: Outline numbered + Level: 1 + Numbering Style: 1, 2, 3, … + Start at: 1 + Alignment: Left + Aligned at: 0.25" + Indent at: 0.5"

Deleted: General factors influencing

Deleted: C cycle across the Mexican crater lakes … [18]

Deleted:

Formatted: None, Outline numbered + Level: 2 + Numbering Style: 1, 2, 3, … + Start at: 1 + Alignment: Left + Aligned at: 0" + Indent at: 0.25"

Deleted: alkalinity (roughly equal to DIC)

Deleted: , Zeyen et al., 2021). The DIC gradient along which these four lakes distribute can be linked with

Deleted: around 2 ± 1 ‰; Armstrong-Altrin et al., 2011; Núñez Useche et al., 2014)

Deleted: purely

Deleted: 3

Deleted: Patches of

Deleted: .

Deleted: almost not

Formatted: Space After: 8 pt

Deleted: Lake

Deleted: Distinct

Moreover, this lake is located on top of a likely active normal fault (Siebe et al., 2012), which is favorable to the ascent of volcanic gases.

Last, different remineralization rates of organic carbon could also be a source of heterogeneity between the DIC contents of the lakes. However, assuming that all organic carbon (OC) from the lakes ultimately remineralized into DIC, it would only represent a relatively small portion of the total carbon (16 % in Lake Atexcac, 9 % in Lake La Alberca de los Espinos and ~5 % for lakes Alchichica and La Preciosa; Havas et al., submitted). From an isotopic mass balance perspective, the $\delta^{13}C_{DIC}$ of the three SOB lakes lie very far from OC isotopic signatures, whereas Lake La Alberca exhibits more negative $\delta^{13}C_{DIC}$ (and $\delta^{13}C_{Carb}$), slightly closer to OC signatures (Fig. 4). This latter lake also stands out from the others because of the dense vegetation surrounding it (Fig. S1). Therefore, La Alberca seems to be the only lake where OC respiration could be a significant source of inorganic C to the water column (potentially influencing the P_{CO2}, [DIC] and pH profiles described above).

Lake	Sample name	Depth	$(C:N)_{SOM}$	SOC	$\delta^{13}C_{SOC}$	DIC	$\delta^{13}C_{DIC}$	Carb.	$\delta^{13}C_{Carb}$
		cm	(molar)	wt. %	‰	mmol/L	‰	wt. %	‰
Alchichica	AL19_C2a_01	0-1	10.4	5.1	-25.7	35.8	0.4	41	4.6
	AL19_C2a_02	1-3	10.2	4.7	-25.7	36.2	0.0	44	4.5
	AL19_C2a_03	3-5	10.6	4.3	-25.3	36.8	-0.1	ND.	4.5
	AL19_C2a_04	5-7	10.4	3.8	-25.1	34.5	-0.3	40	4.7
	AL19_C2a_05	7-10	10.4	3.8	-24.6	34.6	-0.4	35	4.5
	AL19_C2a_06	10-13	10.4	3.7	-24.5	34.9	-0.5	38	4.8
Atexcac	ATX19_C1_1	0-1	8.2	0.9	-26.7	24.4	0.3	61	2.5
	ATX19_C1_2	1-2	7.9	1.3	-26.8	22.5	-0.2	46	2.7
	ATX19_C1_3	2-4	8.0	1.1	-26.8	20.7	0.4	61	2.7
	ATX19_C1_S4	4-7	8.6	0.9	-27.0	ND.	ND.	71	2.5
	ATX19_C1_4	7-9	8.7	0.9	-26.8	22.7	0.5	ND.	2.1
	ATX19_C1_5	9-10	9.3	1.0	-26.9	23.1	0.5	64	2.1
	ATX19_C1_S6	10-12	9.6	0.8	-27.0	25.7	0.0	69	2.1
La Preciosa	LP16_C3_7	0-2	9.8	2.3	-25.1	ND.	ND.	61	2.6
	LP16_C3_8	2-4	9.6	2.3	-25.8	ND.	ND.	63	2.6
	LP16_C3_9	8-10	11.0	2.6	-23.2	ND.	ND.	54	2.5
La Alberca de Los Espinos	ALBESP19_C3_1	0-1	13.1	13.3	-28.6	11.2	9.4	20	-1.5
	ALBESP19_C3_2	1-3	12.3	19.0	-29.4	ND.	ND.	18	ND.
	ALBESP19_C3_3	3-5	11.8	16.2	-29.2	ND.	ND.	17	ND.
	ALBESP19_C3_4	5-9	11.6	11.9	-27.9	11.9	7.7	15	-1.5
	ALBESP19_C3_S	9-10	14.3	7.5	-25.7	ND.	ND.	12	ND.
	ALBESP19_C3_5	10-14	13.5	5.4	-25.4	ND.	ND.	12	ND.

Table 3. Analyses of surficial solid sediments and porewaters: sedimentary organic matter C:N ratio; concentrations and isotopic compositions of sedimentary organic carbon (SOC); concentrations and isotopic compositions of DIC in the porewaters and solid bulk carbonates.

Moved (insertion) [7]

Deleted: between the four lakes

Deleted: DIC content

Deleted: POC and DOC

Deleted: remineralize

Deleted:).

Deleted: $\delta^{13}C_{POC}/\delta^{13}C_{DOC}$

Deleted: (Fig. 4),

Deleted: ,

Deleted: which surrounds

Deleted: . ... [19]

Moved down [8]: , notably because it increases lake pCO_2 and primary productivity which bolsters CO_2 degassing and organic C burial, both having low $\delta^{13}C$ compared to DIC (*e.g.* Li and Ku, 1997; Talbot, 1990).

Formatted: Font:Italic

Deleted: By controlling the DIC speciation ($H_2CO_3/CO_{2(aq)}$, HCO_3^-, CO_3^{2-}),

Moved down [9]: Consistently, the $\delta^{13}C_{DIC}$ of Mexican lakes are in the expected range for lakes with a pH around 9 (Bade et al., 2004), where DIC is dominated by HCO_3^-. However, the pH values of the studied Mexican lakes are too close to each other to explain the significant difference observed between their $\delta^{13}C_{DIC}$ (Fig. 4; p=4.2x10^{-3} for Lakes Atexcac and La Preciosa which have the closest $\delta^{13}C_{DIC}$).

Deleted: also strongly influences $\delta^{13}C_{DIC}$ because there is a fractionation of up to ~9 ‰ between the different DIC species (Emrich et al., 1970; Mook et al., 1974; Bade et al., 2004).

Formatted: Font:Italic

Deleted: Last, lakes with lower DIC concentrations are expected to have a $\delta^{13}C_{DIC}$ more easily influenced by exchanges with other carbon reservoirs, such as organic carbon (through photosynthesis/respiration) or other DIC sources (e.g., depleted volcanic CO_2 or groundwater DIC) – compared with buffered, high DIC lakes (Li and Ku, 1997; Fig. S3). This illustrates another (indirect) influence of the inter-lake chemical gradient on $\delta^{13}C_{DIC}$.

Moved (insertion) [10]

Formatted: Normal, Left, None, Line spacing: single, No bullets or numbering

Formatted: Font:5 pt

Formatted: Left

Deleted: Therefore, the alkalinity gradient and to a first order, the size, isotopic composition and responsiveness of the DIC reservoir to biogeochemical processes are controlled by the local hydro-physico-chemical parameters of th ... [20]

5.1.2. Influence of the lakes' alkalinity on their physico-chemical stratification features

Stratified water columns can sustain strong physico-chemical gradients, where a wide range of biogeochemical reactions impacting the C cycle can take place (*e.g.* Jézéquel et al., 2016). Here, temperature, conductivity and O_2 profiles show that the four lakes were clearly stratified at the time of sampling and had a similar general structure, although depths defining the successive epi-, meta- and hypolimnion layers differed between the lakes (Fig. 2).

The evolution of pH with depth exemplifies the interplay between the alkalinity gradient, the physico-chemical stratification of the lakes, and their respective C cycle. pH showed a stratified profile in La Preciosa and La Alberca, whereas it remained constant in Alchichica and Atexcac. The pH decline at the oxycline of Lake La Preciosa was associated with the decrease of POC and chlorophyll a concentrations and $\delta^{13}C_{DIC}$ values, reflecting the impact of oxygen respiration (*i.e.* carbon remineralization) at this depth (Figs. 2-4). In Lake La Alberca, the surface waters are markedly more alkaline than the bottom waters, with a two-step decrease of pH occurring at around 8 m and 17 m (total drop of 1.5 pH unit). Based on the same observations as in La Preciosa, this likely results from high OM respiration, although input of volcanic acidic gases (*e.g.* dissolved CO_2 with $\delta^{13}C \sim -5$ ‰) might also contribute to the pH decrease in the bottom waters, as reflected by negative $\delta^{13}C_{DIC}$ signatures and the increase of [DIC] and conductivity in the hypolimnion (Figs. 2 and 4). By contrast, while the same pieces of evidence for oxygen respiration ([POC], chlorophyll a) can be detected in the two other lakes, this did not similarly impact their pH profile (Fig. 2). This suggests that the acidity generated by these reactions is buffered by the much higher alkalinity measured in these two lakes. Overall, several external forcings such as lake hydrology or fluid sources impact the alkalinity buffering capacity of these lakes. Thereby, they also influence their vertical pH profile, which is particularly important considering the critical interplay between pH and biogeochemical reactions affecting the C cycle (*e.g.* Soetaert et al., 2007).

5.1.3. Isotopic signatures of inorganic C in the lakes ($\delta^{13}C_{DIC}$ and $\delta^{13}C_{Carbonates}$)

The DIC isotopic composition of the lakes – between ~ -3 and +2 ‰ on average (Table 2) – is consistent with the DIC sources described above. On one hand, those from the SOB lakes are similar to the estimated value of groundwater $\delta^{13}C_{DIC}$ coming from the alteration of the Cretaceous limestone basement. On the other hand, lower $\delta^{13}C_{DIC}$ in Lake La Alberca is consistent with an influence of remineralized OC and/or volcanic CO_2.

By controlling the DIC speciation ($H_2CO_3/CO_{2(aq)}$, HCO_3^-, CO_3^{2-}), pH also strongly influences $\delta^{13}C_{DIC}$ because there is a temperature dependent fractionation of up to ~10 ‰ between the different DIC species (Emrich et al., 1970; Mook et al., 1974; Bade et al., 2004; Table S4). Consistently, the $\delta^{13}C_{DIC}$ of Mexican lakes are in the expected range for lakes with a pH around 9 (Bade et al., 2004), where DIC is dominated by HCO_3^-. However, the pH values of the studied Mexican lakes are too close to each other to explain the significant difference observed between their $\delta^{13}C_{DIC}$ (Fig. 4; p=4.2x10^{-3} for Lakes Atexcac and La Preciosa which have the closest $\delta^{13}C_{DIC}$). Part of the variability of $\delta^{13}C_{DIC}$ among the lakes may result from their varying evaporation stages. This is suggested by the observation that the mean $\delta^{13}C_{DIC}$ values of the lakes broadly correlate with their salinity/alkalinity (Fig. S3b). This relationship is expected as evaporation generally increases the $\delta^{13}C_{DIC}$ of residual waters, notably

Formatted: Font color: Text 1
Formatted: Font:Italic, Font color: Text 1
Formatted: Font color: Text 1
Formatted: Font color: Text 1
Formatted: Font color: Text 1
Deleted: differ between the lakes (Fig. 2). For example, we found a clear offset in Lake Alchichica and Lake La Alberca between the depth of O_2 depletion and the depth below which the ORP decreases. By contrast, ORP sharply dropped below the depth where $O_{2(aq)}$ disappeared in Atexcac and La Preciosa. Meanwhile, in all four lakes the ORP decreased below the depth where chlorophyll a peaks collapsed. This pigment being a tracer of oxygenic photosynthesis, it suggests that ORP was buffered at a high value by photosynthetically produced oxygen during C fixation and only decreased at a depth where aerobic respiration became higher than oxygenic photosynthesis. The offset between the ORP drop and O_2 depletion in Lake Alchichica and Alberca could result from more extended peaks of chlorophyll a that we can observe in these two lakes (Fig. 2). The exact factors causing this distribution of oxygenic primary producers remain to be determined. In the end nonetheless, this impacts the depth distribution of other microbial metabolisms that thrive at different redox levels as well as the depths at which authigenic particles precipitate following redox reactions, as exemplified by the depth profiles of turbidity and the particulate metal concentrations (Fig.
Formatted: Font color: Text 1
Deleted: is another example of
Deleted: DOC,
Deleted: high
Formatted: Font:Italic
Formatted: Font:Italic
Deleted:)
Deleted: -
Deleted: , etc.)
Deleted: Thus,
Deleted: constraints on
Deleted: (e.g., lake hydrology, fluid sources, Sect. 5.1.1)
Formatted: Font:Italic
Moved (insertion) [9]
Formatted: Font:Italic
Moved (insertion) [8]

because it increases lake pCO_2 and primary productivity which bolsters CO_2 degassing and organic C burial, both having low $\delta^{13}C$ compared to DIC (*e.g.* Li and Ku, 1997; Talbot, 1990). Accordingly, the pCO_2 of La Alberca is smaller than in the other lakes (Table S1). Additionally, slightly higher temperatures recorded in La Alberca's surface waters would make degassing $CO_{2(g)}$ slightly less fractionated towards HCO_3^-/CO_3^{2-} ions (Table S4). Thus, even if the four lakes were characterized by similar CO_2-degassing rates, the increase of DIC isotopic composition related to this process would be smaller for La Alberca's $\delta^{13}C_{DIC}$. Lastly, lakes with lower DIC concentrations are expected to have a $\delta^{13}C_{DIC}$ more easily influenced by exchanges with other carbon reservoirs, such as organic carbon (through photosynthesis/respiration) or other DIC sources (*e.g.*, depleted volcanic CO_2 or groundwater DIC) – compared with buffered, high DIC lakes (Li and Ku, 1997). Consistently, low DIC/alkalinity concentration in Lake La Alberca corresponds to the lowest $\delta^{13}C_{DIC}$ of the four lakes, likely reflecting organic and/or volcanic C influence, and thus a higher responsiveness to biogeochemical processes of the inorganic C reservoir.

As a result, the isotopic composition of sedimentary carbonates ($\delta^{13}C_{Carb}$) which precipitate from the water column DIC primarily follows the alkalinity gradient trend with the lowest $\delta^{13}C_{Carb}$ found in the surficial sediments of La Alberca (~ -1.5 ‰), the highest values in Alchichica (~ +4.6 ‰) and La Preciosa and Atexcac having intermediate values (around 2.5 ‰) (Table 3). More precisely, we can estimate the $\delta^{13}C_{DIC}$ from which the carbonates precipitated by correcting for the isotopic fractionation existing between different carbonate phases and the lake DIC (supplementary text S1). From this, it appears that surficial sedimentary carbonates are in isotopic equilibrium with the $\delta^{13}C_{DIC}$ of the upper water columns, more specifically from the oxycline/thermocline, except in Lake Atexcac (Tables S4 and S5). In this latter lake, the $\delta^{13}C$ of carbonate precipitation is slightly lower than the $\delta^{13}C_{DIC}$, possibly related to detrital carbonate inputs from the surrounding microbialites. Thus, some detrital carbonate may contribute to the bulk sediment carbonates and slightly deviate the isotopic record from the theoretical equilibrium fractionation such as observed in Atexcac with a small offset of a few tenth of ‰.

5.1.4. Sinks of DIC along the alkalinity gradient

Interplays between pH and sources of alkalinity/DIC in the lakes also have a strong impact on their C storage capacity as they can result in different fluxes of the C sinks (inorganic and organic C precipitation / sedimentation, CO_2 degassing).

To a first order, alkaline pHs allow a relatively important storage of DIC because they favor the presence of HCO_3^- and CO_3^{2-} species over H_2CO_3* (the intermediate specie between gaseous $CO_{2(g)}$ and the bi-/carbonate ions and defined here as the sum of H_2CO_3 and $CO_{2(aq)}$). In the studied lakes, carbonate and bicarbonate ions represent over 99% of total DIC (Table S1). Nonetheless, large amounts of CO_2 degas out of the surface of lakes Alchichica, Atexcac and La Preciosa, as suggested by their elevated surface water pCO_2, amounting from 2 to 5 times higher the atmospheric pCO_{2atm} (Table S1). Thus, these lakes currently act as CO_2 sources to the atmosphere. Meanwhile, the lake with the lowest DIC (La Alberca de los Espinos) has surface waters in equilibrium or even with lower pCO_2 than pCO_{2atm} (Table S1). These observations are consistent with the idea that higher DIC concentrations favor CO_2 degassing through higher pCO_2 (despite high pH values). For the same pH in the surface waters of lakes Alchichica and La Alberca (the two endmembers of the alkalinity gradient), there is over three times more CO_2 degassing out of Alchichica than La Alberca (for a given value of gas transfer velocity). However, we notice that

Formatted: Font:Italic

most degassing occurs in Lake Atexcac (pCO_{2surf}/pCO_{2atm} = 5 at the moment of sampling; Table S1) due to a lower pH and thus a higher proportion of H_2CO_3*.

Another important sink of C for these lakes is the precipitation of carbonate minerals, composing the microbialites and bottom lake sediments. Here again the respective lake alkalinities and consequent mineral saturation indexes greatly influence the amount of C being precipitated out from the lakes waters. While the four lakes are supersaturated with respect to aragonite, calcite and the precursor phase monohydrocalcite, they show highly contrasting amounts of carbonate deposits (Zeyen et al., 2021). The degree of microbialite occurrence increases along the alkalinity gradient with Alchichica and Atexcac notably harboring massive deposits, whereas La Alberca has limited ones (Zeyen et al., 2021; Fig. S1). Similarly, surficial sediments contain from 40 to 62 wt. % carbonates on average for the SOB lakes but only 16 wt. % for La Alberca (Table 3). Thus, based on this large difference in carbonate precipitate quantities (both in microbialites and bottom sediments), it seems overall that the lakes from the SOB bury more C than Lake La Alberca de los Espinos, although a detailed estimation of these C fluxes (including sedimentation rates, porosity, etc.) would be required to fully constrain this aspect. Nevertheless, based on the data from May 2019, La Alberca was the only of the four lakes to have a pCO_2 in equilibrium with the atmosphere (and not higher) and therefore represents a net sink of C. Classifying the three other lakes as net C sources or sinks – notably in order to see the influence of their respective position in the alkalinity gradient – will require a more detailed description of C in- and out-fluxes since they all store and emit significant amounts of C (as organic and inorganic C deposits and via CO_2 degassing, respectively). However, this is out of the scope of the present study.

In summary, although the four lakes present the same general structure and environmental conditions (*i.e.* being tropical alkaline stratified crater-lakes), external and local factors (such as hydrology, fluid sources or stratification characteristics) result in contrasting compositions of their water chemistries, which in turn, have a critical impact on the physico-chemical depth profiles of each lake and their biogeochemical carbon cycle functioning. Notably, these external factors represent a first order control on the size, the isotopic composition and the responsiveness to biogeochemical processes of the inorganic C reservoir. Interestingly, C storage in mineral carbonates seems to be significant in watersheds where carbonate deposits already pre-exist in the geological substratum (here the Cretaceous limestone basement), providing more alkaline and C-rich sources.

Deleted: ,

Deleted: has

Symbols	Mathematical Expression	Signification
$\delta^{13}C_X$	$\left(\frac{\left(\frac{^{13}C}{^{12}C}\right)_X}{\left(\frac{^{13}C}{^{12}C}\right)_{ref}} - 1\right) * 1000$	Relative difference in ^{13}C:^{12}C isotopic ratio between a sample of a given C reservoir and the international standard "Vienna Pee Dee Bee", expressed in permil (‰). $\delta^{13}C_{total}$ represents the weighted average of $\delta^{13}C$ for all DIC and POC.
$\Delta^{13}C_{X\text{-}Y}$	$= \delta^{13}C_X - \delta^{13}C_Y \approx 1000 ln\alpha_{X\text{-}Y}$	Apparent isotopic fractionation between two reservoirs 'X' and 'Y'. Difference between their measured C isotope compositions approximating the fractionation α in ‰.
$\varepsilon_{X\text{-}CO2}$	$= (\alpha_{X\text{-}CO2} - 1)1000 \approx \delta^{13}C_X - \delta^{13}C_{CO2}$	Calculated isotopic fractionation between a reservoir 'X' and $CO_{2(aq)}$. $\alpha_{X\text{-}CO2}$ is calculated as $(\delta^{13}C_X+1000)/(\delta^{13}C_{CO2}+1000)$ where $\delta^{13}C_X$ is measured and $\delta^{13}C_{CO2}$ is computed based on DIC isotopic composition and speciation (see supplementary text S1).

Table 4

Index for mathematical notations used in the text including C isotopic composition of a reservoir X ($\delta^{13}C_X$), isotopic discrimination between the two carbon reservoirs X and Y ($\Delta^{13}C_{X\text{-}Y}$). In the main text, we report organic C isotopic discrimination *versus* both bulk DIC ($\Delta^{13}C_{POC\text{-}DIC}$) – in a way to facilitate studies intercomparison and because it is the commonly reported raw measured data (Fry, 1996) – and calculated $CO_{2(aq)}$ ($\varepsilon_{POC\text{-}CO2}$) in order to discuss the intrinsic isotopic fractionations associated with the lakes metabolic diversity. All C isotope values and fractionations are reported relative to the international standard VPDB (Vienna Pee Dee Belemnite).

Moved (insertion) [11]

Deleted: From

5.2. Particulate organic carbon: from water column primary production to respiration recycling and sedimentary organic matter

5.2.1. Particulate organic C sources

Primary productivity by oxygenic photosynthesis in the upper water column

All four crater lakes are endorheic basins, *i.e.* there is no surface water inflow or outflow. Therefore, the organic carbon sources are predominantly autochthonous, mainly resulting from planktonic autotrophic C fixation. This is supported by C:N ratios of POM that were comprised between 6 and 12 in the four lakes, *i.e.*, close to the phytoplankton Redfield but far from land plant ratios. Abundant vegetation covers the crater walls of Lake La Alberca and to a lesser extent Lake Atexcac; some plant debris were observed and sampled in the sediment cores of these two lakes. They had high C:N ratios (between 24 and 68), typical of plant tissues and significantly higher than those of the bulk organic matter of surficial sediments (between 8 and 13) and the water column (between 6 and 12) (Fig. 3). Therefore, allochthonous organic carbon in these two lakes – albeit present – does not significantly contribute to their bulk organic signal.

The importance of planktonic autotrophic C fixation as a major source of organic C in the four lakes is further supported by the assessment of the isotopic discrimination between DIC and organic biomass, expressed as $\Delta^{13}C_{POC\text{-}DIC}$ and $\varepsilon_{POC\text{-}CO2}$ (Table 4). The $\Delta^{13}C_{POC\text{-}DIC}$ vary between ~ -29 and -23 ‰ (corresponding to $\varepsilon_{POC\text{-}CO2}$ between ~ -19 and -13 ‰; Table 5) throughout the four water columns, which is in the typical range of planktonic oxygenic phototrophs (Pardue et al., 1976; Sirevag et al., 1977; Thomas et al., 2019). Yet, these values exhibit variability – both within a single water column (up to 4.5 ‰) and between the different lakes (up to 6 ‰, Figs. 4 and 5). This variability may trace several abiotic and biotic factors.

Notably, higher DIC availability in Alchichica and Atexcac probably makes the carboxylation step more limiting during photosynthesis (*e.g.* O'Leary, 1988; Descolas-Gros and Fontungne, 1990; Fry, 1996), increasing $|\varepsilon_{POC\text{-}CO2}|$ in these lakes (between 17.5 and 19.2 ‰ at the peak of Chl. a) compared to La Preciosa and Alberca (Fig. 5a; between 14.5 and 17.7 ‰). Indeed, lower $CO_{2(aq)}$ availability and/or higher reaction rates result in transport-limited rather than carboxylation-limited fixation and thus, smaller C isotope fractionation between POC and DIC (Pardue et al., 1976; Zohary et al., 1994; Fry, 1996; Close and Henderson, 2020). This is because the isotopic fractionation associated with diffusion is much smaller than with carboxylation and because a higher proportion of the DIC entering the cells is converted into organic biomass (*e.g.* Fogel and Cifuentes, 1993). Consistently, we notice a correlation among the lakes between $a(CO_2)_{(aq)}$ (or [DIC]) and $|\varepsilon_{POC\text{-}CO2}|$ at depths where oxygenic photosynthetic peaks (Fig. 6). Furthermore, lakes La Preciosa and Alberca are considered less oligotrophic than the two other lakes (Lugo et al., 1993; Vilaclara et al., 1993; Havas et al., submitted), consistently with higher chlorophyll a contents and thus smaller $|\varepsilon_{POC\text{-}CO2}|$ (Fig. 5). Last, higher water temperatures in La Alberca de los Espinos (by ~ 3 °C) could partly contribute to a smaller $|\varepsilon_{POC\text{-}CO2}|$ in this lake (Sackett et al., 1965; Pardue et al., 1976; Descolas-Gros and Fontungne, 1990).

Unlike $\delta^{13}C_{DIC}$, organic carbon isotopic signatures do not evolve linearly with the alkalinity/salinity gradient, suggesting other lake- and microbial-specific controls on these signatures. These controls include: diffusive or active uptake mechanisms, specific carbon fixation pathways, the fraction of intracellular inorganic carbon

Formatted: Outline numbered + Level: 2 + Numbering Style: 1, 2, 3, … + Start at: 1 + Alignment: Left + Aligned at: 0" + Indent at: 0.25"

Deleted: : insights from POC and DIC signatures

Moved (insertion) [12]

Formatted: Font:Not Bold, Italic

Formatted: Normal, Indent: First line: 0.1", No bullets or numbering

Formatted: Font:Italic

Formatted: Font:Italic

Deleted: In this section, we discuss the different biological processes that can be evidenced based on the depth variations of DIC and POM chemical and isotopic compositions.

Moved up [12]: *Primary productivity by oxygenic photosynthesis in the upper water column* … [21]

Formatted: Font:Not Bold, Italic

Formatted: Font:Italic

Formatted: Font:Italic

Deleted: ,

Deleted: (between 24 and 68)

Deleted: local allochtonous

Deleted: 3).

Deleted: -20

Deleted: 14

Deleted: 4

Deleted: 6) – which could

Formatted: Font:Italic

Deleted: and increase $|\Delta^{13}C_{POC\text{-}DIC}$

Deleted: 6a

Deleted: 24

Deleted: 27 ‰ for these two lakes *versus* 28 to 29.5 ‰ for Alchichica and Atexcac, at the peak of Chl. a).

Deleted: uptake

Formatted: Font:Italic

Deleted: S4

Deleted: Lakes

Deleted: more eutrophic

Deleted: (Lugo et al., 1993; Vilaclara et al., 1993; Callieri et al., 2013) consistently with higher chlorophyll a content and photosynthetic rates and thus smaller $|\Delta^{13}C_{POC\text{-}DIC}|$. Additionally, higher water temperatures in Alberca de los Espinos (by ~ 3 °C) could partly contribute to smaller $|\Delta^{13}C_{POC\text{-}DIC}$

released out of the cells, cell size and geometry (Werne and Hollander, 2004 and references therein) and remineralization efficiency. Moreover, an increasing number of isotopic data has evidenced a significant variability of the isotopic fractionation achieved by different purified RuBisCO enzymes ($\varepsilon_{RuBisCO}$, Iñiguez et al., 2020), and even by a single RuBisCO form (Thomas et al., 2019). Thus, caution should be paid to the interpretation of the origin of small isotopic variations of the biomass in distinct environmental contexts because RuBisCO alone can be an important source of this variability (Thomas et al., 2019).

Formatted: Font:Not Italic, Not Hidden

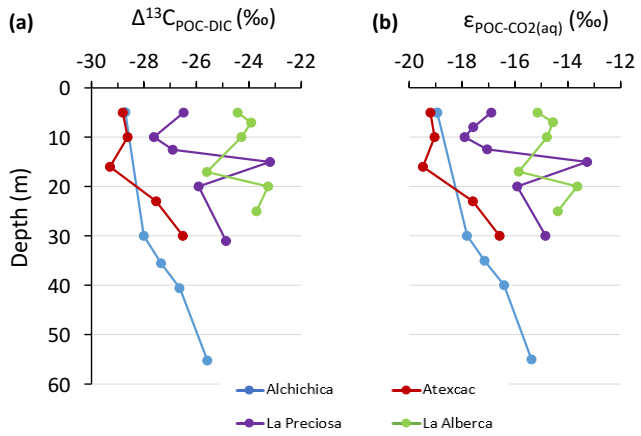

Figure 5.

Isotopic fractionations between POC and DIC in the water columns of the four lakes, expressed as a) $\Delta^{13}C_{x\text{-}y}$ and b) $\varepsilon_{POC\text{-}CO2}$. Refer to Table 4 for more detail about the Δ and ε notations.

Formatted: Font:2 pt, Not Italic, Not Hidden

Formatted: Normal, None, No bullets or numbering

Lake	Sample	$\Delta^{13}C_{POC\text{-}DIC}$	$\varepsilon_{POC\text{-}CO2}$
		‰	
Alchichica	AL 5m	-28.7	-18.7
	AL 30m	-28.0	-17.5
	AL 35m	-27.3	-16.9
	AL 40m	-26.6	-16.1
	AL 55m	-25.6	-15.1
Atexcac	ATX 5m	-28.8	-18.9
	ATX 10m	-28.6	-18.8
	ATX 16m	-29.3	-19.2
	ATX 23m	-27.5	-17.3
	ATX 30m	-26.5	-16.3
La Preciosa	LP 5m	-26.5	-16.7
	LP 10m	-27.6	-17.7
	LP 12.5m	-26.9	-16.9
	LP 15m	-23.2	-13.1
	LP 20m	-25.9	-15.8
	LP 31m	-24.9	-14.7
La Alberca de Los Espinos	Albesp 5m	-24.4	-15.0
	Albesp 7m	-23.9	-14.5
	Albesp 10m	-24.3	-14.7
	Albesp 17m	-25.6	-15.8
	Albesp 20m	-23.3	-13.6
	Albesp 25m	-23.7	-14.4

Table 5

Isotopic fractionations between dissolved inorganic carbon (DIC) and particulate organic carbon (POC). $\Delta^{13}C_{POC\text{-}DIC} = \delta^{13}C_{POC} - \delta^{13}C_{DIC}$ is the apparent fractionation and ε is computed as the actual metabolic isotopic discrimination between CO_2 and POC (see Table 4). The full chemistry of lake Alchichica sample at 35 m depth was not determined, thus, calculation of $\delta^{13}C_{CO2}$ for this sample was based on the composition of samples beneath and above.

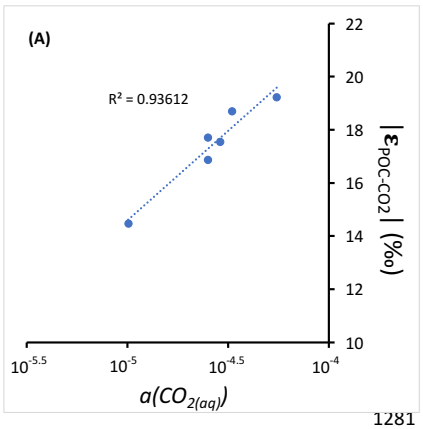

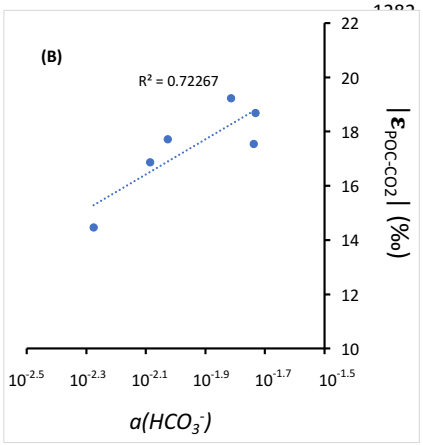

Figure 6.

Cross plots of DIC species activities *versus* absolute values of calculated C isotopic fractionations between POC and CO_2 at depths of peak oxygenic photosynthesis where data was available (5 and 30 m for Alchichica, 16 m for Atexcac, 10 and 12.5 m for La Preciosa and 7 m for La Alberca). (A) Dissolved $CO_{2(aq)}$ activity and (B) bicarbonate activity as functions of $|\varepsilon_{POC\text{-}CO2}|$ in ‰ plus linear correlation trends and corresponding R^2.

Primary production in the anoxic hypolimnion

Anoxygenic autotrophs commonly thrive in anoxic bottom waters of stratified water bodies (*e.g.* (Pimenov et al., 2008; Zyakun et al., 2009; Posth et al., 2017; Fulton et al., 2018; Havig et al., 2018). Consistently, they have been identified at different depths in the four Mexican lakes (Macek et al., 2020; Iniesto et al., 2022). Based on our results obtained on samples collected during the stratification period, anoxygenic autotrophs appear to have a distinctive impact on the C cycle of lakes Atexcac and La Alberca only. Indeed, Lake Atexcac records a concomitant decrease of [DIC] and increase of $\delta^{13}C_{DIC}$ in the anoxic hypolimnion at 23 m, below the peak of chlorophyll a, suggesting autotrophic C fixation by chemoautotrophy or anoxygenic photosynthesis. The calculated $\varepsilon_{POC\text{-}CO2}$ at 23 m (-17.3 ‰) is consistent with C isotopes fractionation by purple- and green-sulfur-anoxygenic bacteria (PSB and GSB), while $\varepsilon_{POC\text{-}CO2}$ in La Alberca's hypolimnion (~ -15 ‰) is closer to GSB canonical signatures (Posth et al., 2017 and references therein) (Fig. 5b). In La Alberca, anoxygenic primary productivity is moreover suggested by increasing POC concentrations below the oxycline. Besides, we also observe a Chl. a peak in the anoxic hypolimnion of this lake (Fig. 2), which likely represents a bias of the probe towards some bacteriochlorophylls typical of GSB (see supplementary text S3). We notice that in Lake Atexcac, C fixation at 23 m by anoxygenic autotrophs causes a shift in the DIC reservoir, while oxygenic photosynthesis at 16 m does not, suggesting that anaerobic autotrophs are the main autotrophic metabolisms in this lake (in terms of DIC uptake). In La Alberca, the increase of [POC] to maximum values at depth also supports the predominance of anoxygenic *versus* oxygenic autotrophy (Fig. 3). This is similar to other stratified water bodies which exhibit primary production clearly dominated by anoxygenic metabolisms (Fulton et al., 2018).

Moved (insertion) [13]

Moved (insertion) [14]

Formatted: Font:Italic

Moved (insertion) [15]

Last, at 23 m in Lake Atexcac and 17 m in Lake La Alberca, we find a striking turbidity peak precisely where the redox potential and the concentration of dissolved Mn drops (Fig. 2). In Lake Atexcac concentrations of dissolved metal such as Cu, Pb or Co also drop at 23 m (Fig. S4). In La Alberca, a peak of particulate Mn concentrations is detected at 15 m (Fig. 2; data not available for Atexcac). This is most likely explained by the precipitation of Mn as mineral particles where reduced bottom waters meet oxidative conditions prevailing in the upper waters. These oxidized Mn phases can be used as electron acceptors during chemoautotrophy (Havig et al., 2015; Knossow et al., 2015; Henkel et al., 2019; van Vliet et al., 2021). Moreover, even at a low particle density, such phases can catalyze abiotic oxidation of sulfide to sulfur compounds (van Vliet et al., 2021), which in turn can be used and further oxidized to sulfate by phototrophic or chemoautotrophic sulfur-oxidizing bacteria. This is also consistent with the small increase of $[SO_4^{2-}]$ observed at 23 m in Atexcac (Table S2).

5.2.2. Sinks of particulate organic carbon: respiration and sedimentation

Aerobic respiration at the oxycline

At the oxycline of stratified water bodies, aerobic respiration of OM by heterotrophic organisms favors the transition from oxygenated upper layers to anoxic bottom waters. In the water column of the four lakes, $\Delta^{13}C_{POC\text{-}DIC}$ (and $\varepsilon_{POC\text{-}CO_2}$) show increasing values in the hypolimnion, and especially below the chlorophyll a peaks (Figs. 2 and 5). This trend also correlates with increasing $\delta^{13}C_{POC}$, decreasing $(C:N)_{POM}$ ratios as well as decreasing POC concentrations (except in La Alberca) (Figs 3 and 4). Decreasing POC concentrations near the oxycline and redoxcline are consistent with the fact that part of the upper primary production is degraded deeper in the water columns and/or that there is less primary production in the anoxic bottom waters. Increase of $\delta^{13}C_{POC}$ in the hypolimnion of the lakes is consistent with heterotrophic activity and points out that POC at these depths could mainly record secondary production rather than being residues of sinking degraded OM formed by primary production. Indeed, heterotrophic bacteria preferentially grow on available ^{13}C-enriched amino acids and sugars, thus becoming more enriched than their C source (Williams and Gordon, 1970; Hayes et al., 1989; Zohary et al., 1994; Briones et al., 1998; Lehmann et al., 2002; Jiao et al., 2010; Close and Henderson, 2020). The decrease in C:N ratios in the POM also reinforces this conclusion since secondary heterotrophic bacteria biomass generally have C:N between 4 and 5 (Lehmann et al., 2002), whereas residual degraded OM from primary producers would carry higher C:N signatures (van Mooy et al., 2002; Buchan et al., 2014). These latter signatures are not recorded by POM in the lower water columns of the lakes (Fig. 3). In Lake La Preciosa, the water column shifts from a highly oxygenated state to anoxia over a ~5 m interval against more than 10 m for Alchichica and Atexcac. This correlates with a sharp $\delta^{13}C_{POC}$ increase (+ 3.4‰), highlighting how efficient and O_2-dependent the remineralization process is in this lake.

The $\delta^{13}C_{DIC}$ signatures in lakes Alchichica and La Preciosa are consistent with the mineralization of OM as they exhibit lower values below the oxycline than in surficial waters (Figs. 2 and 4). Similarly to what is observed in several other water bodies and notably stratified water columns such as the Black Sea (*e.g.* Fry et al., 1991), surface photosynthesis increases $\delta^{13}C_{DIC}$ by fixing light DIC, while respiration transfers light OC back to the DIC pool at depth. Such a decrease of the $\delta^{13}C_{DIC}$ can also be seen in the oxycline of Lake La Alberca between 7 and 10 m.

Moved (insertion) [16] ... [22]

Moved (insertion) [20]

Formatted: Font:Not Bold, Italic

Formatted: Normal, Indent: First line: 0.1", No bullets or numbering

Moved up [10]: ... [23]

Formatted: Font:5 pt

Moved up [11]: Index for mathematical notations used in the text including C isotopic composition of a reservoir X ($\delta^{13}C_X$), isotopic discrimination between the two carbon reservoirs X and Y ($\Delta^{13}C_{X\text{-}Y}$). In the main text, we report organic C isotopic discrimination *versus* both bulk DIC ($\Delta^{13}C_{POC\text{-}DIC}$) – in a way to facilitate studies intercomparison and because it is the commonly reported raw measured data (Fry, 1996) – and calculated $CO_{2(aq)}$ ($\varepsilon_{POC\text{-}CO2}$) in order to discuss the intrinsic isotopic fractionations associated with the lakes metabolic diversity. All C isotope values and fractionations are reported relative to the international standard VPDB (Vienna Pee Dee Belemnite).

Moved up [20]: *Aerobic respiration at the oxycline* ... [26]

Deleted: ... [24]

Deleted: ... [25]

Formatted: Font:Not Bold, Italic

Deleted: Fig. 2; 6)…igs. 2 and 5). This trend also correlates with increasing $\delta^{13}C_{POC}$, decreasing $(C:N)_{POM}$ ratios as well as decreasing POC ... [27]

Moved (insertion) [21]

Moved up [21]: Decreasing POC concentrations near ... [28]

Deleted: Decreasing …he decrease in C:N ratios in th ... [29]

Deleted: ;

Formatted ... [30]

Moved up [18]: can be used as electron acceptors du ... [42]

Deleted: Table 4 ... [31]

Deleted: ... [43]

Formatted: Font:Not Italic, Not Hidden

Formatted ... [32]

Moved up [13]: Besides, we also observe a Chl. a pe ... [33]

Deleted: information).

Moved up [14]: We notice that in Lake Atexcac, C fi ... [34]

Formatted: Font:Italic

Deleted: This is similar with

Moved up [15]: other stratified water bodies which e ... [35]

Deleted: Furthermore, at 23 m in Lake Atexcac and 1 ... [36]

Moved up [16]: 2). In Lake Atexcac concentrations ... [37]

Deleted: This is also consistent with the small in incr ... [41]

Deleted: S5). In La Alberca, a peak of particulate Mn ... [38]

Moved up [17]: 2; data not available for Atexcac).

Deleted: This is most likely explained by the precipit ... [39]

Moved up [19]: can catalyze abiotic oxidation of sul ... [40]

Lake La Alberca shows the least saline/alkaline water column and most peculiar geochemical depth profiles among the four lakes. Notably, its [DIC] and $\delta^{13}C_{DIC}$ (the lowest of the studied lakes) increase from the lower metalimnion to the hypolimnion and further into the porewaters of the first cm of sediments with $\delta^{13}C_{DIC}$ reaching up to ~10 ‰ (Figs. 3; 4). Consistently, the calculated CO_2 partial pressure (P_{CO2}) increases downward from slightly less than 1x that of atmospheric P_{CO2} near the lake surface up to almost 40x at the bottom of the lake (Table S1).

While the increase of [POC] at depth may contribute to the observed $\delta^{13}C_{DIC}$ increase by mass balance, it should also lower the [DIC] instead of increasing it. Similarly, the sinking of POC at depth followed by its remineralization into DIC cannot explain those observations since this would lower the $\delta^{13}C_{DIC}$ in the hypolimnion (Fig. 4). Overall, these observations require that a significant source of inorganic ^{13}C-rich carbon fuels the bottom waters of La Alberca de los Espinos. The source of heavy carbon most likely results from methanogenesis, which consumes organic carbon in the sediments and produces ^{13}C-depleted methane and ^{13}C-rich carbon dioxide diffusing upward in the water column (likely acetoclastic methanogenesis, dominant in lacustrine contexts, Whiticar et al., 1986). Methanogenesis, as an "alternative" OM remineralization pathway could be favored in Lake La Alberca, because this lake is relatively rich in OM (notably with high [DOC], Havas et al., submitted), and depleted in SO_4^{2-} (Wittkop et al., 2014; Birgel et al., 2015; Cadeau et al., 2020) compared with the three other Mexican lakes. Based on the isotopic compositions of sedimentary organic carbon and porewater DIC in Lake La Alberca, we can tentatively calculate the methane isotopic signature (see supplementary text S4). The calculated $\delta^{13}C_{CH4}$ in the first 10 cm of sediments is between -59 and -57 ‰, which is consistent with the range of isotopic composition of methane after biogenic methanogenesis (Whiticar et al., 1986).

Upward diffusing methane may be either (i) partly lost from the lake's surface (*i.e.* escaping the system) by degassing or (ii) totally kept in the water column by complete oxidation (either abiotically by oxygenated surface waters or biologically by methanotrophic organisms). The oxidation of CH_4 in the water column should lead to the formation of ^{13}C-depleted carbon dioxide that would mix back with the lake DIC (and notably with heavy methanogenic CO_2 produced at depth) and/or ^{13}C-depleted biomass (as POC or SOC) if it occurs by methanotrophy. Thus, the net effect of combined methanogenesis and methane oxidation is expected to (i) generate a $\delta^{13}C_{DIC}$ gradient from high to low values between the sediment porewaters and the oxycline as proposed elsewhere (Assayag et al., 2008; Wittkop et al., 2014) and (ii) progressively lower sedimentary $\delta^{13}C_{SOC}$ in case of methanotrophy. Abiotic oxidation of methane by dioxygen is consistent with the observations that $\delta^{13}C_{DIC}$ decreases from porewaters (~ +10 ‰) to the oxycline (-4 ‰), reaching minimum values where dissolved-O_2 starts to appear (Fig. 2). On the other hand, microbial anaerobic oxidation of methane (AOM) could occur at the 17 m depth through Mn-oxides reduction (Cai et al., 2021; Cheng et al., 2021) and possibly bacterial sulfate-reduction closer to the water-sediment interface, as inferred for the surficial sediments of meromictic Lake Cadagno (Posth et al., 2017). Indeed, we observe a net increase of particulate Fe and S concentrations at a depth of 25 m and a peak of solid sulfide minerals in the surficial sediments (Fig. S5). However, $\delta^{13}C_{SOC}$ and $\delta^{13}C_{POC}$ are far from calculated $\delta^{13}C_{CH4}$, suggesting that AOM is not a major process in the bottom lake waters and surface sediments (Lehmann et al., 2004) and thus that methanotrophy is not the main CH_4 oxidation pathway in Lake La Alberca.

Alternatively, if some portion of the methane escaped oxidation and degassed out of the lake, $\delta^{13}C_{DIC}$ would likely be driven to extreme positive values with time, as observed elsewhere (Gu et al., 2004; Hassan, 2014; Birgel et al.,

Formatted: Font:Not Bold, Italic
Deleted: and volcanic-CO_2 degassing from the sediments of
Formatted: Font:Not Bold, Italic
Formatted: Normal, Indent: First line: 0.1", No bullets or numbering
Deleted: pore waters
Deleted: 11
Deleted: ,
Deleted: S4). The total carbon concentration depicts a clear increase from surface waters to the bottom of the lake (Fig. 3
Deleted: OC particles
Deleted: their
Deleted:]),
Deleted: SO_4 compared with the three other Mexican lakes
Deleted: .
Deleted: information
Deleted: 56.8
Deleted: methane
Formatted: Font:Italic
Deleted: as well as
Deleted: chemocline
Deleted: chemocline
Deleted: methane
Deleted: (AMO
Deleted: S6
Deleted: AMO

2015; Cadeau et al., 2020). This is not consistent with the observation that the average $\delta^{13}C_{DIC}$ in Lake La Alberca is about -3 ‰ (Fig. 4), unless an additional counterbalancing source of DIC to this lake exist. This source of DIC could be volcanic CO_2-degassing (see section 5.1.1). Such a contribution may maintain the lake's average $\delta^{13}C_{total}$ close to a mantle isotopic signature and notably away from extreme positive values if CH_4-escape dominated. It is also possible that volcanic CO_2 degassing is coupled to methanogenesis by CO_2 reduction in addition to the acetoclastic one described above. We observe a strong pH decline at depth in this lake (mostly below 17 m, Fig. 2) which could be fostered by both the acidic volcanic gases (Pecoraino et al., 2015) and methanogenesis, although other redox and microbial reactions could impact the pH as well (Soetaert et al., 2007).

Although volcanic CO_2 could be an important source in the C mass balance of Lake La Alberca, we note that it cannot explain the very positive $\delta^{13}C_{DIC}$ in the sediment porewaters alone, thus bolstering the identification of methanogenesis. Only a future quantification of the fluxes of sedimentary methane production, volcanic CO_2 and possible CH_4 efflux out of the lake will help to quantify the peculiar C cycle of Lake La Alberca.

Transfer of OM from the water column to the surficial sediments

The first 12 cm of the sediment cores of the four lakes contain varying quantities of OC between 1 and 13 wt. % (Table 3). This appears to be relatively elevated considering the predominant autochthonous nature of OC and oligotrophic conditions in these lakes (Alcocer et al., 2014; Havas et al., submitted). In Lake Alchichica, the recent OC burial flux in the sediment was estimated to represent between 15 and 26 $g.yr^{-1}.m^{-2}$ (Alcocer et al., 2014). This is within the range of values provided for small lakes around the world (Mulholland and Elwood, 1982; Dean and Gorham, 1998; Mendonça et al., 2017), though most of them receive allochthonous OM inputs. Different factors can favor the preservation of OM including lower respiration and oxidation rates due to anoxic bottom waters and scarce benthic biota and/or high sedimentation rates (Alcocer et al., 2014). Anaerobic respiration clearly occurs in the four lakes to some extent, as detailed for La Alberca in section 5.2.2, and as seen in the surficial sediment data of the other lakes as well (decreasing $\delta^{13}C_{DIC}$ in Alchichica, increasing C:N ratio in Atexcac and La Preciosa; Table 3). Nonetheless, the anoxic conditions prevailing in the hypolimnion most of the year are significantly more favorable to OM preservation than oxic conditions (Sobek et al., 2009; Kuntz et al., 2015). In Alchichica, the large size if phytoplankton was also suggested to favor OM preservation (Adame et al., 2008; Ardiles et al., 2011). In La Alberca the low sulfate content (which is an important electron acceptor for anaerobic respiration) probably favors the preservation of high TOC in the sediments. Again, a complete mass-balance of these lakes C fluxes will be required to estimate their net C emission or sequestration behavior.

Although the nature and geochemical signatures of the OM that deposits in the bottom sediments may vary throughout the year, it is interesting to infer from what part(s) of the water column surficial sedimentary OM comes from during the stratified seasons. In the three lakes from the SOB, $\delta^{13}C_{SOC}$ and $(C:N)_{SOM}$ signatures of the surficial sediments OM lie somewhere in between POM signatures from the upper water columns and from the hypolimnion (Figs. 3, 4). More precisely, in Alchichica, top $\delta^{13}C_{SOC}$ and $(C:N)_{SOM}$ signatures (-25.7 ‰ and 10.4, respectively) lie much closer to values recorded in the upper water column (~ -26.5 ‰ and 10.5, respectively) implying that the upper oxygenic photosynthesis production is primarily recorded. Accordingly, it was suggested that most of the phytoplankton biomass being exported was composed of diatoms (Ardiles et al., 2011). In Lake Atexcac on the

Deleted: In fact, we notice that $\delta^{13}C_{total}$ averages -4.8‰ in Lake La Alberca, which is very similar to mantle-CO_2 signatures (Javoy et al., 1986; Mason et al., 2017). A contribution from mantle CO_2 degassing in this lake may sustain a high P_{CO2} and [DIC] at depth and maintain the lakes

Deleted: (if CH_4-escape dominated). Moreover, Lake La Alberca

Moved up [7]: is located on top of a likely active normal fault (Siebe et al., 2012), which is favorable to the ascent of volcanic gases

Deleted: .

Deleted:

Deleted: Overall,

Deleted: . We

Deleted: however,

Deleted: volcanic CO_2 alone

Deleted: better constraint

Deleted: Which

Formatted: Normal, Indent: First line: 0.1", No bullets or numbering

Formatted: Font:Not Bold, Italic

Deleted: transfers

Deleted: ?

Formatted: Font:Not Bold, Italic

Formatted: Font:Not Bold, Italic

Deleted: -

Deleted: $\delta^{13}C$

Deleted: Nonetheless

Deleted: 5

contrary, $\delta^{13}C_{SOC}$ and $(C:N)_{SOM}$ signatures (~ -26.8 ‰ and 8, respectively) lie closer to values recorded in the hypolimnion (~ -26.5 ‰ and 6.5, respectively) suggesting that SOM records mostly the anaerobic primary production.

In Lake La Alberca, surficial $\delta^{13}C_{SOC}$ are markedly more negative (by ~ 2 to 3 ‰) than the deepest and shallowest water column values (Fig. 4) but they are close to what is recorded at the redoxcline depth of 17 m. However, the $(C:N)_{SOM}$ values are much higher than what is measured anywhere in the water column, which is consistent with remineralization of OM by sulfate-reduction and methanogenesis in the sediments of this lake. Therefore, OM biogeochemical signatures in La Alberca's surficial sediments could be strongly influenced by early diagenesis occurring at the water-sediment interface – despite favorable conditions for OM preservation. Importantly though, methanogenesis/methanotrophy are recorded in the surficial sediments porewaters (notably seen through extremely positive $\delta^{13}C_{DIC}$) but not in the solid sediments that show neither very negative $\delta^{13}C_{SOC}$ nor positive $\delta^{13}C_{carbonates}$ in the first 10 cm.

Overall, this suggests that OM depositing at the bottom of these stratified lakes do not always record geochemical signatures from the same parts of the water columns and can be modified by very early diagenesis. Notably, they do not necessarily record the signatures of primary production by oxygenic photosynthesis from the upper column. For example, in Lake Atexcac, sedimentary OM records instead primary production by anoxygenic photosynthesis, even though POC concentration was maximum in the upper water column. A deeper understanding of the OM transfer process from water columns to sediments will require more detailed analyses and comparison of the different OM pigments and molecules and could have strong implications for interpretation of the fossil record in the deep anoxic time.

6. CONCLUSIONS AND SUMMARY

The carbon cycles of four stratified alkaline crater lakes were described and compared based on the concentration and isotopic compositions of DIC and POC in the water columns and of surficial (~10 cm) sedimentary carbonates and organic carbon. We identify different regimes of C cycling in the four lakes due to different biogeochemical reactions related to slight environmental and ecological variations. In more details, we show that:

- External abiotic factors, such as the hydrological regime and the inorganic C sources to the lakes, control their alkalinity and thus, the buffering capacities of their waters. In turn, it constrains the stratification of the water columns and the inorganic C isotopic signatures of the lakes water columns and sediments. Furthermore, it impacts the C mass balance of the lakes with probable consequences on their net C-emitting or -sequestering status.
- Based on POC and DIC concentrations and isotopic compositions, combined with physico-chemical parameters, we are able to identify the activity of oxygenic photosynthesis and aerobic respiration in the four studied lakes. Anoxygenic photosynthesis and/or chemoautotrophy are also evidenced in some of the lakes, but their POC and DIC signatures can be equivocal.
- Methanogenesis is evidenced in the surficial sediments of the OM-rich Lake La Alberca de los Espinos and influences the lower water column geochemical signatures. However, it is recorded only by analyses of porewater dissolved species, but not imprinted in the sedimentary archives (solid OM and carbonates).

Deleted: 27

Deleted: Finally, in

Deleted: (see also Sect. 1).

Deleted: mainly reflect the effect of

Deleted:

Deleted: sections

Deleted: In Lake La Alberca, OM is rapidly altered by diagenesis processes, but the signal of methanogenesis is not preserved in the sedimentary OM or carbonates, but only recorded by the sediment porewaters

Deleted: <#>A particularly large and central DOC reservoir ... [44]

Formatted: Outline numbered + Level: 1 + Numbering Style: 1, 2, 3, ... + Start at: 1 + Alignment: Left + Aligned at: 0.25" + Indent at: 0.5"

Deleted: cycle

Deleted: extensively

Deleted: , including

Deleted: , DOC,

Deleted: and

Deleted: (SOC) in parallel with their physico-chemical characteristics

Deleted: changes

Deleted: external

Deleted: thus the distribution of microbial communities and their respective metabolic effect on C

Deleted: coupled

Deleted: as well as sediment-related methanogenesis

Deleted: <#>DOC is the largest OC reservoir in the water column of the studied lakes (> 90%). Its concentrations and isotopic compositions bring precious new and complementary information about the C cycle of these stratified water bodies. Depending on environmental factors such as nutrients and DIC availability, diverse photosynthetic planktonic communities appear to release more or less important amounts of DOC depending on the lake, transferring most of the inorganic C fixed to DOC rather than POC. This process is marked by very heavy and distinct isotopic signatures of DOC compared to POC. They reflect different metabolism/C fixation pathways and/or the activity of a DIC-CM coupled with an overflow mechanism (i.e. DOM exudation) for which we propose a novel isotopic model including DOC. These features are invisible to POC analyses and thus are not recorded in the sediments. ... [45]

Deleted: <#>organic

Deleted: <#>pore water

Deleted: <#> and

Deleted: <#>its

- Last, we observe that the SOM geochemical signatures of these stratified lakes do not all record the same "biogeochemical layers" of the water column and can be largely modified by early diagenesis in some cases. Meanwhile, most carbonate phases in bottom lake sediments are in isotopic equilibrium with lake oxyclines, while some might be detrital in origin.

Author Contributions

RH and CT designed the study in a project directed by PLG, KB and CT. CT, MI, DJ, DM, RT, PLG and KB collected the samples on the field. RH carried out the measurements for C data; DJ the physico-chemical parameter probe measurements and EM provided data for trace and major elements. RH and CT analyzed the data. RH wrote the manuscript with important contributions of all co-authors.

Competing Interests

The authors declare that they have no conflict of interest.

Disclaimer

Acknowledgements

This work was supported by Agence Nationale de la Recherche (France; ANR Microbialites, grant number ANR-18-CE02-0013-02). The authors thank Anne-Lise Santoni, Elodie Cognard, Théophile Cocquerez and the GISMO platform (Biogéosciences, Université Bourgogne Franche-Comté, UMR CNRS 6282, France). We thank Céline Liorzou and Bleuenn Guéguen for the analyses at the Pôle Spectrométrie Océan (Laboratoire Géo-Océan, Brest, France) and Laure Cordier for ion chromatography analyses at IPGP (France). We thank Nelly Assayag and Pierre Cadeau for their help on the AP 2003 at IPGP.

References

Adame, M.F., Alcocer, J., Escobar, E., 2008. Size-fractionated phytoplankton biomass and its implications for the dynamics of an oligotrophic tropical lake. Freshw. Biol. 53, 22–31. https://doi.org/10.1111/j.1365-2427.2007.01864.x

Alcocer, J., 2021. Lake Alchichica Limnology, Springer Nature. ed.

Alcocer, J., Ruiz-Fernández, A.C., Escobar, E., Pérez-Bernal, L.H., Oseguera, L.A., Ardiles-Gloria, V., 2014. Deposition, burial and sequestration of carbon in an oligotrophic, tropical lake. J. Limnol. 73. https://doi.org/10.4081/jlimnol.2014.783

Anderson, N.John., Stedmon, C.A., 2007. The effect of evapoconcentration on dissolved organic carbon concentration and quality in lakes of SW Greenland. Freshw. Biol. 52, 280–289. https://doi.org/10.1111/j.1365-2427.2006.01688.x

Ardiles, V., Alcocer, J., Vilaclara, G., Oseguera, L.A., Velasco, L., 2012. Diatom fluxes in a tropical, oligotrophic lake dominated by large-sized phytoplankton. Hydrobiologia 679, 77–90. https://doi.org/10.1007/s10750-011-0853-7

Armienta, M.A., Vilaclara, G., De la Cruz-Reyna, S., Ramos, S., Ceniceros, N., Cruz, O., Aguayo, A., Arcega-Cabrera, F., 2008. Water chemistry of lakes related to active and inactive Mexican volcanoes. J. Volcanol. Geotherm. Res. 178, 249–258. https://doi.org/10.1016/j.jvolgeores.2008.06.019

Deleted: University

Deleted: Adame, M.F., Alcocer, J., Escobar, E.: Size-fractionated phytoplankton biomass and its implications for the dynamics of an oligotrophic tropical lake. Freshw. Biol. 53, 22–31. https://doi.org/10.1111/j.1365-2427.2007.01864.x , 2008. ... [46]

Armstrong-Altrin, J.S., Madhavaraju, J., Sial, A.N., Kasper-Zubillaga, J.J., Nagarajan, R., Flores-Castro, K., Rodríguez, J.L., 2011. Petrography and stable isotope geochemistry of the cretaceous El Abra Limestones (Actopan), Mexico: Implication on diagenesis. J. Geol. Soc. India 77, 349–359. https://doi.org/10.1007/s12594-011-0042-3

Assayag, N., Jézéquel, D., Ader, M., Viollier, E., Michard, G., Prévot, F., Agrinier, P., 2008. Hydrological budget, carbon sources and biogeochemical processes in Lac Pavin (France): Constraints from δ18O of water and δ13C of dissolved inorganic carbon. Appl. Geochem. 23, 2800–2816. https://doi.org/10.1016/j.apgeochem.2008.04.015

Assayag, N., Rivé, K., Ader, M., Jézéquel, D., Agrinier, P., 2006. Improved method for isotopic and quantitative analysis of dissolved inorganic carbon in natural water samples. Rapid Commun. Mass Spectrom. 20, 2243–2251. https://doi.org/10.1002/rcm.2585

Bade, D.L., Carpenter, S.R., Cole, J.J., Hanson, P.C., Hesslein, R.H., 2004. Controls of δ13C-DIC in lakes: Geochemistry, lake metabolism, and morphometry. Limnol. Oceanogr. 49, 1160–1172. https://doi.org/10.4319/lo.2004.49.4.1160

Bekker, A., Holmden, C., Beukes, N.J., Kenig, F., Eglinton, B., Patterson, W.P., 2008. Fractionation between inorganic and organic carbon during the Lomagundi (2.22–2.1 Ga) carbon isotope excursion. Earth Planet. Sci. Lett. 271, 278–291. https://doi.org/10.1016/j.epsl.2008.04.021

Birgel, D., Meister, P., Lundberg, R., Horath, T.D., Bontognali, T.R.R., Bahniuk, A.M., de Rezende, C.E., Vasconcelos, C., McKenzie, J.A., 2015. Methanogenesis produces strong 13C enrichment in stromatolites of Lagoa Salgada, Brazil: a modern analogue for Palaeo-/Neoproterozoic stromatolites? Geobiology 13, 245–266. https://doi.org/10.1111/gbi.12130

Briones, E.E., Alcocer, J., Cienfuegos, E., Morales, P., 1998. Carbon stable isotopes ratios of pelagic and littoral communities in Alchichica crater-lake, Mexico. Int. J. Salt Lake Res. 7, 345–355. https://doi.org/10.1007/BF02442143

Buchan, A., LeCleir, G.R., Gulvik, C.A., González, J.M., 2014. Master recyclers: features and functions of bacteria associated with phytoplankton blooms. Nat. Rev. Microbiol. 12, 686–698. https://doi.org/10.1038/nrmicro3326

Cadeau, P., Jézéquel, D., Leboulanger, C., Fouilland, E., Le Floc'h, E., Chaduteau, C., Milesi, V., Guélard, J., Sarazin, G., Katz, A., d'Amore, S., Bernard, C., Ader, M., 2020. Carbon isotope evidence for large methane emissions to the Proterozoic atmosphere. Sci. Rep. 10, 18186. https://doi.org/10.1038/s41598-020-75100-x

Cai, C., Li, K., Liu, D., John, C.M., Wang, D., Fu, B., Fakhraee, M., He, H., Feng, L., Jiang, L., 2021. Anaerobic oxidation of methane by Mn oxides in sulfate-poor environments. Geology 49, 761–766. https://doi.org/10.1130/G48553.1

Callieri, C., Coci, M., Corno, G., Macek, M., Modenutti, B., Balseiro, E., Bertoni, R., 2013. Phylogenetic diversity of nonmarine picocyanobacteria. FEMS Microbiol. Ecol. 85, 293–301. https://doi.org/10.1111/1574-6941.12118

Camacho, A., Walter, X.A., Picazo, A., Zopfi, J., 2017. Photoferrotrophy: Remains of an Ancient Photosynthesis in Modern Environments. Front. Microbiol. 08. https://doi.org/10.3389/fmicb.2017.00323

Carrasco-Núñez, G., Ort, M.H., Romero, C., 2007. Evolution and hydrological conditions of a maar volcano (Atexcac crater, Eastern Mexico). J. Volcanol. Geotherm. Res. 159, 179–197. https://doi.org/10.1016/j.jvolgeores.2006.07.001

Chako Tchamabé, B., Carrasco-Núñez, G., Miggins, D.P., Németh, K., 2020. Late Pleistocene to Holocene activity of Alchichica maar volcano, eastern Trans-Mexican Volcanic Belt. J. South Am. Earth Sci. 97, 102404. https://doi.org/10.1016/j.jsames.2019.102404

Cheng, C., Zhang, J., He, Q., Wu, H., Chen, Y., Xie, H., Pavlostathis, S.G., 2021. Exploring simultaneous nitrous oxide and methane sink in wetland sediments under anoxic conditions. Water Res. 194, 116958. https://doi.org/10.1016/j.watres.2021.116958

Close, H.G., Henderson, L.C., 2020. Open-Ocean Minima in δ13C Values of Particulate Organic Carbon in the Lower Euphotic Zone. Front. Mar. Sci. 7, 540165. https://doi.org/10.3389/fmars.2020.540165

Crowe, S.A., Katsev, S., Leslie, K., Sturm, A., Magen, C., Nomosatryo, S., Pack, M.A., Kessler, J.D., Reeburgh, W.S., Roberts, J.A., González, L., Douglas Haffner, G., Mucci, A., Sundby, B., Fowle, D.A., 2011. The methane cycle in ferruginous Lake Matano: Methane cycle in ferruginous Lake Matano. Geobiology 9, 61–78. https://doi.org/10.1111/j.1472-4669.2010.00257.x

Dean, W.E., Gorham, E., 1998. Magnitude and significance of carbon burial in lakes, reservoirs, and peatlands. Geology 26, 535. https://doi.org/10.1130/0091-7613(1998)026<0535:MASOCB>2.3.CO;2

Descolas-Gros, C., Fontungne, M., 1990. Stable carbon isotope fractionation by marine phytoplankton during photosynthesis. Plant Cell Environ. 13, 207–218. https://doi.org/10.1111/j.1365-3040.1990.tb01305.x

Emrich, K., Ehhalt, D.H., Vogel, J.C., 1970. Carbon isotope fractionation during the precipitation of calcium carbonate. Earth Planet. Sci. Lett. 8, 363–371. https://doi.org/10.1016/0012-821X(70)90109-3

Ferrari, L., Orozco-Esquivel, T., Manea, V., Manea, M., 2012. The dynamic history of the Trans-Mexican Volcanic Belt and the Mexico subduction zone. Tectonophysics 522–523, 122–149. https://doi.org/10.1016/j.tecto.2011.09.018

Fogel, M.L., Cifuentes, L.A., 1993. Isotope Fractionation during Primary Production, in: Engel, M.H., Macko, S.A. (Eds.), Organic Geochemistry, Topics in Geobiology. Springer US, Boston, MA, pp. 73–98. https://doi.org/10.1007/978-1-4615-2890-6_3

Fry, B., 2021. 13C/12C fractionation by marine diatoms 13.

Fry, B., Jannasch, H.W., Molyneaux, S.J., Wirsen, C.O., Muramoto, J.A., King, S., 1991. Stable isotope studies of the carbon, nitrogen and sulfur cycles in the Black Sea and the Cariaco Trench. Deep Sea Res. Part Oceanogr. Res. Pap. 38, S1003–S1019. https://doi.org/10.1016/S0198-0149(10)80021-4

Fulton, J.M., Arthur, M.A., Thomas, B., Freeman, K.H., 2018. Pigment carbon and nitrogen isotopic signatures in euxinic basins. Geobiology 16, 429–445. https://doi.org/10.1111/gbi.12285

Furian, S., Martins, E.R.C., Parizotto, T.M., Rezende-Filho, A.T., Victoria, R.L., Barbiero, L., 2013. Chemical diversity and spatial variability in myriad lakes in Nhecolândia in the Pantanal wetlands of Brazil. Limnol. Oceanogr. 58, 2249–2261. https://doi.org/10.4319/lo.2013.58.6.2249

Gérard, E., Ménez, B., Couradeau, E., Moreira, D., Benzerara, K., Tavera, R., López-García, P., 2013. Specific carbonate–microbe interactions in the modern microbialites of Lake Alchichica (Mexico). ISME J. 7, 1997–2009. https://doi.org/10.1038/ismej.2013.81

Gonzales-Partida, E., Barragan-R, R.M., Nieva-G, D., 1993. Analisis geoquimico-isotopico de las especies carbonicas del fluido geotermico de Los Humeros, Puebla, México. Geofis. Int. 32, 299–309.

Gröger, J., Franke, J., Hamer, K., Schulz, H.D., 2009. Quantitative Recovery of Elemental Sulfur and Improved Selectivity in a Chromium-Reducible Sulfur Distillation. Geostand. Geoanalytical Res. 33, 17–27. https://doi.org/10.1111/j.1751-908X.2009.00922.x

Gu, B., Schelske, C.L., Hodell, D.A., 2004. Extreme13C enrichments in a shallow hypereutrophic lake: Implications for carbon cycling. Limnol. Oceanogr. 49, 1152–1159. https://doi.org/10.4319/lo.2004.49.4.1152

Hassan, K.M., 2014. Isotope geochemistry of Swan Lake Basin in the Nebraska Sandhills, USA: Large 13C enrichment in sediment-calcite records. Geochemistry 74, 681–690. https://doi.org/10.1016/j.chemer.2014.03.004

Havig, J.R., Hamilton, T.L., McCormick, M., McClure, B., Sowers, T., Wegter, B., Kump, L.R., 2018. Water column and sediment stable carbon isotope biogeochemistry of permanently redox- stratified Fayetteville Green Lake, New York, U.S.A. Limnol. Oceanogr. 63, 570–587. https://doi.org/10.1002/lno.10649

Havig, J.R., McCormick, M.L., Hamilton, T.L., Kump, L.R., 2015. The behavior of biologically important trace elements across the oxic/euxinic transition of meromictic Fayetteville Green Lake, New York, USA. Geochim. Cosmochim. Acta 165, 389–406. https://doi.org/10.1016/j.gca.2015.06.024

Hayes, J.M., Popp, B.N., Takigiku, R., Johnson, M.W., 1989. An isotopic study of biogeochemical relationships between carbonates and organic carbon in the Greenhorn Formation. Geochim. Cosmochim. Acta 53, 2961–2972. https://doi.org/10.1016/0016-7037(89)90172-5

Henkel, J.V., Dellwig, O., Pollehne, F., Herlemann, D.P.R., Leipe, T., Schulz-Vogt, H.N., 2019. A bacterial isolate from the Black Sea oxidizes sulfide with manganese(IV) oxide. Proc. Natl. Acad. Sci. 116, 12153–12155. https://doi.org/10.1073/pnas.1906000116

Hessen, D.O., Anderson, T.R., 2008. Excess carbon in aquatic organisms and ecosystems: Physiological, ecological, and evolutionary implications. Limnol. Oceanogr. 53, 1685–1696. https://doi.org/10.4319/lo.2008.53.4.1685

Hurley, S.J., Wing, B.A., Jasper, C.E., Hill, N.C., Cameron, J.C., 2021. Carbon isotope evidence for the global physiology of Proterozoic cyanobacteria. Sci. Adv. 7, eabc8998. https://doi.org/10.1126/sciadv.abc8998

Iniesto, M., Moreira, D., Benzerara, K., Muller, E., Bertolino, P., Tavera, R., López- García, P., 2021a. Rapid formation of mature microbialites in Lake Alchichica, Mexico. Environ. Microbiol. Rep. 13, 600–605. https://doi.org/10.1111/1758-2229.12957

Iniesto, M., Moreira, D., Benzerara, K., Reboul, G., Bertolino, P., Tavera, R., López- García, P., 2022. Planktonic microbial communities from microbialite- bearing lakes sampled along a salinity- alkalinity gradient. Limnol. Oceanogr. lno.12233. https://doi.org/10.1002/lno.12233

Iniesto, M., Moreira, D., Reboul, G., Deschamps, P., Benzerara, K., Bertolino, P., Saghaï, A., Tavera, R., López- García, P., 2021b. Core microbial communities of lacustrine microbialites sampled along an alkalinity gradient. Environ. Microbiol. 23, 51–68. https://doi.org/10.1111/1462-2920.15252

Iñiguez, C., Capó- Bauçà, S., Niinemets, Ü., Stoll, H., Aguiló- Nicolau, P., Galmés, J., 2020. Evolutionary trends in RuBisCO kinetics and their co- evolution with CO2 concentrating mechanisms. Plant J. 101, 897–918. https://doi.org/10.1111/tpj.14643

Javoy, M., Pineau, F., Delorme, H., 1986. Carbon and nitrogen isotopes in the mantle. Chem. Geol., Isotopes in Geology—Picciotto Volume 57, 41–62. https://doi.org/10.1016/0009-2541(86)90093-8

Jézéquel, D., Michard, G., Viollier, E., Agrinier, P., Albéric, P., Lopes, F., Abril, G., Bergonzini, L., 2016. Carbon Cycle in a Meromictic Crater Lake: Lake Pavin, France, in: Sime-Ngando, T., Boivin, P., Chapron, E., Jezequel, D., Meybeck, M. (Eds.), Lake Pavin: History, Geology, Biogeochemistry, and Sedimentology of a Deep Meromictic Maar Lake. Springer International Publishing, Cham, pp. 185–203. https://doi.org/10.1007/978-3-319-39961-4_11

Jiao, N., Herndl, G.J., Hansell, D.A., Benner, R., Kattner, G., Wilhelm, S.W., Kirchman, D.L., Weinbauer, M.G., Luo, T., Chen, F., Azam, F., 2010. Microbial production of recalcitrant dissolved organic matter: long-term carbon storage in the global ocean. Nat. Rev. Microbiol. 8, 593–599. https://doi.org/10.1038/nrmicro2386

Karhu, J.A., Holland, H.D., 1996. Carbon isotopes and the rise of atmospheric oxygen. Geology 24, 867. https://doi.org/10.1130/0091-7613(1996)024<0867:CIATRO>2.3.CO;2

Klawonn, I., Van den Wyngaert, S., Parada, A.E., Arandia-Gorostidi, N., Whitehouse, M.J., Grossart, H.-P., Dekas, A.E., 2021. Characterizing the "fungal shunt": Parasitic fungi on diatoms affect carbon flow and bacterial communities in aquatic microbial food webs. Proc. Natl. Acad. Sci. 118, e2102225118. https://doi.org/10.1073/pnas.2102225118

Knossow, N., Blonder, B., Eckert, W., Turchyn, A.V., Antler, G., Kamyshny, A., 2015. Annual sulfur cycle in a warm monomictic lake with sub-millimolar sulfate concentrations. Geochem. Trans. 16, 7. https://doi.org/10.1186/s12932-015-0021-5

Kuntz, L.B., Laakso, T.A., Schrag, D.P., Crowe, S.A., 2015. Modeling the carbon cycle in Lake Matano. Geobiology 13, 454–461. https://doi.org/10.1111/gbi.12141

Lehmann, M.F., Bernasconi, S.M., Barbieri, A., McKenzie, J.A., 2002. Preservation of organic matter and alteration of its carbon and nitrogen isotope composition during simulated and in situ early sedimentary diagenesis. Geochim. Cosmochim. Acta 66, 3573–3584. https://doi.org/10.1016/S0016-7037(02)00968-7

Lehmann, M.F., Bernasconi, S.M., McKenzie, J.A., Barbieri, A., Simona, M., Veronesi, M., 2004. Seasonal variation of the δC and δN of particulate and dissolved carbon and nitrogen in Lake Lugano: Constraints on biogeochemical cycling in a eutrophic lake. Limnol. Oceanogr. 49, 415–429. https://doi.org/10.4319/lo.2004.49.2.0415

Lelli, M., Kretzschmar, T.G., Cabassi, J., Doveri, M., Sanchez-Avila, J.I., Gherardi, F., Magro, G., Norelli, F., 2021. Fluid geochemistry of the Los Humeros geothermal field (LHGF - Puebla, Mexico): New constraints for the conceptual model. Geothermics 90, 101983. https://doi.org/10.1016/j.geothermics.2020.101983

Li, H.-C., Ku, T.-L., 1997. δ13C–δ18C covariance as a paleohydrological indicator for closed-basin lakes. Palaeogeogr. Palaeoclimatol. Palaeoecol. 133, 69–80. https://doi.org/10.1016/S0031-0182(96)00153-8

Lorenz, V., 1986. On the growth of maars and diatremes and its relevance to the formation of tuff rings. Bull. Volcanol. 48, 265–274. https://doi.org/10.1007/BF01081755

Lugo, A., Alcocer, J., Sánchez, Ma. del R., Escobar, E., Macek, M., 2000. Temporal and spatial variation of bacterioplankton abundance in a tropical, warm-monomictic, saline lake: Alchichica, Puebla, Mexico. SIL Proc. 1922-2010 27, 2968–2971. https://doi.org/10.1080/03680770.1998.11898217

Lugo, A., Alcocer, J., Sanchez, M.R., Escobar, E., 1993. Trophic status of tropical lakes indicated by littoral protozoan assemblages. SIL Proc. 1922-2010 25, 441–443. https://doi.org/10.1080/03680770.1992.11900159

Lyons, T.W., Reinhard, C.T., Planavsky, N.J., 2014. The rise of oxygen in Earth's early ocean and atmosphere. Nature 506, 307–315. https://doi.org/10.1038/nature13068

Macek, M., Medina, X.S., Picazo, A., Peštová, D., Reyes, F.B., Hernández, J.R.M., Alcocer, J., Ibarra, M.M., Camacho, A., 2020. Spirostomum teres: A Long Term Study of an Anoxic-Hypolimnion Population Feeding upon Photosynthesizing Microorganisms. Acta Protozool. 59, 13–38. https://doi.org/10.4467/16890027AP.20.002.12158

Mason, E., Edmonds, M., Turchyn, A.V., 2017. Remobilization of crustal carbon may dominate volcanic arc emissions. Science 357, 290–294. https://doi.org/10.1126/science.aan5049

Mendonça, R., Müller, R.A., Clow, D., Verpoorter, C., Raymond, P., Tranvik, L.J., Sobek, S., 2017. Organic carbon burial in global lakes and reservoirs. Nat. Commun. 8, 1694. https://doi.org/10.1038/s41467-017-01789-6

Mercedes-Martín, R., Ayora, C., Tritlla, J., Sánchez-Román, M., 2019. The hydrochemical evolution of alkaline volcanic lakes: a model to understand the South Atlantic Pre-salt mineral assemblages. Earth-Sci. Rev. 198, 102938. https://doi.org/10.1016/j.earscirev.2019.102938

Milesi, V.P., Debure, M., Marty, N.C.M., Capano, M., Jézéquel, D., Steefel, C., Rouchon, V., Albéric, P., Bard, E., Sarazin, G., Guyot, F., Virgone, A., Gaucher, É.C., Ader, M., 2020. Early Diagenesis of Lacustrine Carbonates in Volcanic Settings: The Role of Magmatic CO_2 (Lake Dziani Dzaha, Mayotte, Indian Ocean). ACS Earth Space Chem. 4, 363–378. https://doi.org/10.1021/acsearthspacechem.9b00279

Mook, W.G., Bommerson, J.C., Staverman, W.H., 1974. Carbon isotope fractionation between dissolved bicarbonate and gaseous carbon dioxide. Earth Planet. Sci. Lett. 22, 169–176. https://doi.org/10.1016/0012-821X(74)90078-8

Mulholland, P.J., Elwood, J.W., 1982. The role of lake and reservoir sediments as sinks in the perturbed global carbon cycle. Tellus 34, 490–499. https://doi.org/10.1111/j.2153-3490.1982.tb01837.x

O'Leary, M.H., 1988. Carbon Isotopes in Photosynthesis. BioScience 38, 328–336. https://doi.org/10.2307/1310735

Paneth, P., O'Leary, M.H., 1985. Carbon isotope effect on dehydration of bicarbonate ion catalyzed by carbonic anhydrase. Biochemistry 24, 5143–5147. https://doi.org/10.1021/bi00340a028

Pardue, J.W., Scalan, R.S., Van Baalen, C., Parker, P.L., 1976. Maximum carbon isotope fractionation in photosynthesis by blue-green algae and a green alga. Geochim. Cosmochim. Acta 40, 309–312. https://doi.org/10.1016/0016-7037(76)90208-8

Pecoraino, G., D'Alessandro, W., Inguaggiato, S., 2015. The Other Side of the Coin: Geochemistry of Alkaline Lakes in Volcanic Areas, in: Rouwet, D., Christenson, B., Tassi, F., Vandemeulebrouck, J. (Eds.), Volcanic Lakes, Advances in Volcanology. Springer Berlin Heidelberg, Berlin, Heidelberg, pp. 219–237. https://doi.org/10.1007/978-3-642-36833-2_9

Peiffer, L., Carrasco-Núñez, G., Mazot, A., Villanueva-Estrada, R.E., Inguaggiato, C., Bernard Romero, R., Rocha Miller, R., Hernández Rojas, J., 2018. Soil degassing at the Los Humeros geothermal field (Mexico). J. Volcanol. Geotherm. Res. 356, 163–174. https://doi.org/10.1016/j.jvolgeores.2018.03.001

Petrash, D.A., Steenbergen, I.M., Valero, A., Meador, T.B., Pačes, T., Thomazo, C., 2022. Aqueous system-level processes and prokaryote assemblages in the ferruginous and sulfate-rich bottom waters of a post-mining lake. Biogeosciences 19, 1723–1751. https://doi.org/10.5194/bg-19-1723-2022

Pimenov, N.V., Lunina, O.N., Prusakova, T.S., Rusanov, I.I., Ivanov, M.V., 2008. Biological fractionation of stable carbon isotopes at the aerobic/anaerobic water interface of meromictic water bodies. Microbiology 77, 751–759. https://doi.org/10.1134/S0026261708060131

Posth, N.R., Bristow, L.A., Cox, R.P., Habicht, K.S., Danza, F., Tonolla, M., Frigaard, N. - U., Canfield, D.E., 2017. Carbon isotope fractionation by anoxygenic phototrophic bacteria in euxinic Lake Cadagno. Geobiology 15, 798–816. https://doi.org/10.1111/gbi.12254

Rendon-Lopez, M.J., 2008. Limnologia fisica del lago crater los Espinos, Municipio de Jiménez Michoacan.

Ridgwell, A., Arndt, S., 2015. Chapter 1 - Why Dissolved Organics Matter: DOC in Ancient Oceans and Past Climate Change, in: Hansell, D.A., Carlson, C.A. (Eds.), Biogeochemistry of Marine Dissolved Organic Matter (Second Edition). Academic Press, Boston, pp. 1–20. https://doi.org/10.1016/B978-0-12-405940-5.00001-7

Sackett, W.M., Eckelmann, W.R., Bender, M.L., Bé, A.W.H., 1965. Temperature Dependence of Carbon Isotope Composition in Marine Plankton and Sediments. Science 148, 235–237. https://doi.org/10.1126/science.148.3667.235

Saghaï, A., Zivanovic, Y., Moreira, D., Benzerara, K., Bertolino, P., Ragon, M., Tavera, R., López-Archilla, A.I., López-García, P., 2016. Comparative metagenomics unveils functions and genome features of microbialite-associated communities along a depth gradient: Comparative metagenomics of microbialites from Lake Alchichica. Environ. Microbiol. 18, 4990–5004. https://doi.org/10.1111/1462-2920.13456

Saini, J.S., Hassler, C., Cable, R., Fourquez, M., Danza, F., Roman, S., Tonolla, M., Storelli, N., Jacquet, S., Zdobnov, E.M., Duhaime, M.B., 2021. Microbial loop of a Proterozoic ocean analogue (preprint). Microbiology. https://doi.org/10.1101/2021.08.17.456685

Satkoski, A.M., Beukes, N.J., Li, W., Beard, B.L., Johnson, C.M., 2015. A redox-stratified ocean 3.2 billion years ago. Earth Planet. Sci. Lett. 430, 43–53. https://doi.org/10.1016/j.epsl.2015.08.007

Schidlowski, M., 2001. Carbon isotopes as biogeochemical recorders of life over 3.8 Ga of Earth history: evolution of a concept. Precambrian Res. 106, 117–134. https://doi.org/10.1016/S0301-9268(00)00128-5

Schiff, S.L., Tsuji, J.M., Wu, L., Venkiteswaran, J.J., Molot, L.A., Elgood, R.J., Paterson, M.J., Neufeld, J.D., 2017. Millions of Boreal Shield Lakes can be used to Probe Archaean Ocean Biogeochemistry. Sci. Rep. 7, 46708. https://doi.org/10.1038/srep46708

Siebe, C., Guilbaud, M.-N., Salinas, S., Chédeville-Monzo, C., 2012. Eruption of Alberca de los Espinos tuff cone causes transgression of Zacapu lake ca. 25,000 yr BP in Michoacán, México. Presented at the IAS 4IMC Conference, Auckland, New Zeland, pp. 74–75.

Siebe, C., Guilbaud, M.-N., Salinas, S., Kshirsagar, P., Chevrel, M.O., Jiménez, A.H., Godínez, L., 2014. Monogenetic volcanism of the Michoacán-Guanajuato Volcanic Field: Maar craters of the Zacapu basin and domes, shields, and scoria cones of the Tarascan highlands (Paracho-Paricutin region). Presented at the Pre-meeting field guide for the 5th international Maar Conference, Querétaro, México, pp. 1–37.

Sigala, I., Caballero, M., Correa-Metrio, A., Lozano-García, S., Vázquez, G., Pérez, L., Zawisza, E., 2017. Basic limnology of 30 continental waterbodies of the Transmexican Volcanic Belt across climatic and environmental gradients. Bol. Soc. Geológica Mex. 69, 313–370. https://doi.org/10.18268/BSGM2017v69n2a3

Silva Aguilera, R.A., 2019. Analisis del descenso del nivel de agua del lago Alchichica, Puebla, México 120.

Sirevag, R., Buchanan, B.B., Berry, J.A., Troughton, J.H., 1977. Mechanisms of C02 Fixation in Bacterial Photosynthesis Studied by the Carbon Isotope Fractionation Technique. Arch Microbiol 112, 4.

Sobek, S., Durisch-Kaiser, E., Zurbrügg, R., Wongfun, N., Wessels, M., Pasche, N., Wehrli, B., 2009. Organic carbon burial efficiency in lake sediments controlled by oxygen exposure time and sediment source. Limnol. Oceanogr. 54, 2243–2254. https://doi.org/10.4319/lo.2009.54.6.2243

Soetaert, K., Hofmann, A.F., Middelburg, J.J., Meysman, F.J.R., Greenwood, J., 2007. The effect of biogeochemical processes on pH. Mar. Chem. 105, 30–51. https://doi.org/10.1016/j.marchem.2006.12.012

Talbot, M.R., 1990. A review of the palaeohydrological interpretation of carbon and oxygen isotopic ratios in primary lacustrine carbonates. Chem. Geol. Isot. Geosci. Sect. 80, 261–279. https://doi.org/10.1016/0168-9622(90)90009-2

Thomas, P.J., Boller, A.J., Satagopan, S., Tabita, F.R., Cavanaugh, C.M., Scott, K.M., 2019. Isotope discrimination by form IC RubisCO from *Ralstonia eutropha* and *Rhodobacter sphaeroides* , metabolically versatile members of ‘ *Proteobacteria* ’ from aquatic and soil habitats. Environ. Microbiol. 21, 72–80. https://doi.org/10.1111/1462-2920.14423

Ussiri, D.A.N., Lal, R., 2017. Carbon Sequestration for Climate Change Mitigation and Adaptation. Springer International Publishing, Cham. https://doi.org/10.1007/978-3-319-53845-7

Van Mooy, B.A.S., Keil, R.G., Devol, A.H., 2002. Impact of suboxia on sinking particulate organic carbon: Enhanced carbon flux and preferential degradation of amino acids via denitrification. Geochim. Cosmochim. Acta 66, 457–465. https://doi.org/10.1016/S0016-7037(01)00787-6

Vilaclara, G., Chávez, M., Lugo, A., González, H., Gaytán, M., 1993. Comparative description of crater-lakes basic chemistry in Puebla State, Mexico. SIL Proc. 1922-2010 25, 435–440. https://doi.org/10.1080/03680770.1992.11900158

Vliet, D.M., Meijenfeldt, F.A.B., Dutilh, B.E., Villanueva, L., Sinninghe Damsté, J.S., Stams, A.J.M., Sánchez-Andrea, I., 2021. The bacterial sulfur cycle in expanding dysoxic and euxinic marine waters. Environ. Microbiol. 23, 2834–2857. https://doi.org/10.1111/1462-2920.15265

Wang, S., Yeager, K.M., Lu, W., 2016. Carbon isotope fractionation in phytoplankton as a potential proxy for pH rather than for [CO2(aq)]: Observations from a carbonate lake. Limnol. Oceanogr. 61, 1259–1270. https://doi.org/10.1002/lno.10289

Werne, J.P., Hollander, D.J., 2004. Balancing supply and demand: controls on carbon isotope fractionation in the Cariaco Basin (Venezuela) Younger Dryas to present. Mar. Chem. 92, 275–293. https://doi.org/10.1016/j.marchem.2004.06.031

Whiticar, M.J., Faber, E., Schoell, M., 1986. Biogenic methane formation in marine and freshwater environments: CO2 reduction vs. acetate fermentation—Isotope evidence. Geochim. Cosmochim. Acta 50, 693–709. https://doi.org/10.1016/0016-7037(86)90346-7

Williams, P.M., Gordon, L.I., 1970. Carbon-13: carbon-12 ratios in dissolved and particulate organic matter in the sea. Deep Sea Res. Oceanogr. Abstr. 17, 19–27. https://doi.org/10.1016/0011-7471(70)90085-9

Wittkop, C., Teranes, J., Lubenow, B., Dean, W.E., 2014. Carbon- and oxygen-stable isotopic signatures of methanogenesis, temperature, and water column stratification in Holocene siderite varves. Chem. Geol. 389, 153–166. https://doi.org/10.1016/j.chemgeo.2014.09.016

Zeyen, N., Benzerara, K., Beyssac, O., Daval, D., Muller, E., Thomazo, C., Tavera, R., López-García, P., Moreira, D., Duprat, E., 2021. Integrative analysis of the mineralogical and chemical composition of modern microbialites from ten Mexican lakes: What do we learn about their formation? Geochim. Cosmochim. Acta 305, 148–184. https://doi.org/10.1016/j.gca.2021.04.030

Zohary, T., Erez, J., Gophen, M., Berman-Frank, I., Stiller, M., 1994. Seasonality of stable carbon isotopes within the pelagic food web of Lake Kinneret. Limnol. Oceanogr. 39, 1030–1043. https://doi.org/10.4319/lo.1994.39.5.1030

Zyakun, A.M., Lunina, O.N., Prusakova, T.S., Pimenov, N.V., Ivanov, M.V., 2009. Fractionation of stable carbon isotopes by photoautotrophically growing anoxygenic purple and green sulfur bacteria. Microbiology 78, 757–768. https://doi.org/10.1134/S0026261709060137

Page 3: [1] Deleted Rob Havas 12/16/22 3:28:00 PM

Page Break

1.

Page 3: [2] Deleted Rob Havas 12/16/22 3:28:00 PM

Here, the inter-comparison via the same methodology of four redox-stratified lakes of the same type (tropical alkaline volcanic crater-lakes) but with distinct solution chemistries and microbial diversities (Zeyen et al., 2021; Iniesto et al., in press), allows to assess the effects of specific physico-chemical and biological parameters on the C cycle. Thus, we present the main biogeochemical reactions occurring in the water columns (e.g. oxygenic/anoxygenic photosynthesis or methanogenesis) and how they are recorded (or not) in surficial sediments. Then, we shed a new light on the microbial cycling of DOC and how the analysis of its isotopes can provide deeper insights into microbial processes and overall C cycle dynamics in stratified water columns. Finally, we discuss the possible implications of DOC for paleoclimate reconstruction and the interpretation of the sedimentary C isotopes record.

Page 5: [3] Deleted Rob Havas 12/16/22 3:28:00 PM

Lake	General location	Sampling location	Elevation

Page 5: [4] Moved to page 6 (Move #5) Rob Havas 12/16/22 3:28:00 PM

Alchichica	Serdan Oriental Basin, eastern TMVB	19°24'51.5" N; 097°24'09.9" W	2320
Atexcac	Serdan Oriental Basin, eastern TMVB	19°20'2.2'' N; 097°26'59.3'' W	2360
La Preciosa	Serdan Oriental Basin, eastern TMVB	19°22'18.1'' N; 097°23'14.4'' W	2330
La Alberca de los Espinos	Zacapu Basin, MGVF, central TMVB	19°54'23.9'' N; 101°46'07.8'' W	1985

Page 5: [5] Deleted Rob Havas 12/16/22 3:28:00 PM

Lake	Lake Basement	Age	Max Depth (m)	Alkalinity (mmoles/L)	Salinity (psu)	pH

Page 5: [6] Moved to page 6 (Move #6) Rob Havas 12/16/22 3:28:00 PM

Alchichica	limestone, basalts	6-13 ± 5-6 ka	63	~35	7.9	9.22
Atexcac	limestone, andesites, basalts	330 ± 80 ka	39	~26	7.4	8.85
La Preciosa	limestone, basalts	Pleistocene	46	~13.5	1.15	9.01

La Alberca de los Espinos	andesite xenoliths	25 ± 2 ka	30	~7	0.6	9.14

Page 5: [7] Formatted **Rob Havas** **12/16/22 3:28:00 PM**

Outline numbered + Level: 2 + Numbering Style: 1, 2, 3, … + Start at: 1 + Alignment: Left + Aligned at: 0" + Indent at: 0.25"

Page 5: [8] Deleted **Rob Havas** **12/16/22 3:28:00 PM**

For analyses of dissolved inorganic and organic carbon (DIC, DOC), major, minor and trace ions, between 1.5 and 5 L of lake water were filtered at 0.22 μm with Filtropur S filters that were pre-rinsed with the lake water.

Page 7: [9] Deleted **Rob Havas** **12/16/22 3:28:00 PM**

Dissolved organic carbon (DOC) concentrations and isotope measurements

Samples of filtered solutions were first acidified to a pH of about 1-2 in order to degas all the DIC and preserve the DOC only. DOC concentrations were measured with a Vario TOC at the Biogéosciences Laboratory calibrated with a range of potassium hydrogen phthalate (Acros®) solutions. Before isotopic analyses, DOC concentration of the samples was adjusted to match our international standards at 5 ppm (USGS 40 glutamic acid and USGS 62 caffeine). Isotopic compositions were measured at the Biogéosciences Laboratory using an IsoTOC (running under He-continuous flow) coupled with an IsoPrime stable isotope ratio mass spectrometer (IRMS; Isoprime, Manchester, UK). Samples were stirred with a magnetic bar and flushed with He before injection of 1 mL sample aliquots (repeated 3 times). DOC is then transformed into gaseous CO_2 by combustion at about 850 °C, quantitatively oxidized by copper oxides and separated from other combustion products in a reduction column and water condensers. Finally, it is transferred to the IRMS via an open split device. In order to avoid a significant memory effect between consecutive analyses, samples were separated by six aliquots of deionized water and their first aliquot was discarded from the isotopic calculations. Average reproducibility of $\delta^{13}C_{DOC}$ on standards and samples was 1 and 0.5 ‰ (1SD), respectively. Average reproducibility for sample [DOC] measurements was on average 0.3 mM.

Page 9: [10] Deleted **Rob Havas** **12/16/22 3:28:00 PM**

3). $\delta^{13}C_{POC}$ increased from -26.5 ‰ in the top 30 meters to -24.1 ‰ at 55 m in depth. Dissolved organic carbon (DOC) represented about 5% of total carbon, with concentrations around 0.5 mM throughout the water column except in the hypolimnion where it reached up to 5.4 mM. Its isotopic composition varied from -29.3 to -25.1 ‰, with maximum values found in the hypolimnion (Fig. 4).

The sum and weighted average of total carbon concentrations and isotopic compositions were calculated. The total carbon concentration depth profile roughly follows that of DOC, while $\delta^{13}C_{total}$ is roughly comprised between 2 and 0

‰ through the water column, except in the lower part of the hypolimnion where it decreases down to -2.4 ‰ on average (Figs. 3, 4; Table 2).

Total dissolved phosphorus (TDP) is stable down to 20 m where it shows a marked increase from 0.37 to 1.56 µM at 30 m and then progressively increases up to 3.20 µM at the bottom of the lake (Fig. 5, Table S1). Sulfate concentration slightly decreases from ~11.8 to 11.7 mM between the surface and 30 m and then increases to 12.2 mM at 60 m. Dissolved Cl followed a similar profile with values around 107 mM at the surface decreasing below 106 mM at 30 m and increasing back to 111 mM at 60 m (

Page 10: [11] Deleted	**Rob Havas**	**12/16/22 3:28:00 PM**

high (

Page 10: [11] Deleted	**Rob Havas**	**12/16/22 3:28:00 PM**

high (

Page 10: [11] Deleted	**Rob Havas**	**12/16/22 3:28:00 PM**

high (

Page 10: [11] Deleted	**Rob Havas**	**12/16/22 3:28:00 PM**

high (

Page 10: [11] Deleted	**Rob Havas**	**12/16/22 3:28:00 PM**

high (

Page 10: [11] Deleted	**Rob Havas**	**12/16/22 3:28:00 PM**

high (

Page 10: [11] Deleted	**Rob Havas**	**12/16/22 3:28:00 PM**

high (

Page 10: [11] Deleted	**Rob Havas**	**12/16/22 3:28:00 PM**

high (

Page 10: [11] Deleted	**Rob Havas**	**12/16/22 3:28:00 PM**

high (

Page 10: [11] Deleted	**Rob Havas**	**12/16/22 3:28:00 PM**

high (

Page 10: [11] Deleted	Rob Havas	12/16/22 3:28:00 PM

high (

Page 10: [11] Deleted	Rob Havas	12/16/22 3:28:00 PM

high (

Page 10: [11] Deleted	Rob Havas	12/16/22 3:28:00 PM

high (

Page 10: [11] Deleted	Rob Havas	12/16/22 3:28:00 PM

high (

Page 10: [11] Deleted	Rob Havas	12/16/22 3:28:00 PM

high (

Page 10: [12] Deleted	Rob Havas	12/16/22 3:28:00 PM

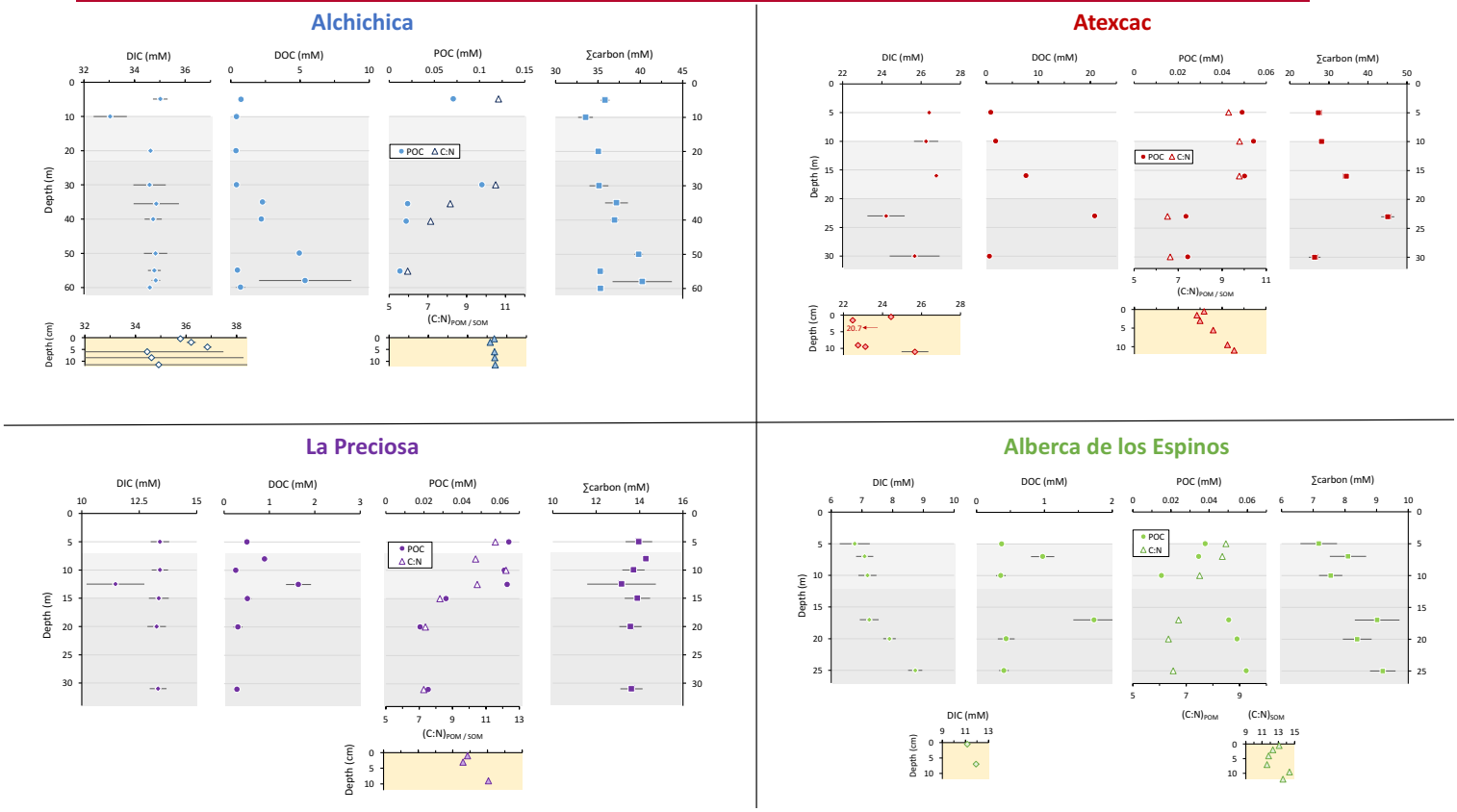

Figure 3. Concentrations in mmoles/L of DIC, DOC, POC and sum of all three reservoirs, C:N molar ratios of POM as a function of depth in the water columns, as well as DIC concentrations in the surficial sediment porewaters and C:N molar ratios of sedimentary OM. Porewaters from La Preciosa's 2016 core were not retrieved.

Page 10: [12] Deleted	Rob Havas	12/16/22 3:28:00 PM

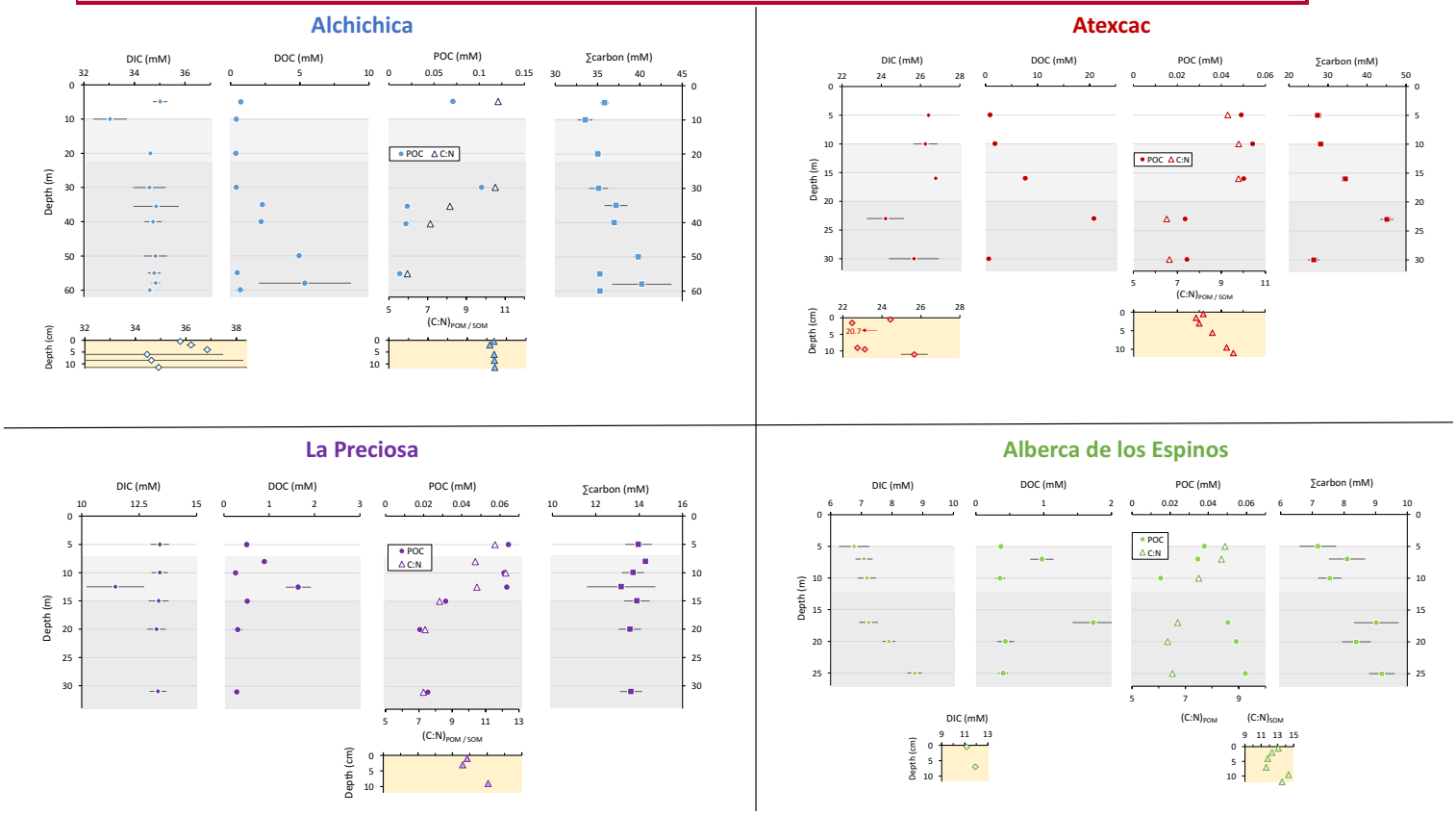

Figure 3. Concentrations in mmoles/L of DIC, DOC, POC and sum of all three reservoirs, C:N molar ratios of POM as a function of depth in the water columns, as well as DIC concentrations in the surficial sediment porewaters and C:N molar ratios of sedimentary OM. Porewaters from La Preciosa's 2016 core were not retrieved.

Page 10: [12] Deleted	Rob Havas	12/16/22 3:28:00 PM

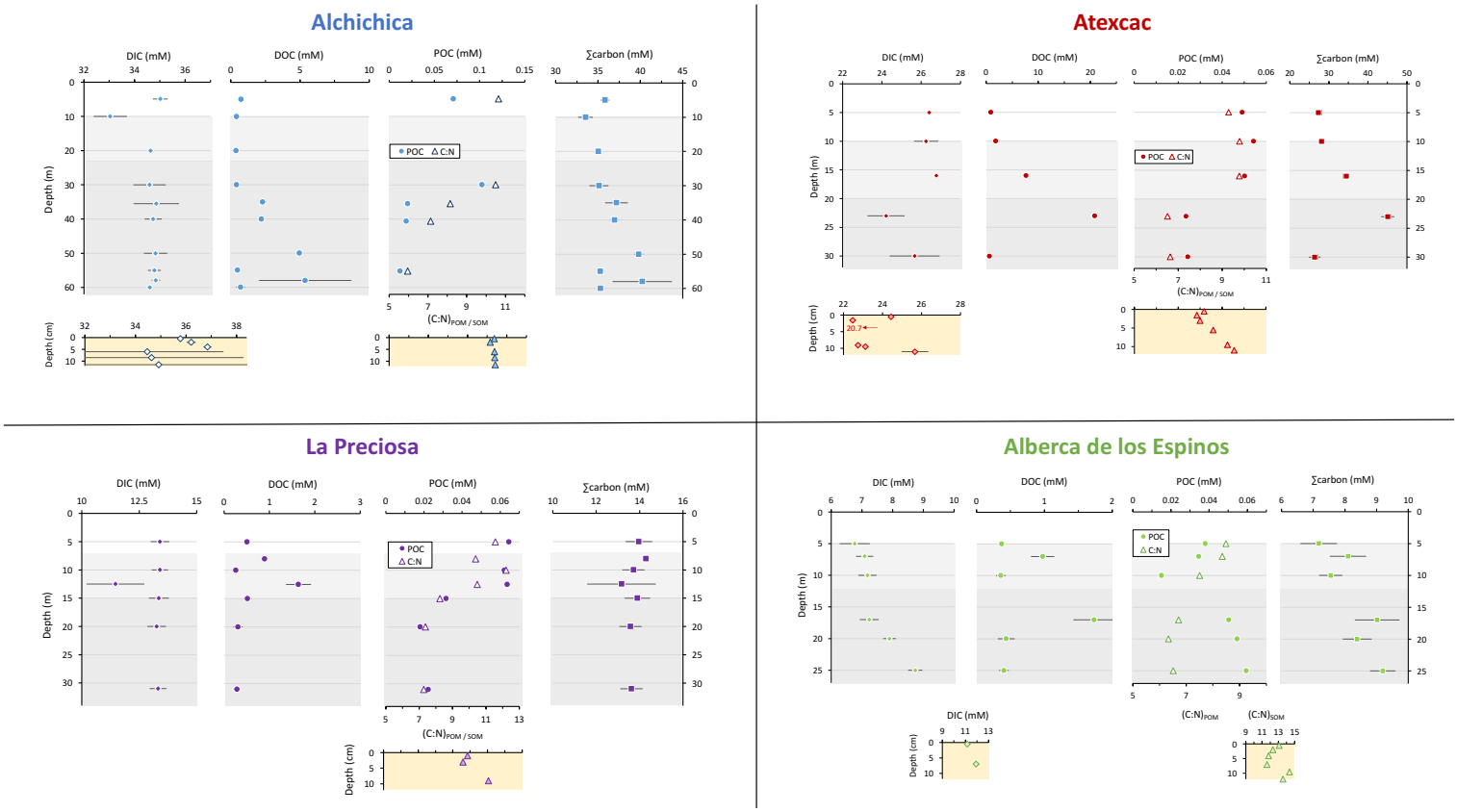

Figure 3. Concentrations in mmoles/L of DIC, DOC, POC and sum of all three reservoirs, C:N molar ratios of POM as a function of depth in the water columns, as well as DIC concentrations in the surficial sediment porewaters and C:N molar ratios of sedimentary OM. Porewaters from La Preciosa's 2016 core were not retrieved.

Page 10: [12] Deleted	Rob Havas	12/16/22 3:28:00 PM

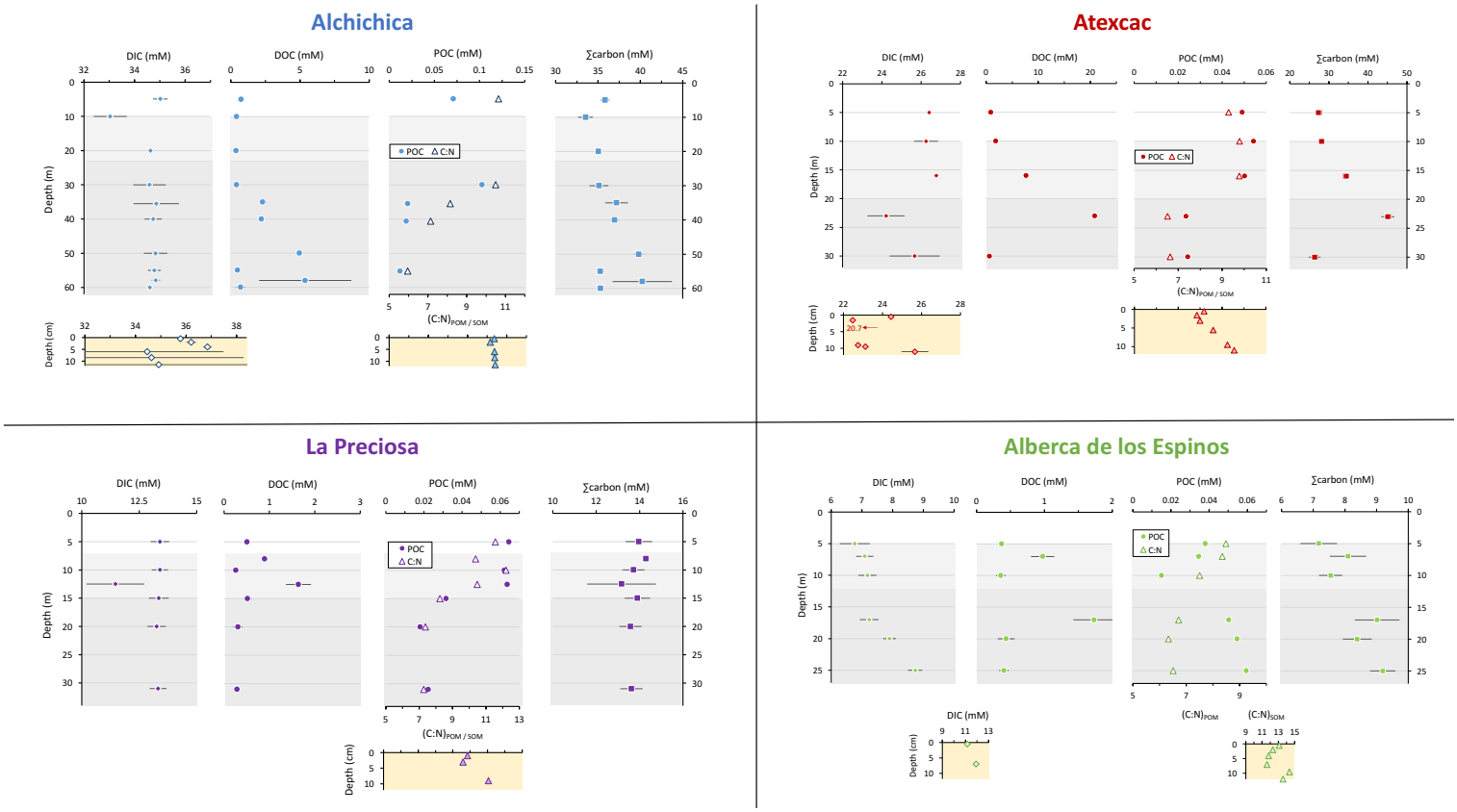

Figure 3. Concentrations in mmoles/L of DIC, DOC, POC and sum of all three reservoirs, C:N molar ratios of POM as a function of depth in the water columns, as well as DIC concentrations in the surficial sediment porewaters and C:N molar ratios of sedimentary OM. Porewaters from La Preciosa's 2016 core were not retrieved.

Page 10: [12] Deleted	Rob Havas	12/16/22 3:28:00 PM

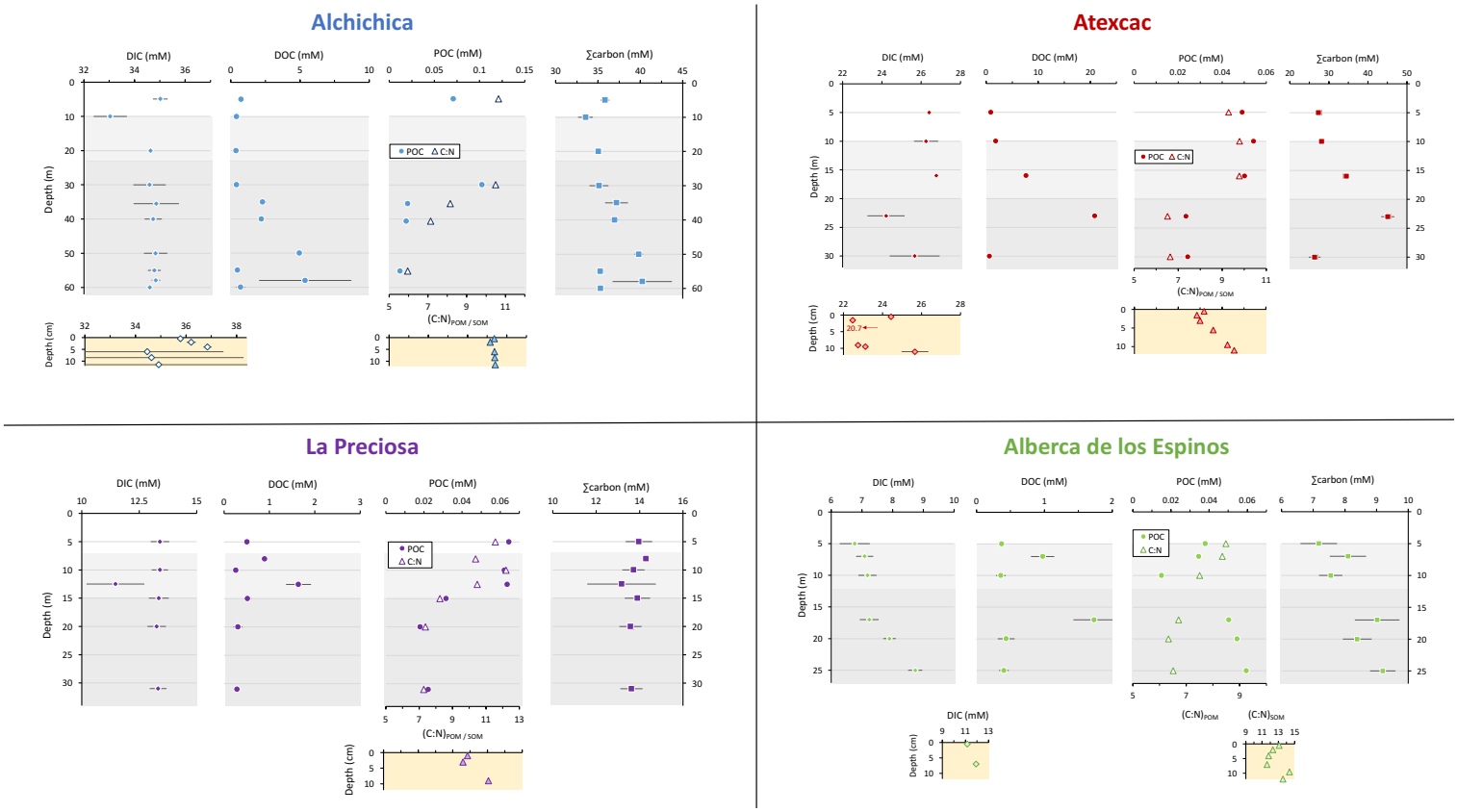

Figure 3. Concentrations in mmoles/L of DIC, DOC, POC and sum of all three reservoirs, C:N molar ratios of POM as a function of depth in the water columns, as well as DIC concentrations in the surficial sediment porewaters and C:N molar ratios of sedimentary OM. Porewaters from La Preciosa's 2016 core were not retrieved.

Page 10: [12] Deleted	Rob Havas	12/16/22 3:28:00 PM

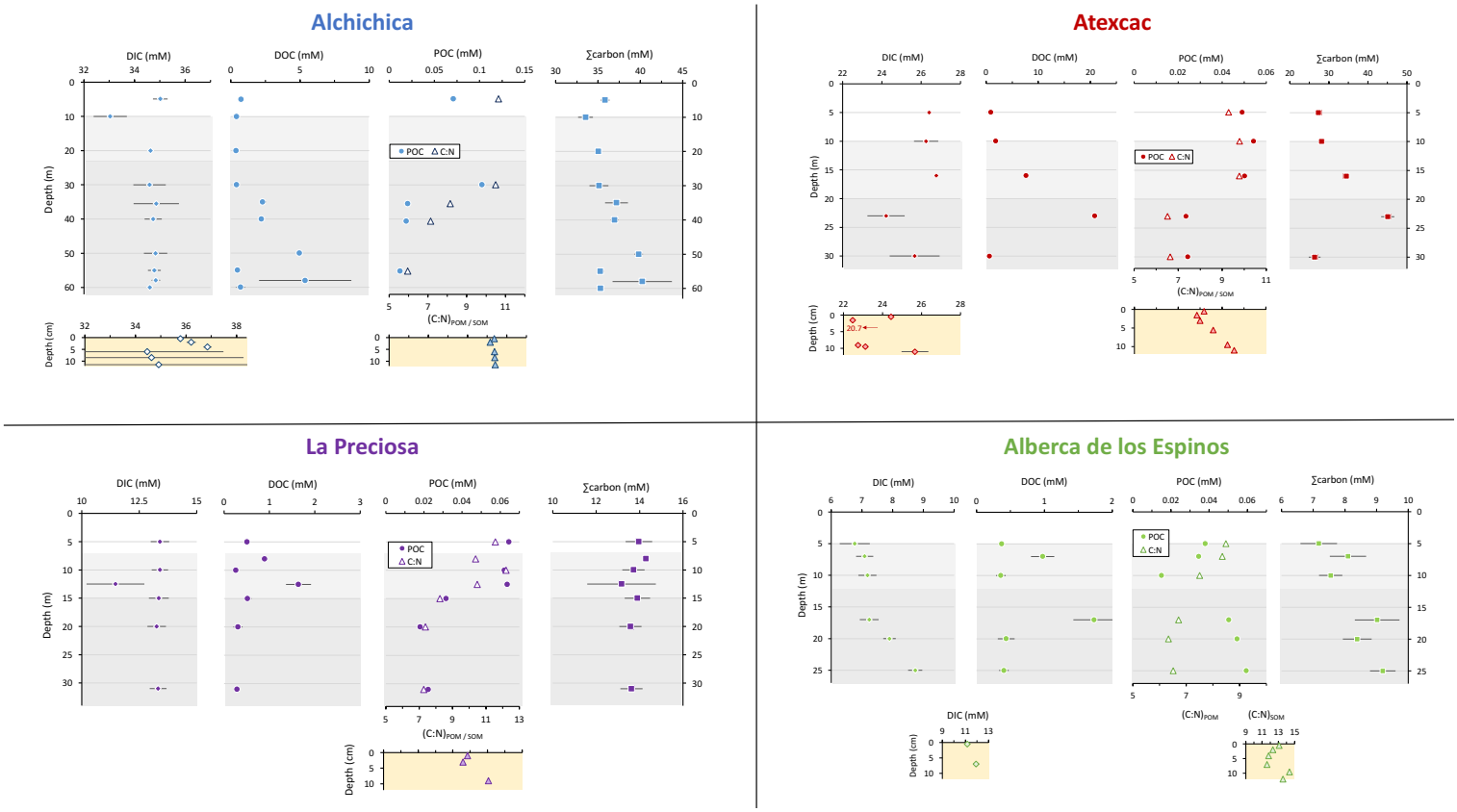

Figure 3. Concentrations in mmoles/L of DIC, DOC, POC and sum of all three reservoirs, C:N molar ratios of POM as a function of depth in the water columns, as well as DIC concentrations in the surficial sediment porewaters and C:N molar ratios of sedimentary OM. Porewaters from La Preciosa's 2016 core were not retrieved.

Page 10: [12] Deleted	Rob Havas	12/16/22 3:28:00 PM

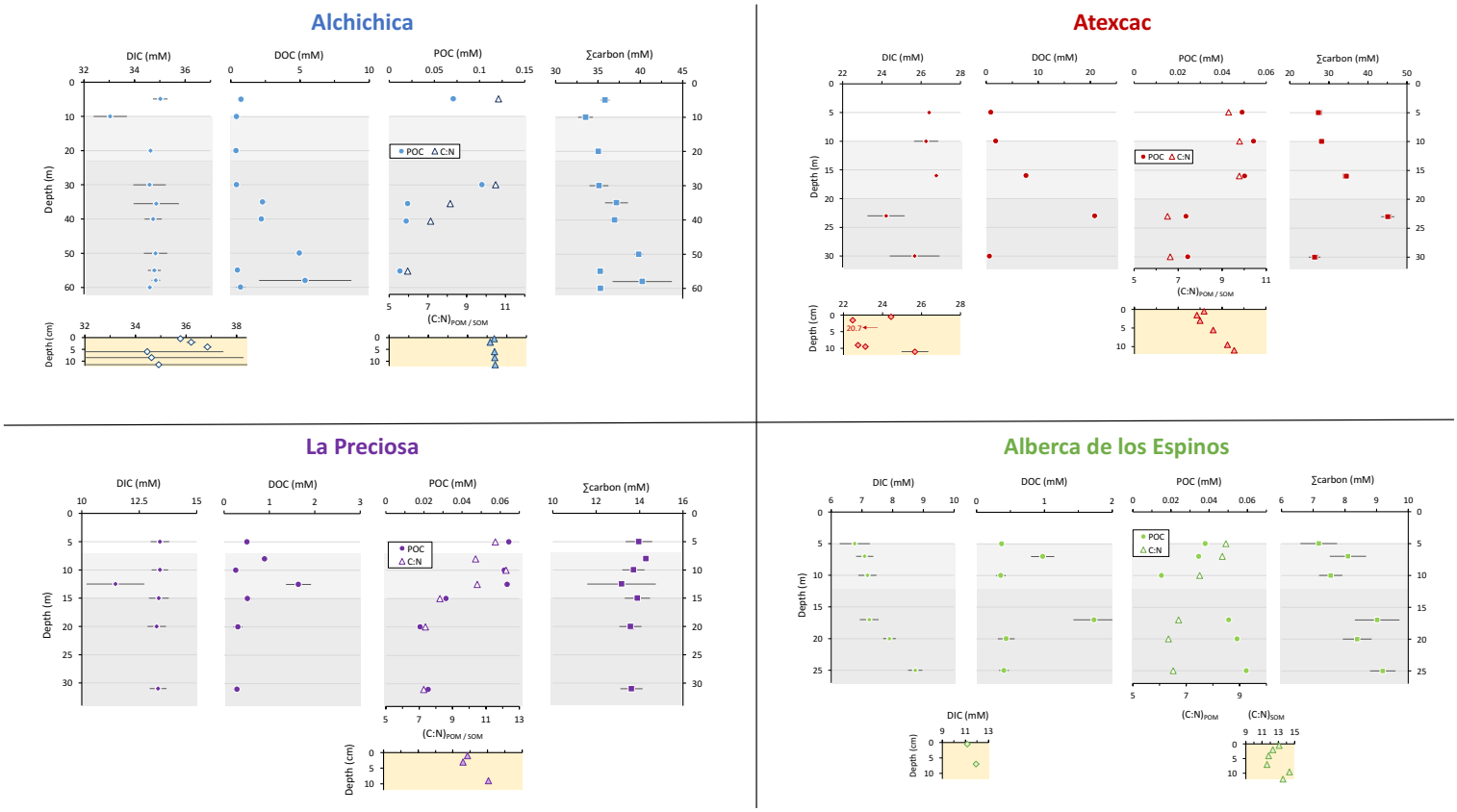

Figure 3. Concentrations in mmoles/L of DIC, DOC, POC and sum of all three reservoirs, C:N molar ratios of POM as a function of depth in the water columns, as well as DIC concentrations in the surficial sediment porewaters and C:N molar ratios of sedimentary OM. Porewaters from La Preciosa's 2016 core were not retrieved.

Page 10: [12] Deleted	Rob Havas	12/16/22 3:28:00 PM

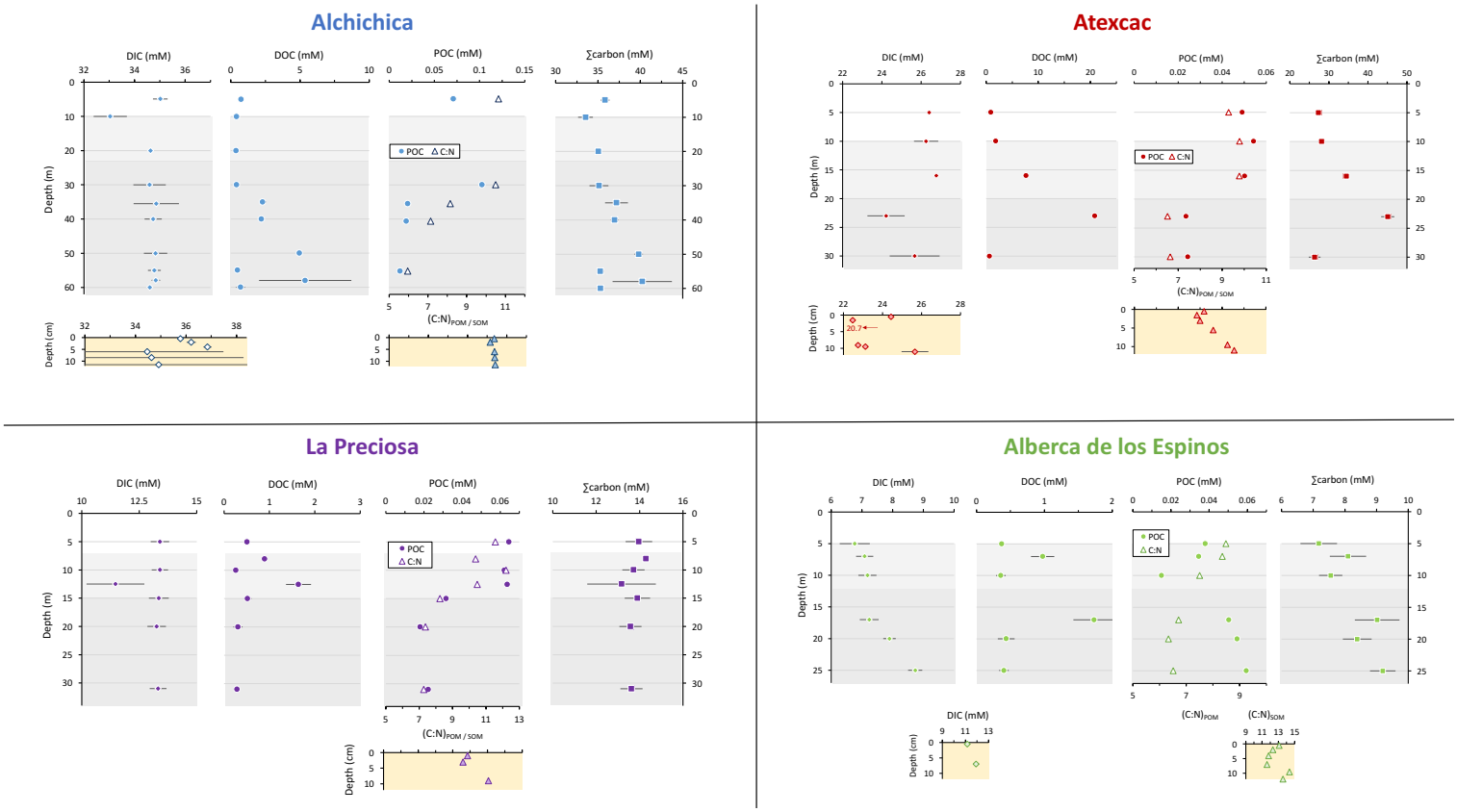

Figure 3. Concentrations in mmoles/L of DIC, DOC, POC and sum of all three reservoirs, C:N molar ratios of POM as a function of depth in the water columns, as well as DIC concentrations in the surficial sediment porewaters and C:N molar ratios of sedimentary OM. Porewaters from La Preciosa's 2016 core were not retrieved.

Page 10: [12] Deleted	Rob Havas	12/16/22 3:28:00 PM

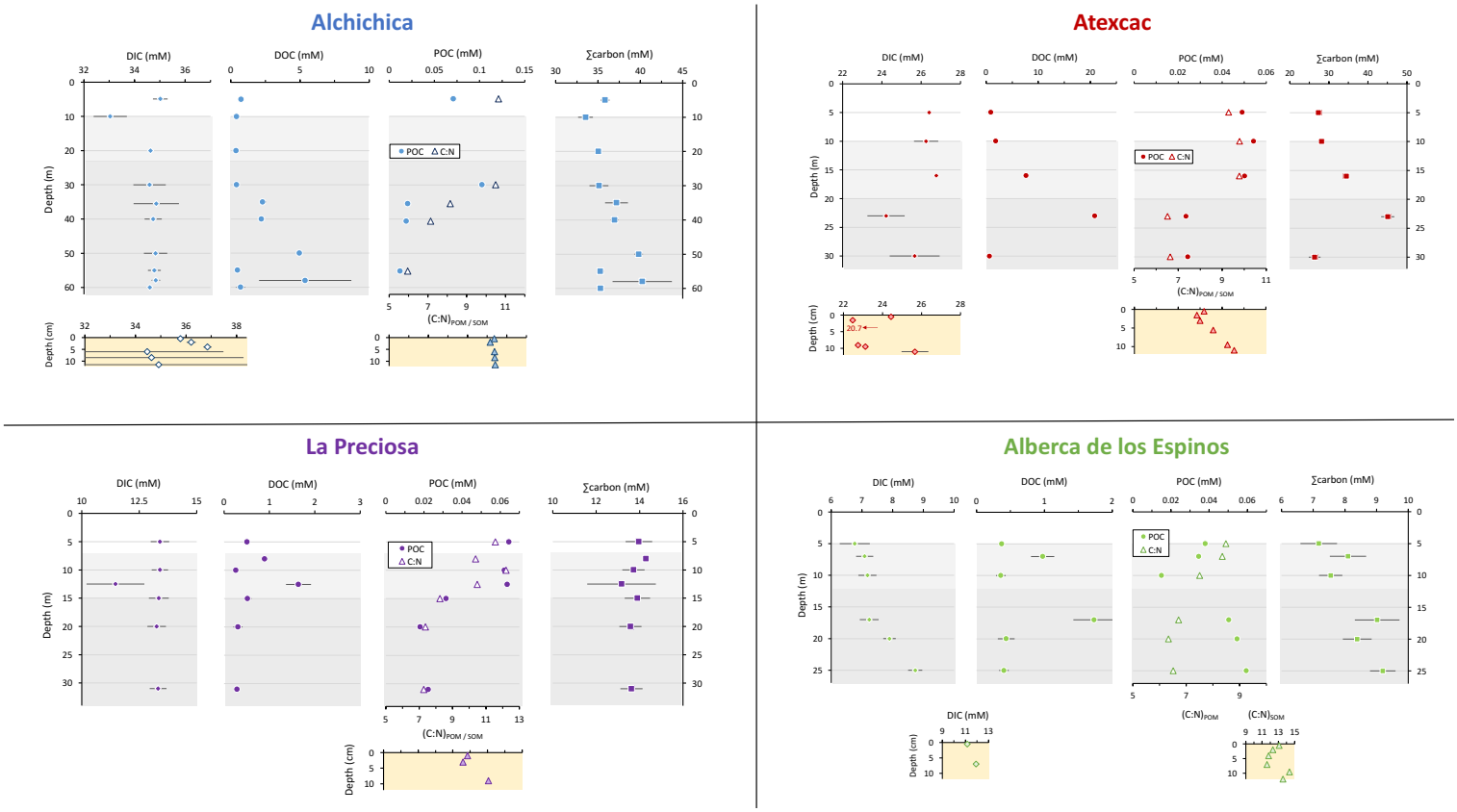

Figure 3. Concentrations in mmoles/L of DIC, DOC, POC and sum of all three reservoirs, C:N molar ratios of POM as a function of depth in the water columns, as well as DIC concentrations in the surficial sediment porewaters and C:N molar ratios of sedimentary OM. Porewaters from La Preciosa's 2016 core were not retrieved.

Page 10: [12] Deleted	Rob Havas	12/16/22 3:28:00 PM

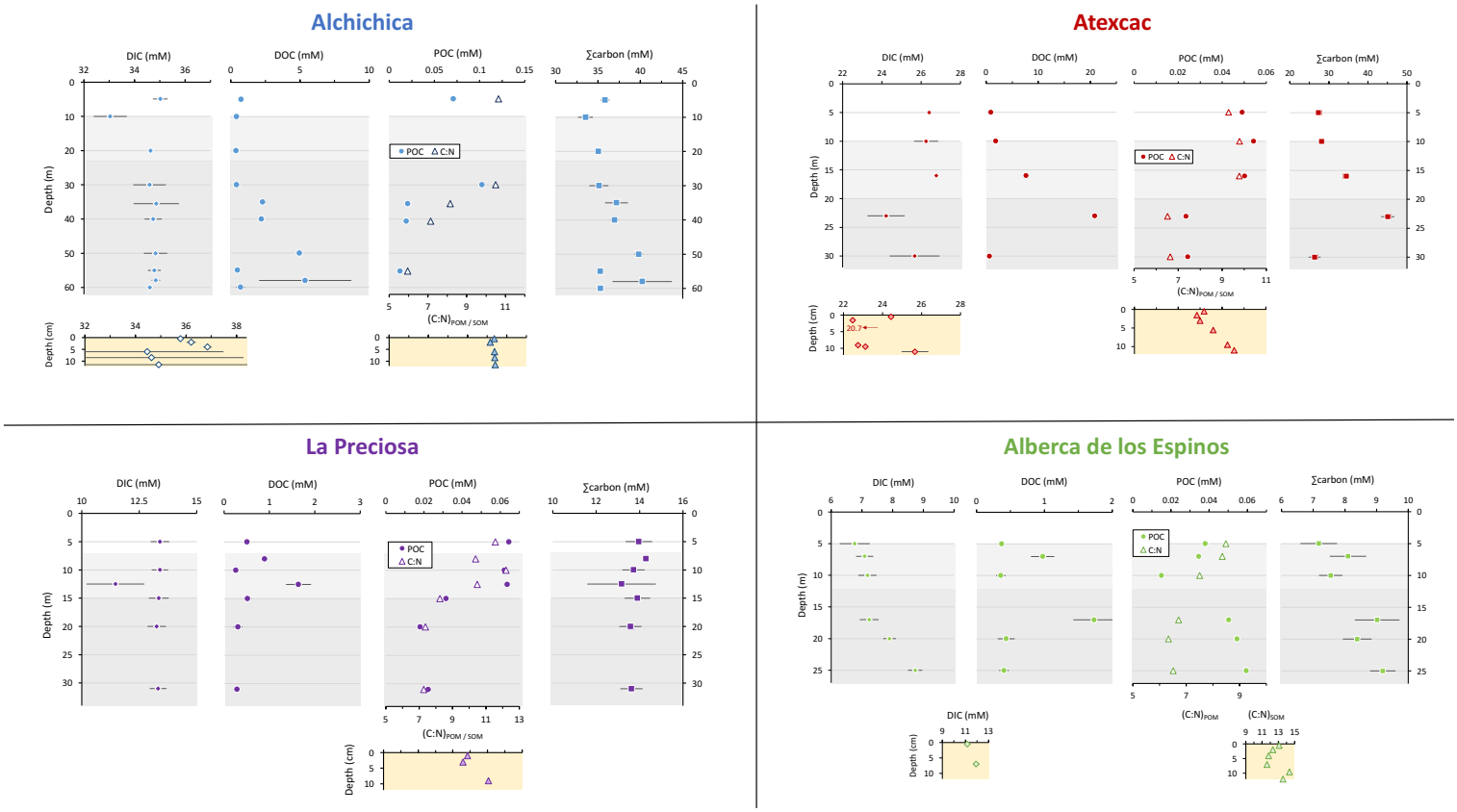

Figure 3. Concentrations in mmoles/L of DIC, DOC, POC and sum of all three reservoirs, C:N molar ratios of POM as a function of depth in the water columns, as well as DIC concentrations in the surficial sediment porewaters and C:N molar ratios of sedimentary OM. Porewaters from La Preciosa's 2016 core were not retrieved.

Page 10: [12] Deleted	Rob Havas	12/16/22 3:28:00 PM

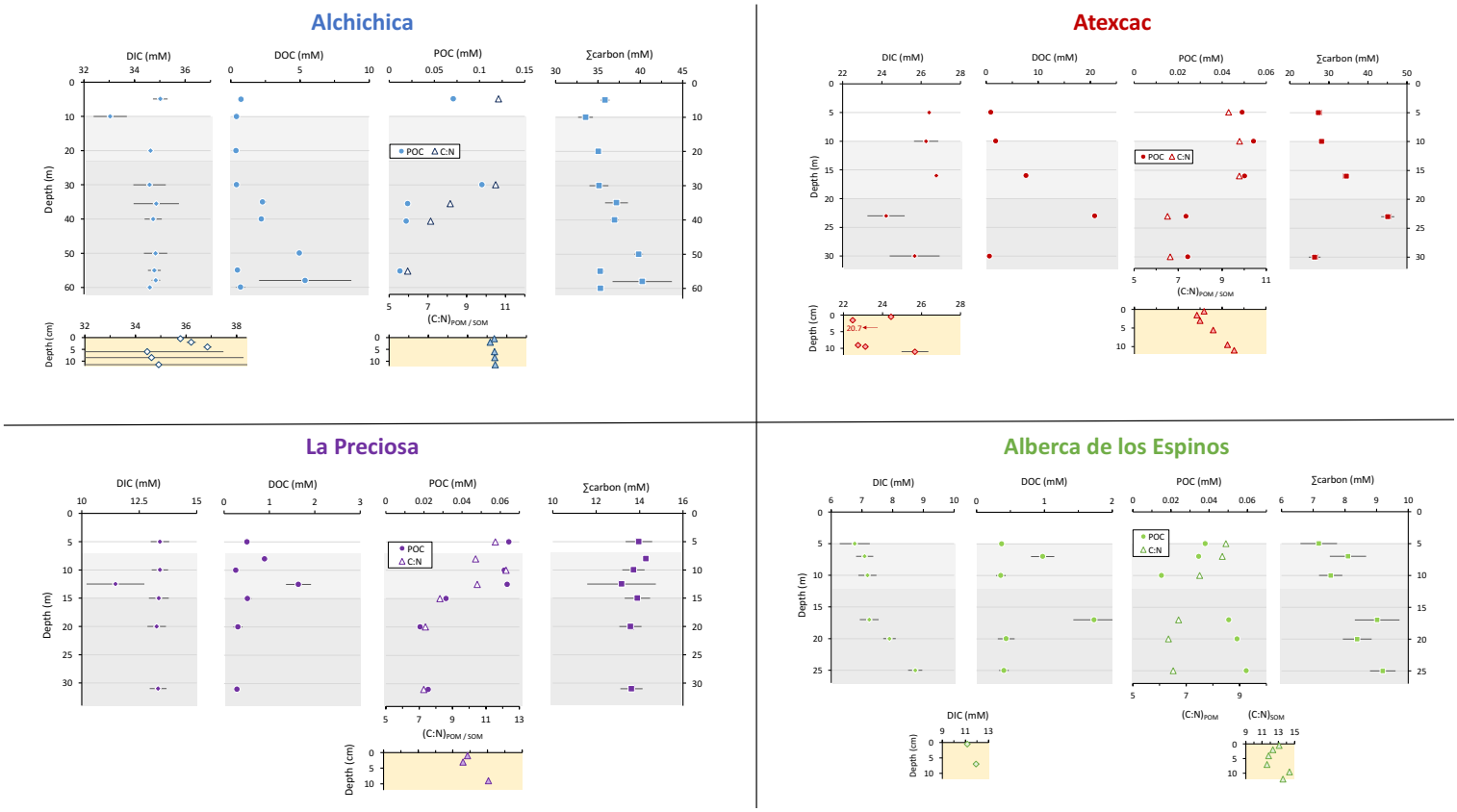

Figure 3. Concentrations in mmoles/L of DIC, DOC, POC and sum of all three reservoirs, C:N molar ratios of POM as a function of depth in the water columns, as well as DIC concentrations in the surficial sediment porewaters and C:N molar ratios of sedimentary OM. Porewaters from La Preciosa's 2016 core were not retrieved.

Page 10: [12] Deleted	Rob Havas	12/16/22 3:28:00 PM

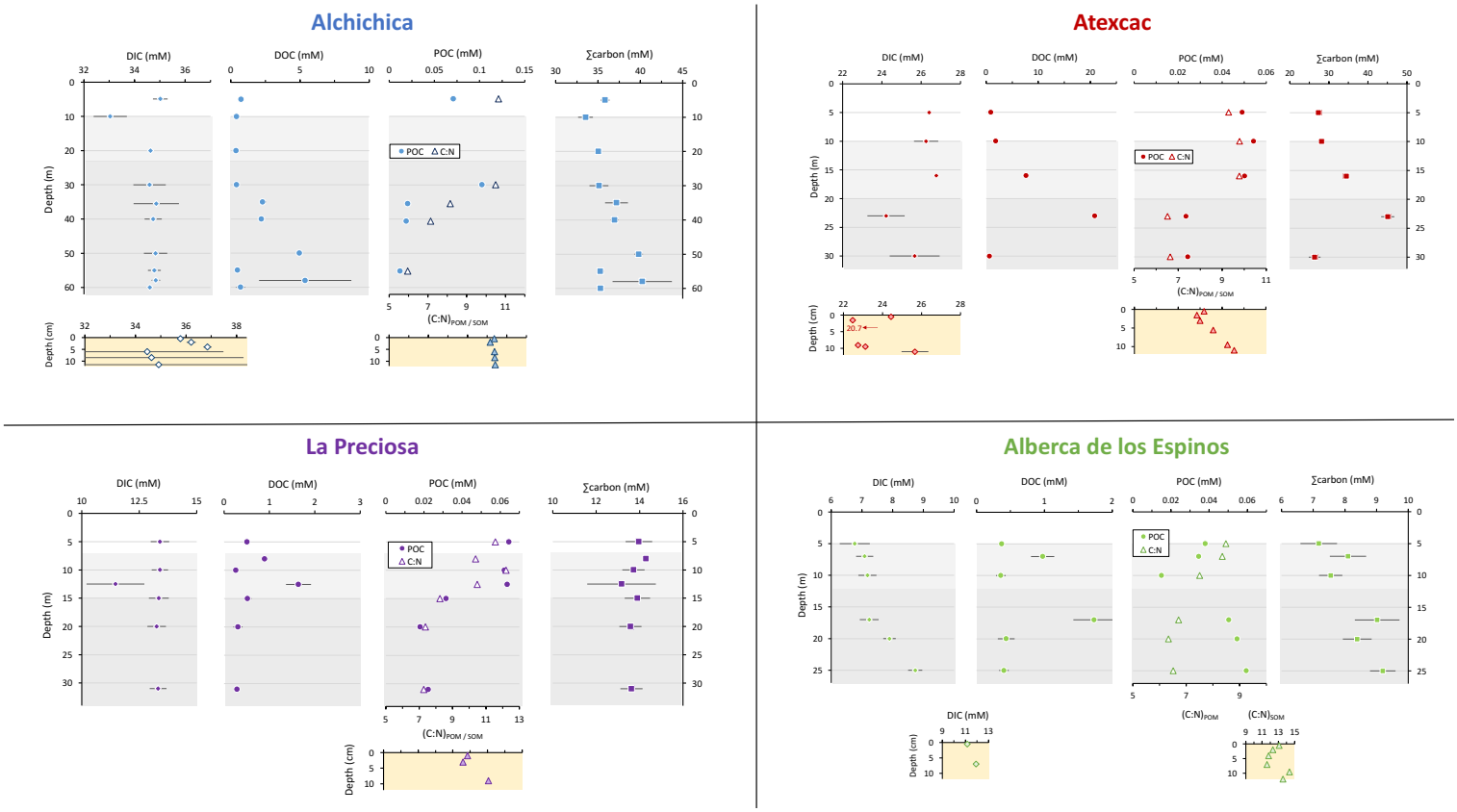

Figure 3. Concentrations in mmoles/L of DIC, DOC, POC and sum of all three reservoirs, C:N molar ratios of POM as a function of depth in the water columns, as well as DIC concentrations in the surficial sediment porewaters and C:N molar ratios of sedimentary OM. Porewaters from La Preciosa's 2016 core were not retrieved.

Page 10: [12] Deleted	Rob Havas	12/16/22 3:28:00 PM

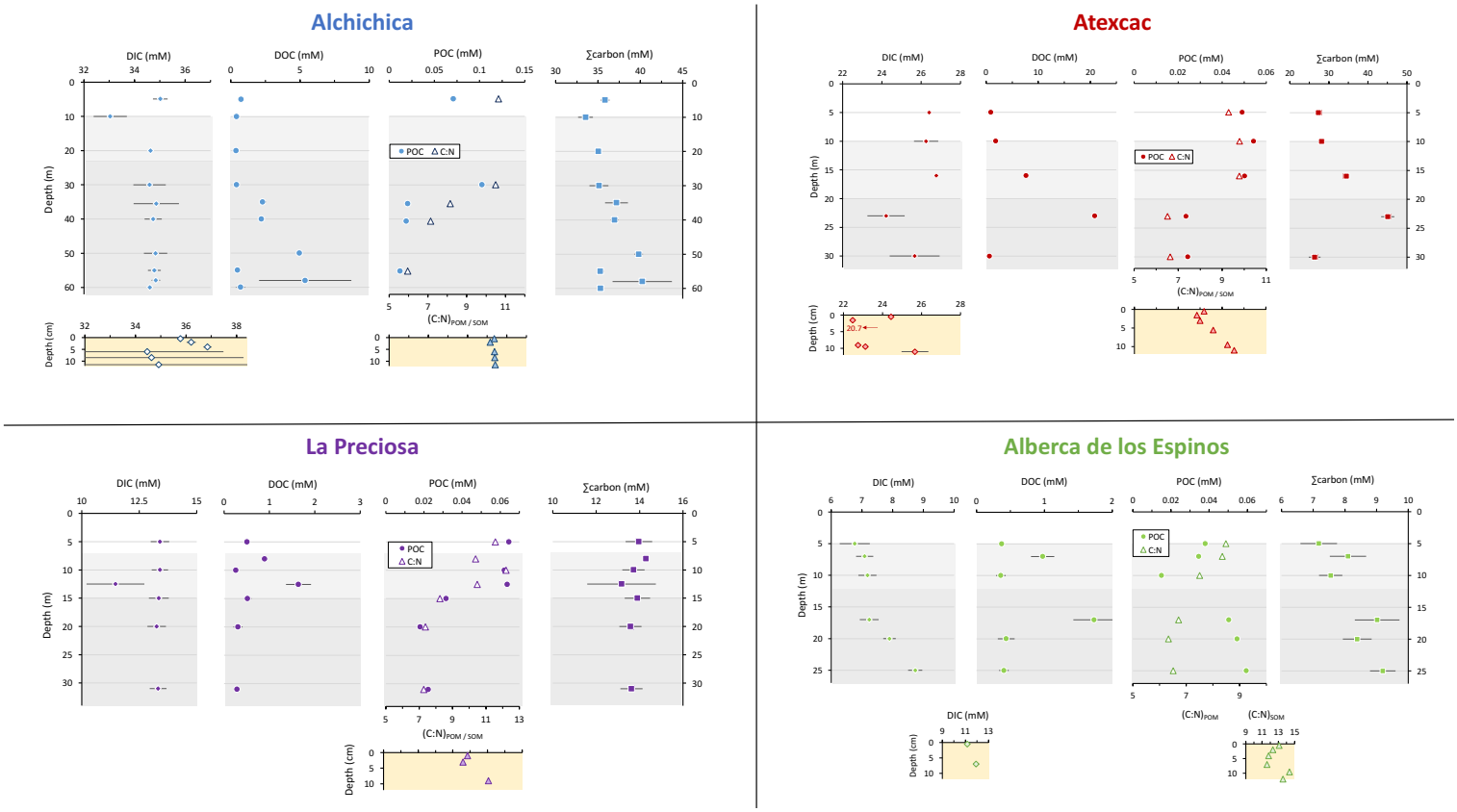

Figure 3. Concentrations in mmoles/L of DIC, DOC, POC and sum of all three reservoirs, C:N molar ratios of POM as a function of depth in the water columns, as well as DIC concentrations in the surficial sediment porewaters and C:N molar ratios of sedimentary OM. Porewaters from La Preciosa's 2016 core were not retrieved.

Page 10: [12] Deleted	Rob Havas	12/16/22 3:28:00 PM

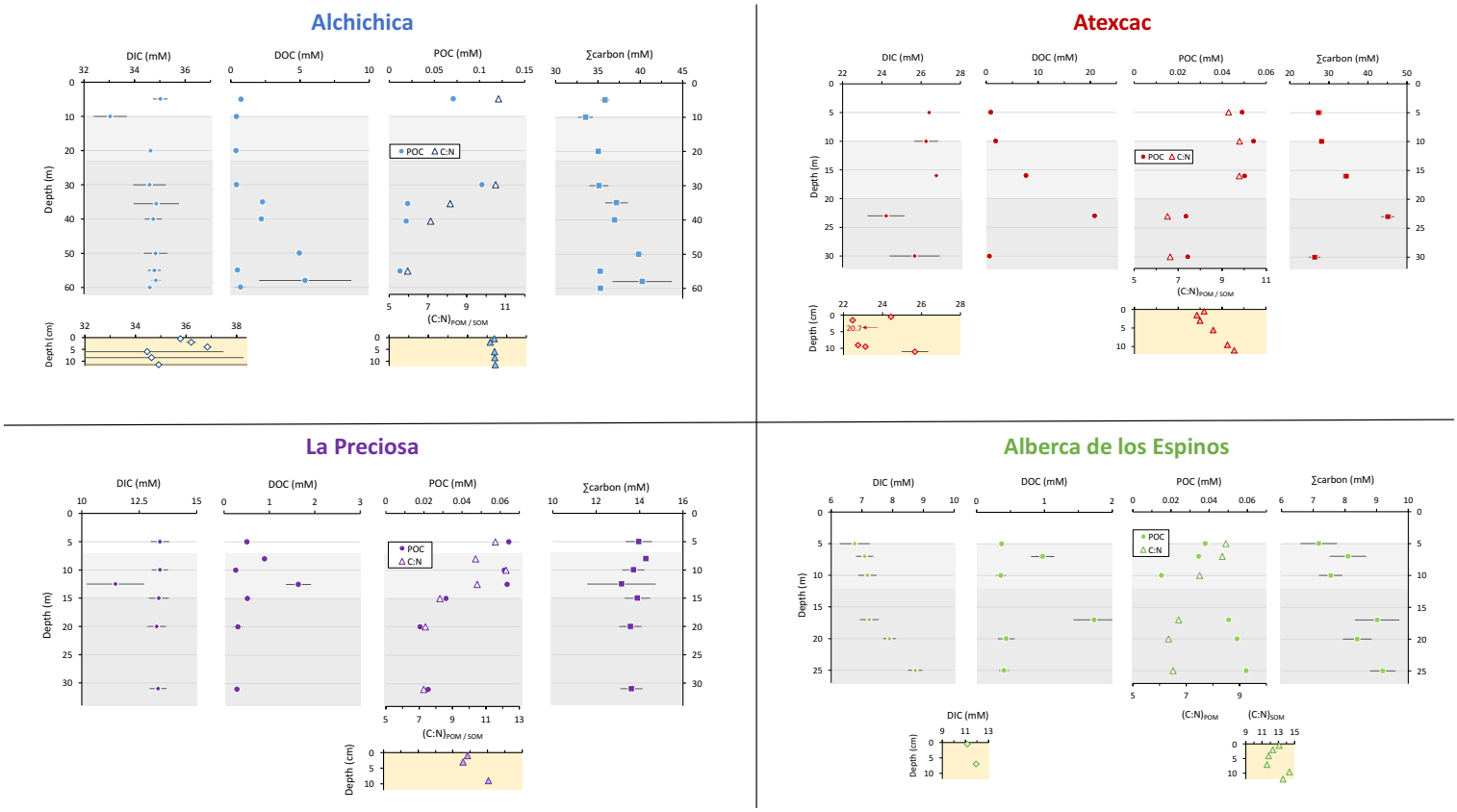

Figure 3. Concentrations in mmoles/L of DIC, DOC, POC and sum of all three reservoirs, C:N molar ratios of POM as a function of depth in the water columns, as well as DIC concentrations in the surficial sediment porewaters and C:N molar ratios of sedimentary OM. Porewaters from La Preciosa's 2016 core were not retrieved.

Page 10: [12] Deleted	Rob Havas	12/16/22 3:28:00 PM

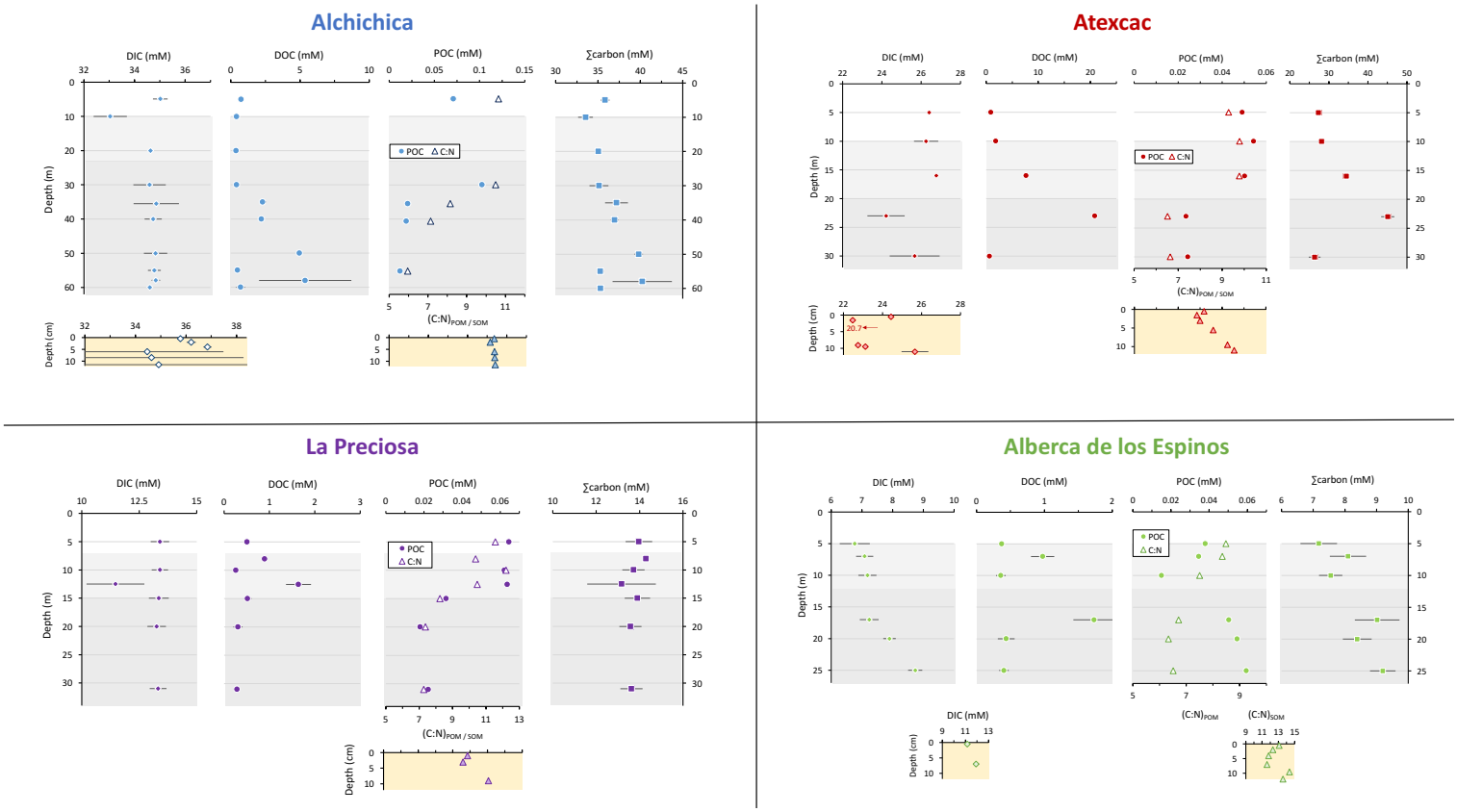

Figure 3. Concentrations in mmoles/L of DIC, DOC, POC and sum of all three reservoirs, C:N molar ratios of POM as a function of depth in the water columns, as well as DIC concentrations in the surficial sediment porewaters and C:N molar ratios of sedimentary OM. Porewaters from La Preciosa's 2016 core were not retrieved.

Page 10: [12] Deleted	Rob Havas	12/16/22 3:28:00 PM

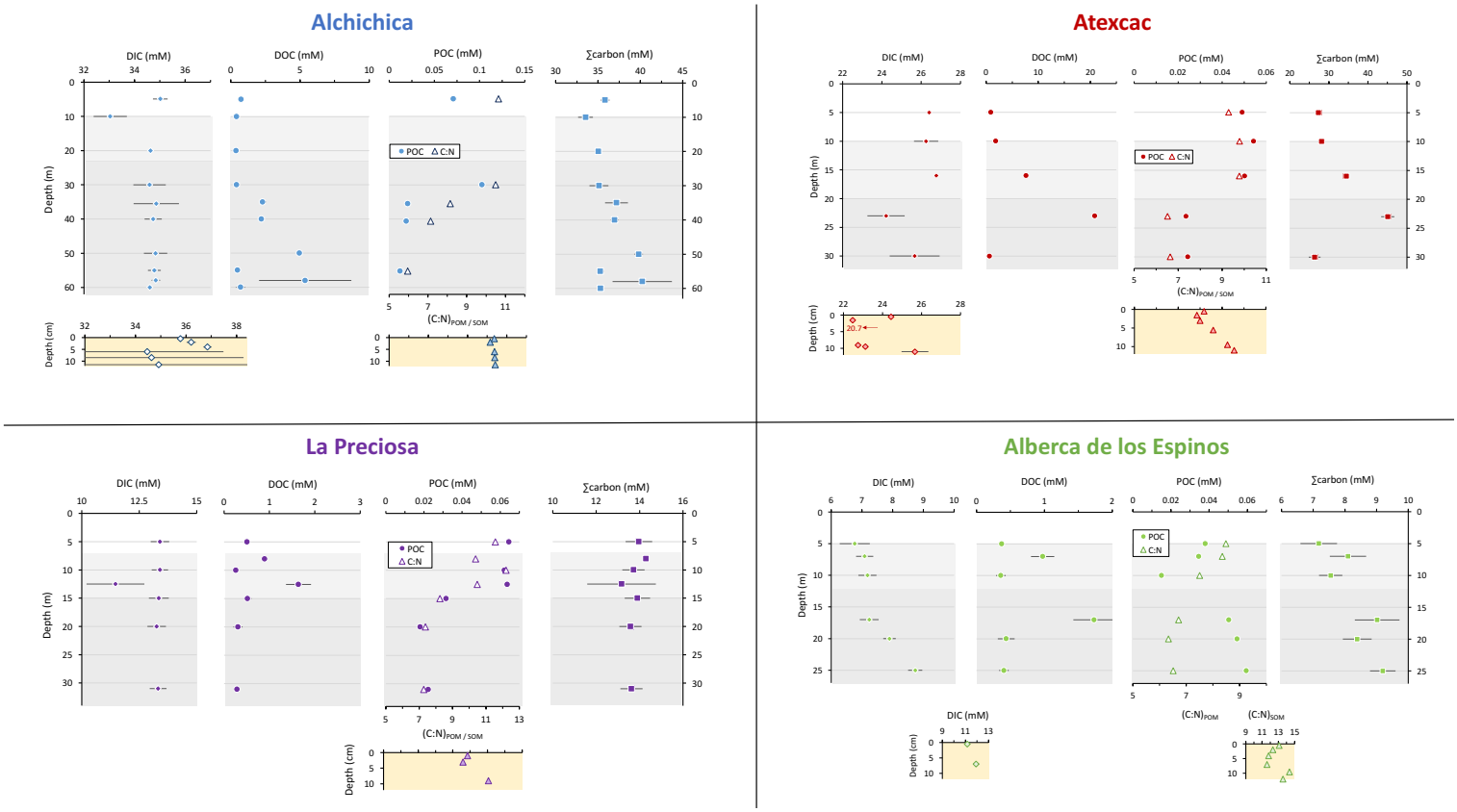

Figure 3. Concentrations in mmoles/L of DIC, DOC, POC and sum of all three reservoirs, C:N molar ratios of POM as a function of depth in the water columns, as well as DIC concentrations in the surficial sediment porewaters and C:N molar ratios of sedimentary OM. Porewaters from La Preciosa's 2016 core were not retrieved.

Page 10: [12] Deleted	Rob Havas	12/16/22 3:28:00 PM

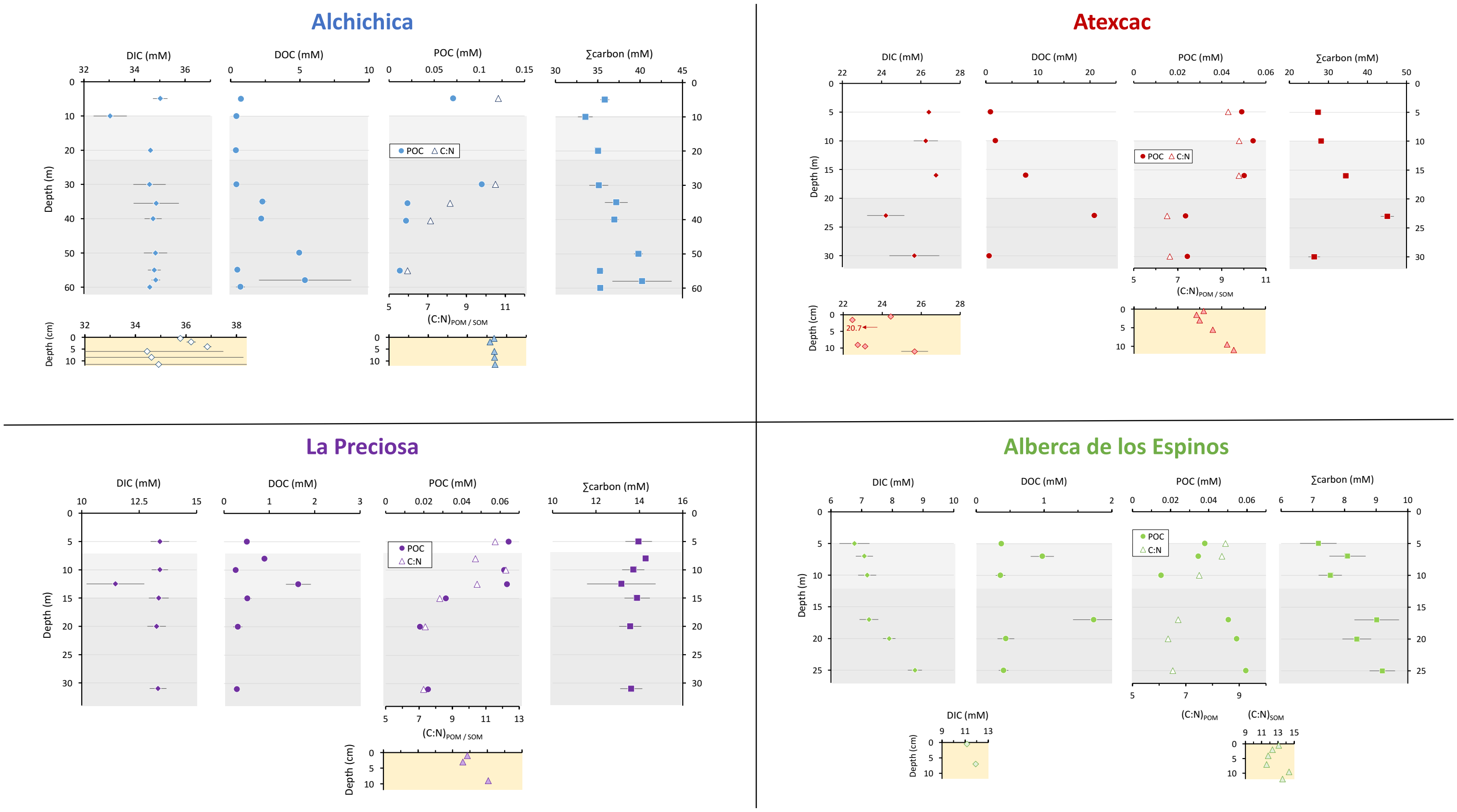

Figure 3. Concentrations in mmoles/L of DIC, DOC, POC and sum of all three reservoirs, C:N molar ratios of POM as a function of depth in the water columns, as well as DIC concentrations in the surficial sediment porewaters and C:N molar ratios of sedimentary OM. Porewaters from La Preciosa's 2016 core were not retrieved.

Page 10: [13] Deleted	Rob Havas	12/16/22 3:28:00 PM

TDP concentrations slightly decreased from ~0.25 µM to 0.19 µM at 16 m, then increased in the hypolimnion to ~ 0.45 µM (Fig. 5; Table S1).

Page 10: [13] Deleted	Rob Havas	12/16/22 3:28:00 PM

TDP concentrations slightly decreased from ~0.25 µM to 0.19 µM at 16 m, then increased in the hypolimnion to ~ 0.45 µM (Fig. 5; Table S1).

Page 10: [13] Deleted	Rob Havas	12/16/22 3:28:00 PM

TDP concentrations slightly decreased from ~0.25 µM to 0.19 µM at 16 m, then increased in the hypolimnion to ~ 0.45 µM (Fig. 5; Table S1).

Page 10: [13] Deleted	Rob Havas	12/16/22 3:28:00 PM

TDP concentrations slightly decreased from ~0.25 µM to 0.19 µM at 16 m, then increased in the hypolimnion to ~ 0.45 µM (Fig. 5; Table S1).

Page 10: [13] Deleted	Rob Havas	12/16/22 3:28:00 PM

TDP concentrations slightly decreased from ~0.25 µM to 0.19 µM at 16 m, then increased in the hypolimnion to ~ 0.45 µM (Fig. 5; Table S1).

Page 10: [13] Deleted	Rob Havas	12/16/22 3:28:00 PM

TDP concentrations slightly decreased from ~0.25 µM to 0.19 µM at 16 m, then increased in the hypolimnion to ~ 0.45 µM (Fig. 5; Table S1).

Page 10: [13] Deleted	Rob Havas	12/16/22 3:28:00 PM

TDP concentrations slightly decreased from ~0.25 µM to 0.19 µM at 16 m, then increased in the hypolimnion to ~ 0.45 µM (Fig. 5; Table S1).

Page 10: [14] Deleted	Rob Havas	12/16/22 3:28:00 PM

Table 2
Concentrations and isotopic compositions for dissolved inorganic and organic carbon (DIC, DOC), particulate organic carbon (POC) and C:N molar ratios of particulate organic matter (POM). Total carbon concentrations is the sum of all carbon reservoirs measured, $\delta^{13}C_{Total}$ is the weighted average of each $\delta^{13}C$.

Lake	Sample	DIC	DOC	POC	Total Carbon	$(C:N)_{POM}$	$\delta^{13}C_{DIC}$	$\delta^{13}C_{POC}$	$\delta^{13}C_{DOC}$	$\delta^{13}C_{Total}$
		mmoles/L				(molar)	‰			
Alchichica	AL 5m	35.0	0.7	0.07	35.8	10.6	2.0	-26.7		1.4
	AL 10m	33.0	0.4		33.5		2.0		-28.3	1.6
	AL 20m	34.6	0.4		35.0		1.6		-29.3	1.3
	AL 30m	34.6	0.4	0.10	35.1	10.5	1.7	-26.3	-28.3	1.2
	AL 35m	34.9	2.3	0.02	37.2	8.1	1.6	-25.7	-26.8	-0.2
	AL 40m	34.7	2.2	0.02	37.0	7.1	1.6	-25.1	-25.8	-0.1
	AL 50m	34.8	5.0		39.8		1.6		-25.1	-1.8
	AL 55m	34.8	0.5	0.01	35.3	5.9	1.5	-24.1	-27.6	1.1
	AL 58m	34.8	5.4		40.2		1.6		-27.7	-2.3
	AL 60m	34.6	0.7		35.3		1.5		-26.1	1.0
Atexcac	ATX 5m	26.4	0.92	0.05	27.4	9.3	0.4	-28.4	-20.0	-0.4
	ATX 10m	26.2	1.8	0.05	28.1	9.8	0.4	-28.2	-15.5	-0.7
	ATX 16m	26.8	7.8	0.05	34.7	9.8	0.3	-29.0		0.2
	ATX 23m	24.2	21.0	0.02	45.2	6.5	0.9	-26.7	-8.7	-3.6
	ATX 30m	25.7	0.7	0.02	26.4	6.6	0.2	-26.4	-11.2	-0.1
La Preciosa	LP 5m	13.4	0.5	0.06	14.0	11.6	0.1	-26.4	-27.2	-0.9
	LP 8m		0.9	0.07		10.4		-27.1	-20.0	
	LP 10m	13.4	0.3	0.06	13.7	12.2	0.2	-27.4	-15.5	-0.4
	LP 12.5m	11.5	1.6	0.06	13.2	10.5	-0.2	-27.1		-2.8
	LP 15m	13.4	0.5	0.03	13.9	8.2	-0.3	-23.5	-8.7	-1.3
	LP 20m	13.3	0.3	0.02	13.6	7.4	-0.4	-26.3	-11.2	-1.0
	LP 31m	13.3	0.3	0.02	13.6	7.3	-0.4	-25.2	-25.4	-0.9
Alberca de Los Espinos	Albesp 5m	6.8	0.4	0.04	7.2	8.5	-2.6	-27.0	-26.7	-3.9
	Albesp 7m	7.1	1.0	0.03	8.1	8.3	-2.3	-26.2	-14.7	-3.9
	Albesp 10m	7.2	0.4	0.02	7.6	7.5	-4.1	-28.3	-25.2	-5.1
	Albesp 17m	7.2	1.7	0.05	9.0	6.7	-3.4	-29.0	-26.3	-7.9
	Albesp 20m	7.9	0.4	0.05	8.4	6.3	-3.3	-26.5	-25.1	-4.5
	Albesp 25m	8.7	0.4	0.06	9.2	6.5	-2.0	-25.7	-27.2	-3.2

Page 10: [14] Deleted	Rob Havas	12/16/22 3:28:00 PM

Table 2
Concentrations and isotopic compositions for dissolved inorganic and organic carbon (DIC, DOC), particulate organic carbon (POC) and C:N molar ratios of particulate organic matter (POM). Total carbon concentrations is the sum of all carbon reservoirs measured, $\delta^{13}C_{Total}$ is the weighted average of each $\delta^{13}C$.

Lake	Sample	DIC	DOC	POC	Total Carbon	$(C:N)_{POM}$	$\delta^{13}C_{DIC}$	$\delta^{13}C_{POC}$	$\delta^{13}C_{DOC}$	$\delta^{13}C_{Total}$
		mmoles/L				(molar)	‰			
Alchichica	AL 5m	35.0	0.7	0.07	35.8	10.6	2.0	-26.7		1.4
	AL 10m	33.0	0.4		33.5		2.0		-28.3	1.6
	AL 20m	34.6	0.4		35.0		1.6		-29.3	1.3
	AL 30m	34.6	0.4	0.10	35.1	10.5	1.7	-26.3	-28.3	1.2
	AL 35m	34.9	2.3	0.02	37.2	8.1	1.6	-25.7	-26.8	-0.2
	AL 40m	34.7	2.2	0.02	37.0	7.1	1.6	-25.1	-25.8	-0.1
	AL 50m	34.8	5.0		39.8		1.6		-25.1	-1.8
	AL 55m	34.8	0.5	0.01	35.3	5.9	1.5	-24.1	-27.6	1.1
	AL 58m	34.8	5.4		40.2		1.6		-27.7	-2.3
	AL 60m	34.6	0.7		35.3		1.5		-26.1	1.0
Atexcac	ATX 5m	26.4	0.92	0.05	27.4	9.3	0.4	-28.4	-20.0	-0.4
	ATX 10m	26.2	1.8	0.05	28.1	9.8	0.4	-28.2	-15.5	-0.7
	ATX 16m	26.8	7.8	0.05	34.7	9.8	0.3	-29.0		0.2
	ATX 23m	24.2	21.0	0.02	45.2	6.5	0.9	-26.7	-8.7	-3.6
	ATX 30m	25.7	0.7	0.02	26.4	6.6	0.2	-26.4	-11.2	-0.1
La Preciosa	LP 5m	13.4	0.5	0.06	14.0	11.6	0.1	-26.4	-27.2	-0.9
	LP 8m		0.9	0.07		10.4		-27.1	-20.0	
	LP 10m	13.4	0.3	0.06	13.7	12.2	0.2	-27.4	-15.5	-0.4
	LP 12.5m	11.5	1.6	0.06	13.2	10.5	-0.2	-27.1		-2.8
	LP 15m	13.4	0.5	0.03	13.9	8.2	-0.3	-23.5	-8.7	-1.3
	LP 20m	13.3	0.3	0.02	13.6	7.4	-0.4	-26.3	-11.2	-1.0
	LP 31m	13.3	0.3	0.02	13.6	7.3	-0.4	-25.2	-25.4	-0.9
Alberca de Los Espinos	Albesp 5m	6.8	0.4	0.04	7.2	8.5	-2.6	-27.0	-26.7	-3.9
	Albesp 7m	7.1	1.0	0.03	8.1	8.3	-2.3	-26.2	-14.7	-3.9
	Albesp 10m	7.2	0.4	0.02	7.6	7.5	-4.1	-28.3	-25.2	-5.1
	Albesp 17m	7.2	1.7	0.05	9.0	6.7	-3.4	-29.0	-26.3	-7.9
	Albesp 20m	7.9	0.4	0.05	8.4	6.3	-3.3	-26.5	-25.1	-4.5
	Albesp 25m	8.7	0.4	0.06	9.2	6.5	-2.0	-25.7	-27.2	-3.2

Page 10: [15] Deleted **Rob Havas** **12/16/22 3:28:00 PM**

at the surface

Page 10: [15] Deleted **Rob Havas** **12/16/22 3:28:00 PM**

at the surface

Page 10: [15] Deleted **Rob Havas** **12/16/22 3:28:00 PM**

at the surface

Page 10: [15] Deleted **Rob Havas** **12/16/22 3:28:00 PM**

at the surface

Page 10: [15] Deleted **Rob Havas** **12/16/22 3:28:00 PM**

at the surface

Page 10: [15] Deleted **Rob Havas** **12/16/22 3:28:00 PM**

at the surface

Page 10: [15] Deleted **Rob Havas** **12/16/22 3:28:00 PM**

at the surface

Page 10: [15] Deleted **Rob Havas** **12/16/22 3:28:00 PM**

at the surface

Page 10: [15] Deleted **Rob Havas** **12/16/22 3:28:00 PM**

at the surface

Page 10: [16] Deleted **Rob Havas** **12/16/22 3:28:00 PM**

. The ORP signal was stable between 213 and 225 mV from

Page 10: [16] Deleted **Rob Havas** **12/16/22 3:28:00 PM**

. The ORP signal was stable between 213 and 225 mV from

Page 10: [16] Deleted **Rob Havas** **12/16/22 3:28:00 PM**

. The ORP signal was stable between 213 and 225 mV from

Page 10: [16] Deleted **Rob Havas** **12/16/22 3:28:00 PM**

. The ORP signal was stable between 213 and 225 mV from

Page 10: [16] Deleted **Rob Havas** **12/16/22 3:28:00 PM**

. The ORP signal was stable between 213 and 225 mV from

Page 10: [16] Deleted **Rob Havas** **12/16/22 3:28:00 PM**

. The ORP signal was stable between 213 and 225 mV from

Page 10: [16] Deleted **Rob Havas** **12/16/22 3:28:00 PM**

. The ORP signal was stable between 213 and 225 mV from

Page 10: [16] Deleted **Rob Havas** **12/16/22 3:28:00 PM**

. The ORP signal was stable between 213 and 225 mV from

Page 10: [16] Deleted **Rob Havas** **12/16/22 3:28:00 PM**

. The ORP signal was stable between 213 and 225 mV from

Page 10: [16] Deleted **Rob Havas** **12/16/22 3:28:00 PM**

. The ORP signal was stable between 213 and 225 mV from

Page 10: [16] Deleted	Rob Havas	12/16/22 3:28:00 PM

. The ORP signal was stable between 213 and 225 mV from

Page 10: [16] Deleted	Rob Havas	12/16/22 3:28:00 PM

. The ORP signal was stable between 213 and 225 mV from

Page 13: [17] Deleted	Rob Havas	12/16/22 3:28:00 PM

Figure 5. Concentrations of dissolved nutrients in micromoles.L^{-1} in the water columns of the four lakes as a function of depth. TDP and TDS stands for 'total dissolved P' and S', respectively, and were measured by ICP-AES. Fe and Mn were measured by ICP-MS. Nitrogen species were measured by colorimetry.

Page 14: [18] Deleted	Rob Havas	12/16/22 3:28:00 PM

C cycle across the Mexican crater lakes

The

1.1.

Page 15: [19] Deleted	Rob Havas	12/16/22 3:28:00 PM

.

Mean $\delta^{13}C_{DIC}$ values of the lakes broadly correlate with their alkalinity/salinity. This relationship is expected as evaporation generally increases the $\delta^{13}C_{DIC}$ of residual

Page 15: [20] Deleted	Rob Havas	12/16/22 3:28:00 PM

Therefore, the alkalinity gradient and to a first order, the size, isotopic composition and responsiveness of the DIC reservoir to biogeochemical processes are controlled by the local hydro-physico-chemical parameters of the lakes.

Stratification of the lakes

Page 20: [21] Moved to page 20 (Move #12)	Rob Havas	12/16/22 3:28:00 PM

Primary productivity by oxygenic photosynthesis in the upper water column

All four crater lakes are endorheic basins, *i.e.* there is no surface water inflow or outflow. Therefore, the organic carbon sources are predominantly autochthonous, mainly resulting from planktonic autotrophic C fixation. This is supported by C:N ratios of POM that were comprised between 6 and 12 in the four lakes, *i.e.*, close to the

Page 23: [22] Moved from page 23 (Move #16)	Rob Havas	12/16/22 3:28:00 PM

2). In Lake Atexcac concentrations of dissolved metal such as Cu, Pb or Co also drop at 23 m (Fig.

Page 23: [22] Moved from page 23 (Move #16) **Rob Havas** **12/16/22 3:28:00 PM**

2). In Lake Atexcac concentrations of dissolved metal such as Cu, Pb or Co also drop at 23 m (Fig.

Page 23: [22] Moved from page 23 (Move #16) **Rob Havas** **12/16/22 3:28:00 PM**

2). In Lake Atexcac concentrations of dissolved metal such as Cu, Pb or Co also drop at 23 m (Fig.

Page 23: [22] Moved from page 23 (Move #16) **Rob Havas** **12/16/22 3:28:00 PM**

2). In Lake Atexcac concentrations of dissolved metal such as Cu, Pb or Co also drop at 23 m (Fig.

Page 23: [23] Moved to page 15 (Move #10) **Rob Havas** **12/16/22 3:28:00 PM**

Table 3

Page 23: [24] Deleted **Rob Havas** **12/16/22 3:28:00 PM**

Symboles	Mathematical Expression	Signification
$\delta^{13}C_X$	$\left(\frac{\left(\frac{^{13}C}{^{12}C}\right)_X}{\left(\frac{^{13}C}{^{12}C}\right)_{VPDB}} - 1\right) * 1000$	Relative difference in ^{13}C:^{12}C isotopic ratio between a sample of a given C reservoir and the international standard "Vienna Pee Dee Bee", expressed in permil (‰). $\delta^{13}C_{total}$ represents the weighted average of $\delta^{13}C$ for all DIC, DOC and POC.
$\Delta^{13}C_{X\text{-}Y}$	$= \delta^{13}C_X - \delta^{13}C_Y \approx 1000 ln\alpha_{X\text{-}Y}$	Apparent isotopic fractionation between two reservoirs 'X' and 'Y'. Difference between their measured C isotope compositions approximating the fractionation α in ‰.
$\varepsilon_{X\text{-}CO2}$	$= (\alpha_{X\text{-}CO2} - 1)1000 \approx \delta^{13}C_X - \delta^{13}C_{CO2}$	Calculated isotopic fractionation between a reservoir 'X' and $CO_{2(aq)}$. $\alpha_{X\text{-}CO2}$ is calculated as $(\delta^{13}C_X+1000)/(\delta^{13}C_{CO2}+1000)$ where $\delta^{13}C_X$ is measured and $\delta^{13}C_{CO2}$ is computed based on DIC isotopic composition and speciation (see supplementary information).
Indexes	DIC DOC POC SOC	Dissolved Inorganic- , Dissolved Organic- , Particulate Organic- , Sedimentary Organic-Carbon

Page 23: [25] Deleted **Rob Havas** **12/16/22 3:28:00 PM**

Page 23: [26] Moved to page 23 (Move #20) **Rob Havas** **12/16/22 3:28:00 PM**

Aerobic respiration at the oxycline

At the oxycline of stratified water bodies, aerobic respiration of OM by heterotrophic organisms favors the transition from oxygenated upper layers to anoxic bottom waters. In the water column of the four lakes, $\Delta^{13}C_{POC\text{-}DIC}$ (and $\varepsilon_{POC\text{-}CO2}$) show increasing values in the hypolimnion, and especially below the chlorophyll a peaks (

Page 23: [27] Deleted	Rob Havas	12/16/22 3:28:00 PM

Fig. 2; 6).

Page 23: [27] Deleted	Rob Havas	12/16/22 3:28:00 PM

Fig. 2; 6).

Page 23: [28] Moved to page 23 (Move #21)	Rob Havas	12/16/22 3:28:00 PM

Decreasing POC concentrations near the oxycline and redoxcline are consistent with the fact that part of the upper primary production is degraded deeper in the water columns and/or that there is less primary production in the anoxic bottom waters. Increase of $\delta^{13}C_{POC}$ in the hypolimnion of the lakes is consistent with heterotrophic activity and points out that POC at these depths could mainly record secondary production rather than

Page 23: [29] Deleted	Rob Havas	12/16/22 3:28:00 PM

Decreasing

Page 23: [29] Deleted	Rob Havas	12/16/22 3:28:00 PM

Decreasing

Page 23: [29] Deleted	Rob Havas	12/16/22 3:28:00 PM

Decreasing

Page 23: [29] Deleted	Rob Havas	12/16/22 3:28:00 PM

Decreasing

Page 23: [29] Deleted	Rob Havas	12/16/22 3:28:00 PM

Decreasing

Page 23: [29] Deleted	Rob Havas	12/16/22 3:28:00 PM

Decreasing

Page 23: [29] Deleted	Rob Havas	12/16/22 3:28:00 PM

Decreasing

Page 23: [29] Deleted Rob Havas 12/16/22 3:28:00 PM

Decreasing

Page 23: [30] Formatted Rob Havas 12/16/22 3:28:00 PM

Font:Italic

Page 23: [30] Formatted Rob Havas 12/16/22 3:28:00 PM

Font:Italic

Page 23: [31] Deleted Rob Havas 12/16/22 3:28:00 PM

Table 4

Isotopic fractionations between dissolved inorganic and organic carbon (DIC, DOC) and particulate organic carbon (POC), where $\Delta^{13}C_{x\text{-}y} = \delta^{13}C_x - \delta^{13}C_y$ is the apparent fractionation and ε is computed as the actual metabolic isotopic discrimination between CO_2 and POC/DOC (see Table 3). $\delta^{13}C_{DOC}$ was not measured at 5 m depth and its value at 10 m was used in this calculation of $\Delta^{13}C_{DOC\text{-}POC}$.

Lake	Sample	$\Delta^{13}C_{POC\text{-}DIC}$	$\Delta^{13}C_{DOC\text{-}DIC}$	$\Delta^{13}C_{DOC\text{-}POC}$	$\varepsilon_{POC\text{-}DIC}$	$\varepsilon_{DOC\text{-}DIC}$
		‰			‰	
Alchichica	AL 5m	-28.7		*-1.6**	-19.1	
	AL 10m		-30.3			-20.4
	AL 20m		-30.9			-20.6
	AL 30m	-28.0	-30.0	-2.0		-20.9
	AL 35m	-27.3	-28.4	-1.0	-17.9	-19.9
	AL 40m	-26.6	-27.3	-0.7	-17.3	-18.3
	AL 50m		-26.7		-16.5	-17.2
	AL 55m	-25.6	-29.1	-3.5		-16.6
	AL 58m		-29.3		-15.5	-19.0
	AL 60m		-27.6			-17.5
Atexcac	ATX 5m	-28.8	-20.4	8.4	-19.3	-10.9
	ATX 10m	-28.6	-16.0	12.6	-19.1	-6.5
	ATX 16m	-29.3			-19.5	
	ATX 23m	-27.5	-9.7	17.9	-17.6	0.3
	ATX 30m	-26.5	-11.4	15.2	-16.6	-1.5
La Preciosa	LP 5m	-26.5	-25.5	1.0	-16.9	-15.9
	LP 10m	-27.6	-25.9	1.7	-17.9	-16.2
	LP 12.5m	-26.9	-19.8	7.1	-17.1	-10.0
	LP 15m	-23.2	-23.6	-0.4	-13.3	-13.7
	LP 20m	-25.9	-25.8	0.1	-15.9	-15.9
	LP 31m	-24.9	-25.8	-1.0	-14.9	-15.8
La Alberca de Los Espinos	Albesp 5m	-24.4	-24.2	0.2	-15.2	-15.0
	Albesp 7m	-23.9	-12.4	11.5	-14.6	-3.1
	Albesp 10m	-24.3	-21.2	3.1	-14.8	-11.7
	Albesp 17m	-25.6	-22.9	2.7	-15.9	-13.2
	Albesp 20m	-23.3	-21.8	1.5	-13.6	-12.2
	Albesp 25m	-23.7	-25.2	-1.5	-14.4	-15.9

Primary production in the hypolimnion

Anoxygenic autotrophs commonly thrive in anoxic bottom waters of stratified water bodies (e.g. (Pimenov et al., 2008; Zyakun et al., 2009; Posth et al., 2017; Fulton et al., 2018; Havig et al., 2018). They have been identified at different depths in the four Mexican lakes (Macek et al., 2020; Iniesto et al., in press). Based on our results obtained on samples collected during the stratification period, anoxygenic autotrophs appear to have an impact on the C cycle of lakes Atexcac and La Alberca only. Lake Atexcac records a concomitant decrease of [DIC] and increase of $\delta^{13}C_{DIC}$ in the anoxic hypolimnion at 23 m, below the peak of chlorophyll a, suggesting autotrophic C fixation by chemoautotrophy or anoxygenic photosynthesis. The calculated $\varepsilon_{POC\text{-}CO2}$ at 23 m (-17.5 ‰) is consistent with C isotopes fractionation by purple- and green sulphur-anoxygenic bacteria (PSB and GSB), while $\varepsilon_{POC\text{-}CO2}$ in La Alberca's hypolimnion (~ -15 ‰) is closer to GSB canonical signatures (Posth et al., 2017 and references therein) (Fig. 6c). In La Alberca, anoxygenic primary productivity is moreover suggested by increasing POC concentrations.

Page 23: [32] Formatted **Rob Havas** **12/16/22 3:28:00 PM**

Normal, None, Line spacing: multiple 1.15 li, No bullets or numbering

Page 23: [33] Moved to page 22 (Move #13) **Rob Havas** **12/16/22 3:28:00 PM**

Besides, we also observe a Chl. a peak in the anoxic hypolimnion of this lake (Fig. 2), which likely represents a bias of the probe towards some bacteriochlorophylls typical of GSB (see supplementary

Page 23: [34] Moved to page 22 (Move #14) **Rob Havas** **12/16/22 3:28:00 PM**

We notice that in Lake Atexcac, C fixation at 23 m by anoxygenic autotrophs causes a shift in the DIC reservoir, while oxygenic photosynthesis at 16 m does not, suggesting that anaerobic autotrophs are the main autotrophic metabolisms in this lake (in terms of DIC uptake). In La Alberca, the increase of [POC] to maximum values at depth also supports the predominance of anoxygenic *versus* oxygenic autotrophy (Fig. 3).

Page 23: [35] Moved to page 22 (Move #15) **Rob Havas** **12/16/22 3:28:00 PM**

other stratified water bodies which exhibit primary production clearly dominated by anoxygenic metabolisms (Fulton et al., 2018).

Page 23: [36] Deleted **Rob Havas** **12/16/22 3:28:00 PM**

Furthermore, at 23 m in Lake Atexcac and 17 m in Lake La Alberca, we find a striking turbidity peak precisely where the redox potential and concentrations of dissolved Mn drop (Fig.

Page 23: [37] Moved to page 23 (Move #16) **Rob Havas** **12/16/22 3:28:00 PM**

2). In Lake Atexcac concentrations of dissolved metal such as Cu, Pb or Co also drop at 23 m (Fig.

Page 23: [38] Deleted **Rob Havas** **12/16/22 3:28:00 PM**

S5). In La Alberca, a peak of particulate Mn concentrations is also detected at 15 m (Fig.

Page 23: [39] Deleted **Rob Havas** **12/16/22 3:28:00 PM**

This is most likely explained by the precipitation of Mn as oxide particles where reduced bottom waters meet oxidative conditions prevailing in the upper waters. Such Mn-oxides, even at low µM concentrations,

Page 23: [40] Moved to page 23 (Move #19) **Rob Havas** **12/16/22 3:28:00 PM**

can catalyze abiotic oxidation of sulfide to sulfur compounds (van Vliet et al., 2021), which in turn can be used and further oxidized to sulfate by phototrophic or chemoautotrophic sulfur-oxidizing bacteria.

Page 23: [41] Deleted **Rob Havas** **12/16/22 3:28:00 PM**

This is also consistent with the small in increase of [SO_4^{2-}] observed at 23 m in Atexcac (Table S1). Besides Mn-oxides

Page 23: [42] Moved to page 23 (Move #18)	Rob Havas	12/16/22 3:28:00 PM

can be used as electron acceptors during chemoautotrophy (Havig et al., 2015; Knossow et al., 2015; Henkel et al., 2019; van Vliet et al., 2021).

Page 23: [43] Deleted	Rob Havas	12/16/22 3:28:00 PM

Page 26: [44] Deleted	Rob Havas	12/16/22 3:28:00 PM

A particularly large and central DOC reservoir

In all four Mexican lakes studied here, the DOC reservoir occupies a predominant role, while showing quite diverse dynamics and characteristics between the lakes. Indeed, the four lakes have a high DOC content but very different [DOC] / $\delta^{13}C_{DOC}$ profiles and signatures despite quite similar ones for the DIC and POC reservoirs (Fig. 3; 4). Evaporation may be one process increasing DOC concentrations (Anderson and Stedmon, 2007; Zeyen et al., 2021). However, it is likely marginal here because on the contrary to what was observed for DIC, there is no correlation between the average [DOC] in the Mexican lakes and their salinity. Moreover, evaporation would not explain the significant intra-lake DOC depth variability.

In this section, we explore the different patterns of DOC production and fate, which depend on slight environmental and biological variations between the Mexican lakes. Moreover, we further describe the role of the DOC reservoir on other processes of the lakes C cycle and its potential implications in past oceans C cycle perturbations.

Sources and fate of DOC

Dissolved organic carbon is an operationally defined fraction of aqueous organic carbon (here separated from particulate organic carbon by filtration at 0.22 µm) within a continuum of organic molecules spanning a large range of sizes, compositions, degrees of reactivity and bioavailability (Kaplan et al., 2008; Hansell, 2013; Beaupré, 2015; Carlson and Hansell, 2015; Brailsford, 2019). The endorheic nature of the studied lakes allows to specifically focus on the effects of autochthonous primary production, and notably its effects on the DOC reservoir. Autochthonous DOC can form through multiple processes broadly including: higher-rank OM degradation processes such as sloppy feeding by predators, UV photolysis or bacterial and viral cell lysis (Lampert, 1978; Hessen, 1992; Bade et al., 2007; Thornton, 2014; Brailsford, 2019) as well as passive (leakage) or active (exudation) release by healthy cells (e.g. Baines and Pace, 1991; Hessen and Anderson, 2008; Thornton, 2014; Ivanovsky et al., 2020). In general, this C release (either "active" or "passive") tends to be enhanced in nutrient-limited conditions because some recently fixed C is in excess compared with other essential nutrients such as N or P (Hessen and Anderson, 2008; Morana et al., 2014;

Ivanovsky et al., 2020). Moreover, oligotrophic conditions tend to limit heterotrophic bacterial activity and thus preserve the DOC stocks (Thornton, 2014; Dittmar, 2015). In the studied lakes, this may partly explain the trend of increasing DOC concentrations from the more eutrophic Lake Alberca and La Preciosa's waters (0.7 mM on average) to the more oligotrophic Alchichica (1.8 mM) and Atexcac's (6.5 mM).

DOC release by autotrophs

In the four Mexican lakes, [DOC] depth profiles exhibit one or several peaks standing out from low background values and occurring both in oxic and anoxic waters (Fig. 3). In La Alberca and La Preciosa they correlate with chlorophyll a peaks. In the two other lakes, they do not match chlorophyll increase. However, in Atexcac, a remarkable DOC peak (over 10-fold increase, Fig. 3) occurs at the same depth as anoxygenic photosynthesis (Sect. 5.2.3). These co-occurrences support that a large portion of DOC in these three lakes (at least at these depths) arise from the release of photosynthetic C fixed in excess. Phytoplankton release of DOM is generally thought to be carried out by (i) an active "overflow mechanism" (DOM exudation) or (ii) a passive diffusion throughout the cell membranes. In the first case, DOM is actively released out of the cells as a result of C fixation rates higher than growth and molecular synthesis rates (e.g. Baines and Pace, 1991). Hence, DOM exudation depends on environmental factors such as irradiance and nutrient availability (e.g. Morana et al., 2014). Besides, it may serve "fitness-promoting purposes" such as storage, defense or mutualistic goals (Hessen and Anderson, 2008). In the second case (passive diffusion), DOC release depends on cells permeability and the outward DOC gradient, and is more directly connected to the amount of phytoplankton biomass (e.g. Marañón et al., 2004). Thus, any new photosynthate production insures a steady DOM release rate, regardless of the environmental conditions (Marañón et al., 2004; Morana et al., 2014). In the studied lakes, the fact that lakes La Preciosa and Alberca have lower DOC but overall higher chlorophyll a concentrations than Atexcac and Alchichica suggests that DOC production does not directly relate with phytoplankton biomass and is not passively released. Alternatively, an active DOC release is bolstered by DOC isotopic signatures (see below). Furthermore, the studied Mexican lakes precisely correspond to environmental contexts (high irradiance and oligotrophic freshwater bodies) where DOM exudation has been observed and is predicted (e.g. Baines and Pace, 1991; Morana et al., 2014; Thornton, 2014).

At depths where oxygenic photosynthesis occurs, the DOC over total OC ratio averages approximately 85, 99, 94 and 95 % for lakes Alchichica, Atexcac, La Preciosa and La Alberca, respectively. Release of DOC by primary producers can be characterized by the percentage of extracellular release (PER), which corresponds to the fraction of DOM over total (dissolved and particulate) OM primary production (e.g. Thornton et al., 2014). PER is highly variable and averages about 13% of C biomass over a wide range of environments (e.g. Baines and Pace, 1991; Thornton, 2014). But values as high as 99% have been reported (see Bertilsson and Jones, 2003). Thus, although some of the DOC measured in the Mexican lakes may correspond to an older long-term DOC reservoir, these DOC fractions are consistent with extremely high phytoplankton release rates.

An interesting feature is that DOC peaks associated with primary production (mainly photosynthesis) are characterized

by very positive $\Delta^{13}C_{DOC\text{-}POC}$ (from +3 to +18 ‰, Fig. 6b). It should be noticed that a switch from $CO_{2(aq)}$ to HCO_3^- as an inorganic C source (and their 10 ‰ isotopic difference, e.g. Mook et al., 1974) could not explain alone the isotopic difference between POC and DOC. The isotopic enrichment of DOC molecules compared to POC could have different origins. First, it supports that DOC may correspond to new photosynthate release rather than a product of cell lysis or zooplankton sloppy feeding, since the latter would likely produce $\delta^{13}C_{DOC}$ close to $\delta^{13}C_{POC}$ values. Second, this heavy DOC could originate from photosynthetic organisms using a different C-fixation pathway inducing smaller isotopic fractionation. In lakes Atexcac and La Alberca anoxygenic phototrophic bacteria, and notably GSB, could release important amounts of DOC, especially under nutrient-limiting conditions (Ivanovsky et al., 2020). In contrary to PSB (another group of anoxygenic phototrophs) or cyanobacteria which use the CCB pathway, GSB use the reductive citric acid cycle or reverse tricarboxylic-TCA cycle, which tends to induce smaller isotopic fractionations (between ~ 3-13 ‰, Hayes, 2001). If the DOC reservoirs in lakes Atexcac and La Alberca's hypolimnion originate from GSB fixed C, then their isotopic composition ($\varepsilon_{DOC\text{-}CO2} \approx -5 \pm 5$ and $\varepsilon_{DOC\text{-}CO2} \approx -13$ ‰, respectively) are in good agreement with fractionations found for this type of organisms in laboratory cultures and other stratified water bodies (Posth et al., 2017). The DOC and POC signatures would deviate from each other if GSB only marginally participated to the POC reservoir but released most of the DOC. Third, phytoplankton blooms could specifically release isotopically heavy organic molecules. For example, carbohydrates could be preferentially released under nutrient-limiting conditions as they are devoid of N and P (Bertilsson and Jones, 2003; Wetz and Wheeler, 2007; Thornton, 2014). Carbohydrates typically have ^{13}C-enriched (heavy) isotopic composition (Blair et al., 1985; Jiao et al., 2010; Close and Henderson, 2020). Yet, this molecular hypothesis would hardly explain the full range of $\Delta^{13}C_{DOC\text{-}POC}$ variations measured in Atexcac and La Alberca according to isotopic mass balance of cell specific organic compounds (Hayes, 2001). At last, such enrichments require otherwise that DOC and DIC first accumulate in the cells. Indeed, if DOC molecules were released as soon as they were produced, their isotopic composition should approach that of the biomass (i.e. $\delta^{13}C_{POC,}$ within the range of molecules-specific isotopic compositions), which is not the case. If DIC could freely exchange between inner and outer cell media, maximum "carboxylation-limited" fractionation (mostly between ~ 18 and 30 ‰ depending on RuBisCO form, Thomas et al., 2019) would be **expressed** in all synthetized organic molecules as represented in Fig. 7a (e.g. O'Leary, 1988; Descolas-Gros and Fontungne, 1990; Fry, 1996), which is also not what DOC records (see $\varepsilon_{DOC\text{-}CO2}$ in Fig. 6d).

Under the environmental conditions of the studied lakes, i.e., low CO_2 quantities relative to HCO_3^-, local planktonic competition for CO_2 and low nutrient availability, the activation of intracellular DIC concentrating mechanism (DIC-CM) is expected (Beardall et al., 1982; Burns and Beardall, 1987; Fogel and Cifuentes, 1993; Badger et al., 1998; Iñiguez et al., 2020). This mechanism is particularly relevant in oligotrophic aqueous media (Beardall et al., 1982), where CO_2 diffusion is slower than in the air (O'Leary, 1988; Fogel and Cifuentes, 1993; Iñiguez et al., 2020). DIC-CM have been proposed to reduce the efflux of DIC from the cells back to the extracellular solution. This internal DIC is eventually converted into organic biomass, thereby drawing the cells isotopic composition closer to that of $\delta^{13}C_{DIC}$ (Fig. 7; Beardall et al., 1982; Fogel and Cifuentes, 1993; Werne and Hollander, 2004). However, we suggest that the activation of a DIC-CM could preserve a large $\Delta^{13}C_{POC\text{-}DIC}$ while generating an apparent fractionation between

the DOC and POC molecules instead. Indeed, initially fixed OC would be discriminated against the heavy C isotopes and incorporated into the cellular biomass (Fig. 7c, 't_i'). Further, following the overflow mechanism scenario, high photosynthetic rates (due to high irradiance, temperature and high DIC despite low CO_2) coupled with low population growth rates and organic molecules synthesis (due to limited abundances of P, N, Fe, etc.) would result in the exudation of excess organic molecules with heavy $\delta^{13}C_{DOC}$ as they are synthetized from residual internal DIC, which progressively becomes ^{13}C-enriched (Fig. 7c, 't_{ii}'). This suggests that oligotrophic conditions could be a determinant factor in the generation of significantly heavy $\delta^{13}C_{DOC}$., and even more if they are coupled to high irradiance.

DOM accumulation in Lake Alchichica

From the previous discussion, it appears that environmental conditions of the Mexican lakes might favor an important phytoplanktonic production of DOM. Alcocer et al. (2014) also proposed that an early spring cyanobacterial bloom in Lake Alchichica favored the production of DOC in the epilimnion. However, at the time of sampling, the DOC reservoir in this lake was not correlated with any sizeable autotrophic activity at any depth. Indeed, the large epilimnetic chlorophyll a peak did not correlate with any changes of [DOC] nor $\delta^{13}C_{DOC}$ (Figs. 2-4). Compared with the other lakes, the geochemical conditions at which chlorophyll a is produced in Alchichica could have been incompatible with the activation of a DIC-CM and significant DOM exudation. For example, Alchichica had similar [$CO_{2(aq)}$] as La Preciosa, but higher P and NH_4^+ concentrations (Table S1, S3); Lake La Alberca had higher P concentrations, but presented similar [NH_4^+] and lower [$CO_{2(aq)}$]. We measure a large DOC increase in the middle of the anoxic hypolimnion of Lake Alchichica, but it did not correspond to any change in the DIC reservoir as observed for lakes La Preciosa (at 12.5 m) or Atexcac (at 23 m). Moreover at these depths, photosynthetic active radiation (PAR) is below 0.1% in Alchichica during the stratified season (Macek et al., 2020), which might not be sufficient to trigger important anoxygenic phytoplankton DOC release.

The DOC reservoir in Alchichica is characterized by a $\delta^{13}C_{DOC}$ (and $\Delta^{13}C_{DOC\text{-}DIC}$) lower than in the other lakes and systematically showing ^{13}C-depleted signatures relative to POC (i.e. $\delta^{13}C_{DOC} < \delta^{13}C_{POC}$; Fig. 6e). Thus, if the DOC increase in Alchichica's hypolimnion resulted from the release of photosynthetic OC like in the other lakes, it was not associated to the same C isotopes fractionation (e.g. if anoxygenic phototrophs did not actively take up DIC, Fig. 7a).

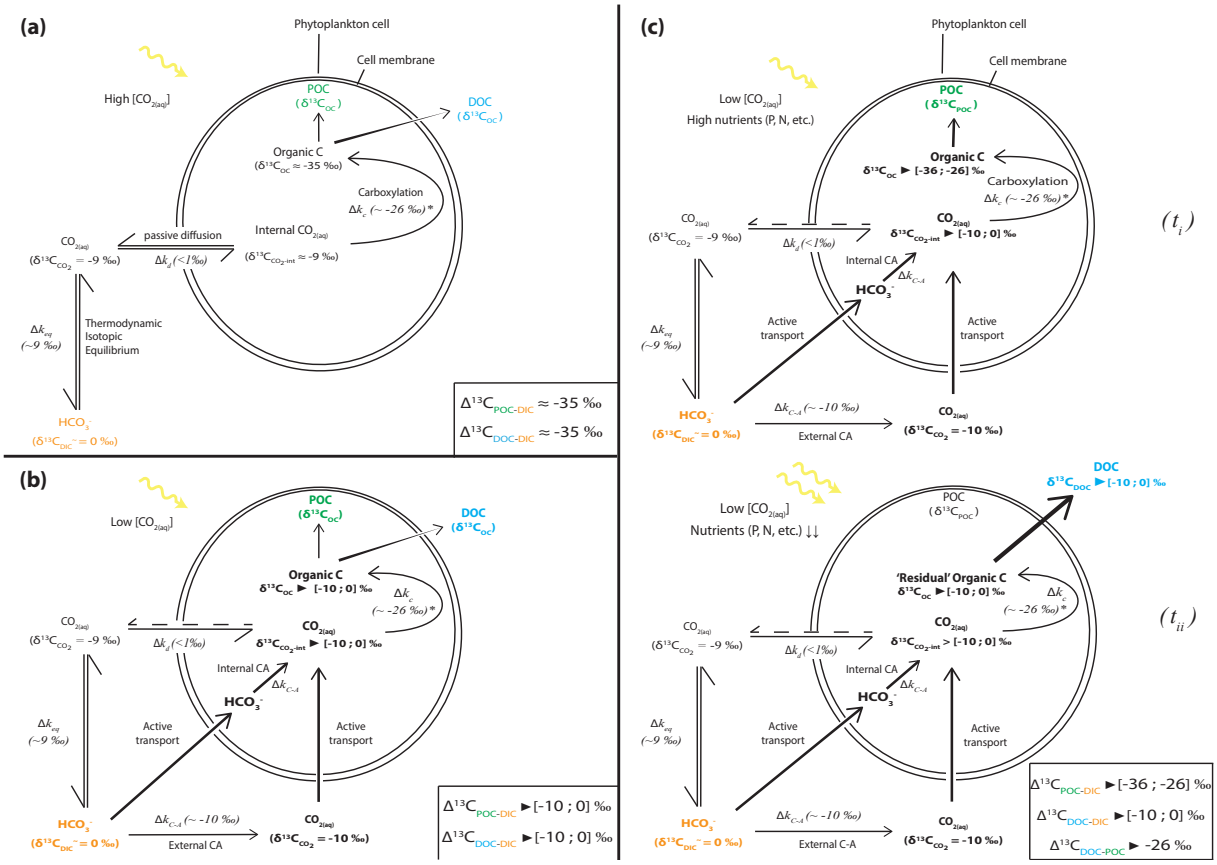

Figure 7. Schematic view of phytoplankton cells during autotrophic C fixation through different C supply strategies and associated apparent isotopic fractionation between DIC and POC/DOC and between DOC and POC (*cf*. Table 3). (a) Case where [$CO_{2(aq)}$] is high enough to allow for a DIC supply by passive $CO_{2(aq)}$ diffusion through the cell membrane and $CO_{2(aq)}$ is at equilibrium with other DIC species. There, isotopic fractionation is maximum (minimum $\delta^{13}C_{OC}$) because C fixation is limited by the carboxylation step. DOC is released following an in- to outward cell concentration gradient and has a similar composition to POC. (b) "Classic" view of C isotopic cycling resulting from active DIC transport within the cell because of low ambient [$CO_{2(aq)}$] (through a DIC-CM). Carbonic anhydrase (CA) catalyzes the conversion between HCO_3 and $CO_{2(aq)}$ inside or outside the cell with an isotopic fractionation close to equilibrium fractionation (~ 10 ‰). While inward passive $CO_{2(aq)}$ diffusion can still occur, the DIC-CM activation reduces the reverse diffusion, resulting in internal $CO_{2(aq)}$ isotopic composition approaching that of the incoming DIC (depending on the fraction of internal $CO_{2(aq)}$ leaving the cell). Acting as a "closed-system", most of internal DIC is fixed as OC and minimum isotopic fractionation is expressed for both POC and DOC. (c) Proposed model for C isotopic fractionation with active DIC transport including an isotopic discrimination between POC and DOC. (t_i) Initially fixed C is isotopically depleted and incorporates the cell's biomass as long as there are sufficient nutrients to enable "complex" organic molecules synthesis. (t_{ii}) In low nutrient conditions, but high photosynthetic activity – fixed OC is released out of the cell as DOC following the "overflow" hypothesis and inherits heavier isotopic compositions from the residual internal DIC. This leads to distinct POC and DOC isotopic signatures, with small fractionation between DOC and DIC, the amplitude of which will depend notably on the rate of CO_2 backward diffusion and ratio of biomass C (POC) and released C (DOC).

Alternatively, this hypolimnetic DOC increase could reflect the preservation and accumulation of DOM over the years in Lake Alchichica, consistently with higher [DOC] measured in 2019 than in the previous years (Alcocer et al., 2014).

While alteration of the DOM reservoir by UV-photolysis would induce a positive isotopic fractionation (Chomicki, 2009), the slightly negative $\Delta^{13}C_{DOC\text{-}POC}$ signatures give support to DOC being mainly a recalcitrant residual product of primary OM degradation by heterotrophic organisms (Alcocer et al., 2014). Indeed, the preferential consumption of labile ^{13}C-enriched molecules by heterotrophic bacteria would leave the residual OM with more negative isotopic signatures (Sect. 5.2.2.). Moreover, degradation by heterotrophic bacteria leaves more recalcitrant DOM in the water column which tends to accumulate over longer periods of time (Ogawa et al., 2001; Jiao et al., 2010; Kawasaki et al., 2013). DOM content is a balance between its production by autotrophs and consumption by heterotrophs, especially in environments where both types of organisms compete for nutrients at a low content (Dittmar, 2015). If Alchichica's DOC actually represents a long-term reservoir, its presence might favor the development of bacterial populations growing on it. Alcocer et al. (2014) describe the shift of the cyanobacterial DOC towards the hypolimnion of Lake Alchichica at the end of the spring. Deeper and darker anoxic waters in Alchichica could better preserve DOM from intense microbial and light degradation, hence allowing its accumulation.

In conclusion, Alchichica's DOC reservoir (and notably in the hypolimnion) more likely represents an older and evolved DOM pool. The time required for its accumulation and its stability over the years remain to be investigated. Nevertheless, we cannot fully rule out that part of it this DOC was produced by anoxygenic photosynthetic plankton. If so, the reasons why it did not bear the same isotopic enrichment as in the other lakes also remain to be elucidated.

DOC analysis provides deeper insights into planktonic cells functioning and water column C cycle dynamics

With concentrations ranging from 0.6 and 6.5 mM on average, DOC amounts between 14 and 160 times the POC concentrations. It represents from about 5 to 16% of total C measured in the four lakes. In comparison, although DOC is the main organic pool in the ocean, its concentration hardly exceeds 0.08 mM (Hansell, 2013) while in large scale anoxic basin such as the Black Sea, it remains under 0.3 mM (Ducklow et al., 2007). Hence DOC is a major C reservoir in these Mexican lakes.

The depth profiles of DOC concentration and isotopic composition differ significantly from those of POC. Notably in Lake La Preciosa, the photosynthetic DOC production (+1.5 mM) at the Chl. a peak depth matches the decrease of DIC (- 2 mM) (Fig. 3) with no change in [POC] or $\delta^{13}C_{POC}$. Just below, at a 15 m depth, the marked increase of $\delta^{13}C_{POC}$ related with heterotrophic activity (Sect. 0) might be better understood when considering the heavier DOC isotopes compositions as a C source between 12.5 and 15 m depth (Fig. 4). In Lake La Alberca, only a small portion of C is transferred from the inorganic to the POC by primary productivity, while the DIC reservoir is largely dominated by methanogenesis and possible volcanic degassing in the bottom of the lake. In Lake Atexcac, anoxygenic photosynthesis clearly stands out based on [DOC] and $\delta^{13}C_{DOC}$ data, but is not recorded by the POC reservoir and only slightly by the DIC reservoir. Overall, it implies that recently fixed OC is quickly released out of the cells as DOM, thereby transferring most of C from DIC to DOC, rather than POC which, therefore, is an incomplete archive of the biogeochemical reactions occurring in water columns. Furthermore, this shows that the isotopic analysis of DIC and

by extension authigenic carbonates, especially in alkaline-buffered waters, might not be sensitive enough to faithfully archive environmental and biological changes.

The heavy $\delta^{13}C_{DOC}$ recorded in lakes La Preciosa, La Alberca and Atexcac provides important constraints on the way planktonic cells deal with and cycle C: it may arise from the activation of a DIC-CM or from a specific metabolism or C fixation pathway. By contrast, the use of a DIC-CM is poorly captured by $\delta^{13}C_{POC}$ analyses, although recognition of active DIC uptake has often been based on this signal (by reduced isotopic fractionation with the DIC; e.g. Beardall et al., 1982; Erez et al., 1998; Riebesell et al., 2000). Most interestingly, intra-cellular amorphous Ca-carbonates (iACC) are formed in some of the cyanobacteria from Alchichica microbialites, possibly due to supersaturated intra-cell media following active DIC uptake through a DIC-CM (Couradeau et al., 2012; Benzerara et al., 2014). While this link is still debated (Benzerara et al., 2014), the active use of DIC-CMs in the studied Mexican lakes is independently supported by the DOC isotopic signature.

The report that DOC is a major C reservoir in lakes has several other implications. First, the fact that a major fraction of primary and secondary productivity may be released and cycled as DOM instead of POM contrasts with the conventional view that autochtonous SOM strictly records water columns biological processes. Then, if a larger fraction of DOC incorporated the POM (e.g. due to higher nutrient availability), which later deposits as SOM, it may tend to shift both POM and SOM isotopic compositions towards higher values (e.g. Fig. 7b *vs* 7c). However, we notice that $\delta^{13}C_{SOC}$ does not seem to keep track of peculiar DOC isotopic signatures, although OC carbon of the lakes is by far dominated by DOC over POC. Finally, in lakes such as Lake La Alberca, where alkalinity is not high enough to have a high buffering effect, production or consumption of DOC should increase or decrease, respectively, the $\delta^{13}C$ of the residual lake DIC and ultimately the isotopic signatures of authigenic carbonates accumulated in the sediments (see below).

Implications for the inference of past big DOC reservoirs

The studied Mexican lakes have large DOC pools, allowing to draw comparisons with studies that have invoked past occurrences of oceanic carbon cycles dominated by big DOC reservoirs (e.g. Rothman et al., 2003; Sexton et al., 2011). Ventilation/oxidation cycles of a large deep ocean DOC reservoir have been inferred to explain carbonate isotopic records of successive warming events through the Eocene (Sexton et al., 2011). Briefly, the release of carbon dioxide into the ocean/atmosphere system following DOC oxidation would generate both the precipitation of low $\delta^{13}C$ carbonates and an increase of the atmospheric greenhouse gas content. It was assessed that the size of this DOC reservoir should have been at least 1600 PgC (about twice the size of the modern ocean DOC reservoir) to account for a 2-4°C increase of deep ocean temperatures (Sexton et al., 2011). However, the main counter argument to this hypothesis is that the buildup of such a DOC reservoir at modern DOC production rates implies a sustained deep ocean anoxia over hundreds of thousand years, while independent geochemical proxies do not suggest such a sustained anoxia during this time interval (Rigwell and Arndt, 2015). However, our study suggests that this counter argument may be weak. Indeed, in the studied Mexican lakes, the lowest recorded [DOC] is 260 µM (Table 1), i.e., about 6

times the deep modern ocean concentrations (~ 45 µM; Hansell, 2013). Yet, the entire water columns of these lakes down to the surficial sediments are seasonally mixed with oxygen showing that high [DOC] (notably in Alchichica which likely harbor a "long-term" DOC reservoir) can be achieved despite frequent oxidative (oxygen-rich) conditions. Besides, the oxidation of only half of the DOC in the studied lakes would generate average $\delta^{13}C_{DIC}$ deviations between -0.6 and -1 ‰, corresponding to the C isotopes excursion magnitudes described by Sexton et al. (2011).

Similarly, Black Sea's deep anoxic waters hold about 3 times the amount of DOC found in the modern deep open ocean (Sexton et al., 2011; Dittmar; 2015). In the Black Sea and Mexican lakes, the low nutrient availability may limit sulfate-reduction despite high sulfate and labile organic matter concentrations, thence favoring DOM preservation and accumulation (Dittmar, 2015 and references therein). Margolin et al. (2016) argued that important DOM was only sustained by important terrigenous inputs. Our study attests the possibility for "autochthonous systems" to reach DOC concentrations well above what is found in the Black Sea and that terrigenous inputs are not needed for that. Therefore, it can be argued that the buildup of a large DOC reservoir which may have influenced the carbonates isotopic record of Eocene warming events is plausible.

The presence of a large oceanic DOC reservoir has also been used to account for the Neoproterozoic C isotopic record, where carbonates show $\delta^{13}C$ negative excursions of more than 10 ‰ over tens of Ma, while paired sedimentary organic carbon isotope signal remain stable (Rothman et al., 2003; Fike et al., 2006; Swanson-Hysell et al., 2010; Tziperman et al., 2011). However, once again, this hypothesis has been questioned because of the too high DOC reservoir's size (10 times the contemporaneous DIC, i.e., 10^2 to 10^3 times that of modern DOC) and amount of oxidants required to generate such a sustained DOC oxidation excursion (see Ridgwell and Arndt, 2015). Modeling approaches have both supported or contradicted this hypothesis: some suggested that partial oxidation of a large DOC reservoir would suffice to explain such excursions (Shi et al., 2017), while others concluded that DOC abundance in the past Earth's oceans could not have significantly departed from today's values (Fakhraee et al., 2021). Critically, although multiple studies have built on the Neoproterozoic big DOC scenario (e.g. Li et al., 2017; Canadas et al., 2022), there is at the moment no evidence – to the best of our knowledge – for the existence of such high oceanic DOC levels in the past or present days. Modern analogous systems such as the Black Sea or Mexican lakes studied here support the possibility of important DOC contents accumulation but those remain substantially lower than the levels required to account for the Neoproterozoic events (Ducklow et al., 2007; Ridgwell and Arndt, 2015).

In the studied lakes, a full DOC oxidation would generate a maximum $\delta^{13}C_{DIC}$ deviation of -2 ‰, in Alberca de los Espinos, which has the lowest alkalinity, and the lowest $\delta^{13}C_{DIC}$. The other lakes $\delta^{13}C_{DIC}$ are less impacted, notably because they are largely buffered by high DIC content (Table 1). Bade et al. (2004) showed that low alkalinity/low pH lakes generally show more negative $\delta^{13}C_{DIC}$ (down to ~ -30‰), partly due to a higher response to remineralization of OM and especially DOC. Compiling our data with those of Bade et al. (2004) we consistently show a clear negative trend of $\delta^{13}C_{DIC}$ with increasing DOC:DIC ratio over a broad range of lacustrine DOC and DIC concentrations (Fig. S3a). This observation is consistent with the inference that systems where DOC:DIC >> 1 should drive $\delta^{13}C_{DIC}$ to very negative values (Rothman et al., 2003). In high DOC:DIC environments, the biomass is largely influenced by

heterotrophs and usually lean towards acidic pHs (Fig. S3b; Bade et al., 2004). Hence, environmental conditions where DOC:DIC >> 1 might be inconsistent with large carbonate deposits. Accordingly, in light of the present results, Neoproterozoic carbonate carbon isotope excursions seem unlikely to be explained by the big DOC scenario, unless DOC and DIC pools are spatially decoupled (e.g. through terrestrial DOM inputs).

Page 26: [45] Deleted **Rob Havas** **12/16/22 3:28:00 PM**

DOC is the largest OC reservoir in the water column of the studied lakes (> 90%). Its concentrations and isotopic compositions bring precious new and complementary information about the C cycle of these stratified water bodies. Depending on environmental factors such as nutrients and DIC availability, diverse photosynthetic planktonic communities appear to release more or less important amounts of DOC depending on the lake, transferring most of the inorganic C fixed to DOC rather than POC. This process is marked by very heavy and distinct isotopic signatures of DOC compared to POC. They reflect different metabolism/C fixation pathways and/or the activity of a DIC-CM coupled with an overflow mechanism (i.e. DOM exudation) for which we propose a novel isotopic model including DOC. These features are invisible to POC analyses and thus are not recorded in the sediments.

Our results bring further constraints on the environmental conditions in which autochthonous DOM can accumulate in anoxic water bodies and provides boundary conditions to the "big DOC reservoir" scenario.

We observe that the SOM geochemical signatures of these stratified lakes do not all record the same biogeochemical layers of the water column and can be largely modified by early diagenesis in some cases.

Page 27: [46] Deleted **Rob Havas** **12/16/22 3:28:00 PM**

Adame, M.F., Alcocer, J., Escobar, E.: Size-fractionated phytoplankton biomass and its implications for the dynamics of an oligotrophic tropical lake. Freshw. Biol. 53, 22–31. https://doi.org/10.1111/j.1365-2427.2007.01864.x , 2008.

Alcocer, J.: Lake Alchichica Limnology, Springer Nature. ed. https://link.springer.com/book/10.1007/978-3-030-79096-7 , 2021.

Alcocer, J., Guzmán-Arias, A., Oseguera, L.A., Escobar, E.: Dinámica del carbono orgánico disuelto y particulado asociados al florecimiento de Nodularia spumigena en un lago tropical oligotrófico. Programma Mex. Carbono 13, 2014.

Anderson, N.John., Stedmon, C.A.: The effect of evapoconcentration on dissolved organic carbon concentration and quality in lakes of SW Greenland. Freshw. Biol. 52, 280–289. https://doi.org/10.1111/j.1365-2427.2006.01688.x , 2007.

Armienta, M.A., Vilaclara, G., De la Cruz-Reyna, S., Ramos, S., Ceniceros, N., Cruz, O., Aguayo, A., Arcega-Cabrera, F.: Water chemistry of lakes related to active and inactive Mexican volcanoes. J. Volcanol. Geotherm. Res. 178, 249–258. https://doi.org/10.1016/j.jvolgeores.2008.06.019 , 2008.

Armstrong-Altrin, J.S., Madhavaraju, J., Sial, A.N., Kasper-Zubillaga, J.J., Nagarajan, R., Flores-Castro, K., Rodríguez, J.L.:Petrography and stable isotope geochemistry of the cretaceous El Abra Limestones (Actopan), Mexico: Implication on diagenesis. J. Geol. Soc. India 77, 349–359. https://doi.org/10.1007/s12594-011-0042-3 , 2011.

Assayag, N., Jézéquel, D., Ader, M., Viollier, E., Michard, G., Prévot, F., Agrinier, P.: Hydrological budget, carbon sources and biogeochemical processes in Lac Pavin (France): Constraints from δ18O of water and δ13C of dissolved inorganic carbon. Appl. Geochem. 23, 2800–2816. https://doi.org/10.1016/j.apgeochem.2008.04.015 , 2008.

Assayag, N., Rivé, K., Ader, M., Jézéquel, D., Agrinier, P.: Improved method for isotopic and quantitative analysis of dissolved inorganic carbon in natural water samples. Rapid Commun. Mass Spectrom. 20, 2243–2251. https://doi.org/10.1002/rcm.2585 , 2006.

Bade, D.L., Carpenter, S.R., Cole, J.J., Hanson, P.C., Hesslein, R.H.: Controls of δ^{13}C-DIC in lakes: Geochemistry, lake metabolism, and morphometry. Limnol. Oceanogr. 49, 1160–1172. https://doi.org/10.4319/lo.2004.49.4.1160 , 2004.

Bade, D.L., Carpenter, S.R., Cole, J.J., Pace, M.L., Kritzberg, E., Van de Bogert, M.C., Cory, R.M., McKnight, D.M.: Sources and fates of dissolved organic carbon in lakes as determined by whole-lake carbon isotope additions. Biogeochemistry 84, 115–129. https://doi.org/10.1007/s10533-006-9013-y , 2007.

Badger, M.R., Andrews, T.J., Whitney, S.M., Ludwig, M., Yellowlees, D.C., Leggat, W. and Price, G.D.: The diversity and coevolution of Rubisco, plastids, pyrenoids, and chloroplast-based CO_2-concentrating mechanisms in algae. Canadian Journal of Botany, *76*(6), pp.1052-1071 , https://doi.org/10.1139/b98-074 , 1998.

Baines, S.B., Pace, M.L.: The production of dissolved organic matter by phytoplankton and its importance to bacteria: Patterns across marine and freshwater systems. Limnol. Oceanogr. 36, 1078–1090. https://doi.org/10.4319/lo.1991.36.6.1078 , 1991.

Beardall, J., Griffiths, H., Raven, J.A.: Carbon Isotope Discrimination and the CO_2 Accumulating Mechanism in Chlorella emersonii. J. of Expe. Botany, 33, 729–737. https://doi.org/10.1093/jxb/33.4.729 , 1982.

Beaupré, S.R.: The Carbon Isotopic Composition of Marine DOC, in: Biogeochemistry of Marine Dissolved Organic Matter. Elsevier, pp. 335–368. https://doi.org/10.1016/B978-0-12-405940-5.00006-6 , 2015.

Bekker, A., Holmden, C., Beukes, N.J., Kenig, F., Eglinton, B., Patterson, W.P.: Fractionation between inorganic and organic carbon during the Lomagundi (2.22–2.1 Ga) carbon isotope excursion. Earth Planet. Sci. Lett. 271, 278–291. https://doi.org/10.1016/j.epsl.2008.04.021 , 2008.

Benzerara, K., Skouri-Panet, F., Li, J., Férard, C., Gugger, M., Laurent, T., Couradeau, E., Ragon, M., Cosmidis, J., Menguy, N., Margaret-Oliver, I., Tavera, R., López-García, P., Moreira, D.: Intracellular Ca-carbonate biomineralization is widespread in cyanobacteria. Proc. Natl. Acad. Sci. 111, 10933–10938. https://doi.org/10.1073/pnas.1403510111 , 2014.

Bertilsson, S., Jones, J.B.: Supply of Dissolved Organic Matter to Aquatic Ecosystems: Autochthonous Sources, in: Findlay, S.E.G., Sinsabaugh, R.L. (Eds.), Aquatic Ecosystems, Aquatic Ecology. Academic Press, Burlington, pp. 3–24. https://doi.org/10.1016/B978-012256371-3/50002-0 , 2003.

Birgel, D., Meister, P., Lundberg, R., Horath, T.D., Bontognali, T.R.R., Bahniuk, A.M., de Rezende, C.E., Vasconcelos, C., McKenzie, J.A.: Methanogenesis produces strong ^{13}C enrichment in stromatolites of Lagoa Salgada, Brazil: a modern analogue for Palaeo-/Neoproterozoic stromatolites? Geobiology 13, 245–266. https://doi.org/10.1111/gbi.12130 , 2015.

Blair, N., Leu, A., Muñoz, E., Olsen, J., Kwong, E., Des Marais, D. : Carbon isotopic fractionation in heterotrophic microbial metabolism. Appl. Environ. Microbiol. 50, 996–1001. https://doi.org/10.1128/aem.50.4.996-1001.1985 , 1985.

Brailsford, F.L.: *Dissolved organic matter (DOM) in freshwater ecosystems*. Bangor University (UK) , 2019

Briones, E.E., Alcocer, J., Cienfuegos, E., Morales, P.: Carbon stable isotopes ratios of pelagic and littoral communities in Alchichica crater-lake, Mexico. Int. J. Salt Lake Res. 7, 345–355. https://doi.org/10.1007/BF02442143 , 1998.

Buchan, A., LeCleir, G.R., Gulvik, C.A., González, J.M.: Master recyclers: features and functions of bacteria associated with phytoplankton blooms. Nat. Rev. Microbiol. 12, 686–698. https://doi.org/10.1038/nrmicro3326 , 2014.

Burns, B.D., Beardall, J.: Utilization of inorganic carbon by marine microalgae. J. Exp. Mar. Biol. Ecol. 107, 75–86. https://doi.org/10.1016/0022-0981(87)90125-0 , 1987.

Cadeau, P., Jézéquel, D., Leboulanger, C., Fouilland, E., Le Floc'h, E., Chaduteau, C., Milesi, V., Guélard, J., Sarazin, G., Katz, A., d'Amore, S., Bernard, C., Ader, M.: Carbon isotope evidence for large methane emissions to the Proterozoic atmosphere. Sci. Rep. 10, 18186. https://doi.org/10.1038/s41598-020-75100-x , 2020.

Cai, C., Li, K., Liu, D., John, C.M., Wang, D., Fu, B., Fakhraee, M., He, H., Feng, L., Jiang, L.: Anaerobic oxidation of methane by Mn oxides in sulfate-poor environments. Geology 49, 761–766. https://doi.org/10.1130/G48553.1 , 2021.

Callieri, C., Coci, M., Corno, G., Macek, M., Modenutti, B., Balseiro, E., Bertoni, R.: Phylogenetic diversity of nonmarine picocyanobacteria. FEMS Microbiol. Ecol. 85, 293–301. https://doi.org/10.1111/1574-6941.12118 , 2013.

Camacho, A., Walter, X.A., Picazo, A., Zopfi, J.: Photoferrotrophy: Remains of an Ancient Photosynthesis in Modern Environments. Front. Microbiol. 08. https://doi.org/10.3389/fmicb.2017.00323 , 2017.

Cañadas, F., Papineau, D., Leng, M.J. and Li, C.: Extensive primary production promoted the recovery of the Ediacaran Shuram excursion. Nature communications, 13, 1-9. https://doi.org/10.1038/s41467-021-27812-5 , 2022.

Carlson, C.A., Hansell, D.A.: DOM Sources, Sinks, Reactivity, and Budgets, in: Biogeochemistry of Marine Dissolved Organic Matter. Elsevier, pp. 65–126. https://doi.org/10.1016/B978-0-12-405940-5.00003-0 , 2015.

Carrasco-Núñez, G., Ort, M.H., Romero, C.: Evolution and hydrological conditions of a maar volcano (Atexcac crater, Eastern Mexico). J. Volcanol. Geotherm. Res. 159, 179–197. https://doi.org/10.1016/j.jvolgeores.2006.07.001 , 2007.

Chako Tchamabé, B., Carrasco-Núñez, G., Miggins, D.P., Németh, K.: Late Pleistocene to Holocene activity of Alchichica maar volcano, eastern Trans-Mexican Volcanic Belt. J. South Am. Earth Sci. 97, 102404. https://doi.org/10.1016/j.jsames.2019.102404 , 2020.

Cheng, C., Zhang, J., He, Q., Wu, H., Chen, Y., Xie, H., Pavlostathis, S.G.: Exploring simultaneous nitrous oxide and methane sink in wetland sediments under anoxic conditions. Water Res. 194, 116958. https://doi.org/10.1016/j.watres.2021.116958 , 2021.

Chomicki, K.: The use of stable carbon and oxygen isotopes to examine the fate of dissolved organic matter in two small, oligotrophic Canadian Shield lakes. University of Waterloo (Canada) , 2009.

Close, H.G., Henderson, L.C.: Open-Ocean Minima in $\delta^{13}C$ Values of Particulate Organic Carbon in the Lower Euphotic Zone. Front. Mar. Sci. 7, 540165. https://doi.org/10.3389/fmars.2020.540165 , 2020.

Couradeau, E., Benzerara, K., Gérard, E., Moreira, D., Bernard, S., Brown, G.E., López-García, P.: An Early-Branching Microbialite Cyanobacterium Forms Intracellular Carbonates. Science 336, 459–462. https://doi.org/10.1126/science.1216171 , 2012.

Crowe, S.A., Katsev, S., Leslie, K., Sturm, A., Magen, C., Nomosatryo, S., Pack, M.A., Kessler, J.D., Reeburgh, W.S., Roberts, J.A., González, L., Douglas Haffner, G., Mucci, A., Sundby, B., Fowle, D.A.: The methane cycle in ferruginous Lake Matano: Methane cycle in ferruginous Lake Matano. Geobiology 9, 61–78. https://doi.org/10.1111/j.1472-4669.2010.00257.x , 2011.

Descolas-Gros, C., Fontungne, M.: Stable carbon isotope fractionation by marine phytoplankton during photosynthesis. Plant Cell Environ. 13, 207–218. https://doi.org/10.1111/j.1365-3040.1990.tb01305.x , 1990.

Dittmar, T.: Reasons Behind the Long-Term Stability of Dissolved Organic Matter, in: Biogeochem. of Marine Dissolved Organic Matter (pp. 369–388). Academic Press. https://doi.org/10.1016/B978-0-12-405940-5.00007-8 , 2015.

Ducklow, H.W., Hansell, D.A., Morgan, J.A.: Dissolved organic carbon and nitrogen in the Western Black Sea. Mar. Chem. 105, 140–150. https://doi.org/10.1016/j.marchem.2007.01.015 , 2007.

Emrich, K., Ehhalt, D.H., Vogel, J.C.: Carbon isotope fractionation during the precipitation of calcium carbonate. Earth Planet. Sci. Lett. 8, 363–371. https://doi.org/10.1016/0012-821X(70)90109-3 , 1970.

Erez, J., Bouevitch, A., Kaplan, A.: Carbon isotope fractionation by photosynthetic aquatic microorganisms: experiments with *Synechococcus* PCC7942, and a simple carbon flux model. Can. J. Bot. 76, 1109–1118. https://doi.org/10.1139/b98-067 , 1998.

Fakhraee, M., Tarhan, L.G., Planavsky, N.J., Reinhard, C.T.: A largely invariant marine dissolved organic carbon reservoir across Earth's history. Proc. Natl. Acad. Sci. 118, e2103511118. https://doi.org/10.1073/pnas.2103511118 , 2021.

Ferrari, L., Orozco-Esquivel, T., Manea, V., Manea, M.: The dynamic history of the Trans-Mexican Volcanic Belt and the Mexico subduction zone. Tectonophysics 522–523, 122–149. https://doi.org/10.1016/j.tecto.2011.09.018 , 2012.

Fike, D.A., Grotzinger, J.P., Pratt, L.M., Summons, R.E.: Oxidation of the Ediacaran Ocean. Nature 444, 744–747. https://doi.org/10.1038/nature05345 , 2006.

Fogel, M.L., Cifuentes, L.A.: Isotope Fractionation during Primary Production, in: Engel, M.H., Macko, S.A. (Eds.), Organic Geochemistry, Topics in Geobiology. Springer US, Boston, MA, pp. 73–98. https://doi.org/10.1007/978-1-4615-2890-6_3 , 1993.

Fry, B.: 13C/12C fractionation by marine diatoms. Mar. Ecol. Prog. Ser. 134, 283–294. https://doi.org/10.3354/meps134283 , 1996.

Fry, B., Jannasch, H.W., Molyneaux, S.J., Wirsen, C.O., Muramoto, J.A., King, S.: Stable isotope studies of the carbon, nitrogen and sulfur cycles in the Black Sea and the Cariaco Trench. Deep Sea Res. Part Oceanogr. Res. Pap. 38, S1003–S1019. https://doi.org/10.1016/S0198-0149(10)80021-4 , 1991

Fulton, J.M., Arthur, M.A., Thomas, B., Freeman, K.H.: Pigment carbon and nitrogen isotopic signatures in euxinic basins. Geobiology 16, 429–445. https://doi.org/10.1111/gbi.12285 , 2018.

Furian, S., Martins, E.R.C., Parizotto, T.M., Rezende-Filho, A.T., Victoria, R.L., Barbiero, L.: Chemical diversity and spatial variability in myriad lakes in Nhecolândia in the Pantanal wetlands of Brazil. Limnol. Oceanogr. 58, 2249–2261. https://doi.org/10.4319/lo.2013.58.6.2249 , 2013.

Gérard, E., Ménez, B., Couradeau, E., Moreira, D., Benzerara, K., Tavera, R. and López-García, P.: Specific carbonate–microbe interactions in the modern microbialites of Lake Alchichica (Mexico). The ISME journal, 7, 1997-2009. https://doi:10.1038/ismej.2013.81 , 2013.

Gröger, J., Franke, J., Hamer, K., Schulz, H.D.: Quantitative Recovery of Elemental Sulfur and Improved Selectivity in a Chromium-Reducible Sulfur Distillation. Geostand. Geoanalytical Res. 33, 17–27. https://doi.org/10.1111/j.1751-908X.2009.00922.x , 2009.

Gu, B., Schelske, C.L., Hodell, D.A.: Extreme ^{13}C enrichments in a shallow hypereutrophic lake: Implications for carbon cycling. Limnol. Oceanogr. 49, 1152–1159. https://doi.org/10.4319/lo.2004.49.4.1152 , 2004.

Hansell, D.A.: Recalcitrant Dissolved Organic Carbon Fractions. Annu. Rev. Mar. Sci. 5, 421–445. https://doi.org/10.1146/annurev-marine-120710-100757 , 2013.

Hassan, K.M.: Isotope geochemistry of Swan Lake Basin in the Nebraska Sandhills, USA: Large ^{13}C enrichment in sediment-calcite records. Geochemistry 74, 681–690. https://doi.org/10.1016/j.chemer.2014.03.004 , 2014.

Havig, J.R., Hamilton, T.L., McCormick, M., McClure, B., Sowers, T., Wegter, B., Kump, L.R.: Water column and sediment stable carbon isotope biogeochemistry of permanently redox- stratified Fayetteville Green Lake, New York, U.S.A. Limnol. Oceanogr. 63, 570–587. https://doi.org/10.1002/lno.10649 , 2018.

Havig, J.R., McCormick, M.L., Hamilton, T.L., Kump, L.R.: The behavior of biologically important trace elements across the oxic/euxinic transition of meromictic Fayetteville Green Lake, New York, USA. Geochim. Cosmochim. Acta 165, 389–406. https://doi.org/10.1016/j.gca.2015.06.024 , 2015.

Hayes, J.M.: Fractionation of Carbon and Hydrogen Isotopes in Biosynthetic Processes*. Rev. Mineral. Geochem. 43, 225–277. https://doi.org/10.2138/gsrmg.43.1.225 , 2001.

Hayes, J.M., Popp, B.N., Takigiku, R., Johnson, M.W.: An isotopic study of biogeochemical relationships between carbonates and organic carbon in the Greenhorn Formation. Geochim. Cosmochim. Acta 53, 2961–2972. https://doi.org/10.1016/0016-7037(89)90172-5 , 1989.

Henkel, J.V., Dellwig, O., Pollehne, F., Herlemann, D.P.R., Leipe, T., Schulz-Vogt, H.N.: A bacterial isolate from the Black Sea oxidizes sulfide with manganese(IV) oxide. Proc. Natl. Acad. Sci. 116, 12153–12155. https://doi.org/10.1073/pnas.1906000116 , 2019.

Hessen, D.O.: Dissolved organic carbon in a humic lake: effects on bacterial production and respiration. Hydrobiologia, 229(1), pp.115-123. https://doi.org/10.1007/978-94-011-2474-4_9 , 1992.

Hessen, D.O., Anderson, T.R.: Excess carbon in aquatic organisms and ecosystems: Physiological, ecological, and evolutionary implications. Limnol. Oceanogr. 53, 1685–1696. https://doi.org/10.4319/lo.2008.53.4.1685 , 2008.

Iniesto, M., Moreira, D., Benzerara, K., Muller, E., Bertolino, P., Tavera, R. and López- García, P.: Rapid formation of mature microbialites in Lake Alchichica, Mexico. Env. Microbio. Reports, 13, 600-605. https://doi.org/10.1111/1758-2229.12957 , 2021a.

Iniesto, M., Moreira, D., Reboul, G., Deschamps, P., Benzerara, K., Bertolino, P., Saghaï, A., Tavera, R. and López- García, P.: Core microbial communities of lacustrine microbialites sampled along an alkalinity gradient. Env. Microbio., 23, 51-68. https://doi.org/10.1111/1462-2920.15252 , 2021b.

Iniesto, M., Moreira, D., Benzerara, K., Reboul G., Bertolino, P., Tavera, R. and López- García, P.: Planktonic microbial communities from microbialite-bearing lakes sampled along a salinity-alkalinity gradient. Limnol. Oceanogr. In press.

Iñiguez, C., Capó- Bauçà, S., Niinemets, Ü., Stoll, H., Aguiló- Nicolau, P., Galmés, J.: Evolutionary trends in RuBisCO kinetics and their co- evolution with CO_2 concentrating mechanisms. Plant J. 101, 897–918. https://doi.org/10.1111/tpj.14643 , 2020.

Ivanovsky, R.N., Lebedeva, N.V., Keppen, O.I., Chudnovskaya, A.V.: Release of Photosynthetically Fixed Carbon as Dissolved Organic Matter by Anoxygenic Phototrophic Bacteria. Microbiology 89, 28–34. https://doi.org/10.1134/S0026261720010075 , 2020.

Javoy, M., Pineau, F., Delorme, H.: Carbon and nitrogen isotopes in the mantle. Chem. Geol., Isotopes in Geology—Picciotto Volume 57, 41–62. https://doi.org/10.1016/0009-2541(86)90093-8 , 1986.

Jézéquel, D., Michard, G., Viollier, E., Agrinier, P., Albéric, P., Lopes, F., Abril, G. and Bergonzini, L.: Carbon cycle in a meromictic crater lake: Lake Pavin, France. In Lake Pavin (pp. 185-203). Springer, Cham. https://doi.org/10.1007/978-3-319-39961-4_11 , 2016.

Jiao, N., Herndl, G.J., Hansell, D.A., Benner, R., Kattner, G., Wilhelm, S.W., Kirchman, D.L., Weinbauer, M.G., Luo, T., Chen, F., Azam, F.: Microbial production of recalcitrant dissolved organic matter: long-term carbon storage in the global ocean. Nat. Rev. Microbiol. 8, 593–599. https://doi.org/10.1038/nrmicro2386 , 2010.

Kaplan, L.A., Wiegner, T.N., Newbold, J.D., Ostrom, P.H., Gandhi, H.: Untangling the complex issue of dissolved organic carbon uptake: a stable isotope approach. Freshw. Biol. 53, 855–864. https://doi.org/10.1111/j.1365-2427.2007.01941.x , 2008.

Karhu, J.A. and Holland, H.D.: Carbon isotopes and the rise of atmospheric oxygen. Geology 24, 867-870 , https://doi.org/10.1130/0091-7613(1996)024<0867:CIATRO>2.3.CO;2 , 1996.

Kawasaki, N., Komatsu, K., Kohzu, A., Tomioka, N., Shinohara, R., Satou, T., Watanabe, F.N., Tada, Y., Hamasaki, K., Kushairi, M.R.M., Imai, A.: Bacterial Contribution to Dissolved Organic Matter in Eutrophic Lake Kasumigaura, Japan. Appl. Environ. Microbiol. 79, 7160–7168. https://doi.org/10.1128/AEM.01504-13 , 2013.

Klawonn, I., Van den Wyngaert, S., Parada, A.E., Arandia-Gorostidi, N., Whitehouse, M.J., Grossart, H.-P., Dekas, A.E.: Characterizing the "fungal shunt": Parasitic fungi on diatoms affect carbon flow and bacterial communities in aquatic microbial food webs. Proc. Natl. Acad. Sci. 118, e2102225118. https://doi.org/10.1073/pnas.2102225118 , 2021.

Knossow, N., Blonder, B., Eckert, W., Turchyn, A.V., Antler, G., Kamyshny, A.: Annual sulfur cycle in a warm monomictic lake with sub-millimolar sulfate concentrations. Geochem. Trans. 16, 7. https://doi.org/10.1186/s12932-015-0021-5 , 2015.

Kuntz, L.B., Laakso, T.A., Schrag, D.P., Crowe, S.A.: Modeling the carbon cycle in Lake Matano. Geobiology 13, 454–461. https://doi.org/10.1111/gbi.12141 , 2015.

Lampert, W.: Release of dissolved organic carbon by grazing zooplankton. Limnol. Oceanogr. 23, 831–834. https://doi.org/10.4319/lo.1978.23.4.0831 , 1978.

Lehmann, M.F., Bernasconi, S.M., Barbieri, A., McKenzie, J.A.: Preservation of organic matter and alteration of its carbon and nitrogen isotope composition during simulated and in situ early sedimentary diagenesis. Geochim. Cosmochim. Acta 66, 3573–3584. https://doi.org/10.1016/S0016-7037(02)00968-7 , 2002.

Lehmann, M.F., Bernasconi, S.M., McKenzie, J.A., Barbieri, A., Simona, M., Veronesi, M.: Seasonal variation of the δC and δN of particulate and dissolved carbon and nitrogen in Lake Lugano: Constraints on biogeochemical cycling in a eutrophic lake. Limnol. Oceanogr. 49, 415–429. https://doi.org/10.4319/lo.2004.49.2.0415 , 2004.

Lelli, M., Kretzschmar, T.G., Cabassi, J., Doveri, M., Sanchez-Avila, J.I., Gherardi, F., Magro, G., Norelli, F.: Fluid geochemistry of the Los Humeros geothermal field (LHGF - Puebla, Mexico): New constraints for the conceptual model. Geothermics 90, 101983. https://doi.org/10.1016/j.geothermics.2020.101983 , 2021.

Li, C., Hardisty, D.S., Luo, G., Huang, J., Algeo, T.J., Cheng, M., Shi, W., An, Z., Tong, J., Xie, S. and Jiao, N.: Uncovering the spatial heterogeneity of Ediacaran carbon cycling. Geobio., 15, 211-224. https://doi.org/10.1111/gbi.12222 , 2017.

Li, H.-C., Ku, T.-L.: $\delta^{13}C$–$\delta^{18}C$ covariance as a paleohydrological indicator for closed-basin lakes. Palaeogeogr. Palaeoclimatol. Palaeoecol. 133, 69–80. https://doi.org/10.1016/S0031-0182(96)00153-8 , 1997.

Lorenz, V.: On the growth of maars and diatremes and its relevance to the formation of tuff rings. Bull. Volcanol. 48, 265–274. https://doi.org/10.1007/BF01081755 , 1986.

Lugo, A., Alcocer, J., Sánchez, Ma. del R., Escobar, E., Macek, M.: Temporal and spatial variation of bacterioplankton abundance in a tropical, warm-monomictic, saline lake: Alchichica, Puebla, Mexico. SIL Proc. 1922-2010 27, 2968–2971. https://doi.org/10.1080/03680770.1998.11898217 , 2000.

Lugo, A., Alcocer, J., Sanchez, M.R., Escobar, E.: Trophic status of tropical lakes indicated by littoral protozoan assemblages. SIL Proc. 1922-2010 25, 441–443. https://doi.org/10.1080/03680770.1992.11900159 , 1993.

Lyons, T.W., Reinhard, C.T., Planavsky, N.J.: The rise of oxygen in Earth's early ocean and atmosphere. Nature 506, 307–315. https://doi.org/10.1038/nature13068 , 2014.

Macek, M., Medina, X.S., Picazo, A., Peštová, D., Reyes, F.B., Hernández, J.R.M., Alcocer, J., Ibarra, M.M., Camacho, A.: Spirostomum teres: A Long Term Study of an Anoxic-Hypolimnion Population Feeding upon Photosynthesizing Microorganisms. Acta Protozool. 59, 13–38. https://doi.org/10.4467/16890027AP.20.002.12158 , 2020.

Marañón, E., Cermeño, P., Fernández, E., Rodríguez, J., Zabala, L.: Significance and mechanisms of photosynthetic production of dissolved organic carbonin a coastal eutrophic ecosystem. Limnol. Oceanogr. 49, 1652–1666. https://doi.org/10.4319/lo.2004.49.5.1652 , 2004.

Margolin, A.R., Gerringa, L.J., Hansell, D.A. and Rijkenberg, M.J.: Net removal of dissolved organic carbon in the anoxic waters of the Black Sea. Marine Chemistry, 183, pp.13-24. https://doi.org/10.1016/j.marchem.2016.05.003 , 2016.

Mason, E., Edmonds, M., Turchyn, A.V.: Remobilization of crustal carbon may dominate volcanic arc emissions. Science 357, 290–294. https://doi.org/10.1126/science.aan5049 , 2017.

Mercedes-Martín, R., Ayora, C., Tritlla, J., Sánchez-Román, M.: The hydrochemical evolution of alkaline volcanic lakes: a model to understand the South Atlantic Pre-salt mineral assemblages. Earth-Sci. Rev. 198, 102938. https://doi.org/10.1016/j.earscirev.2019.102938 , 2019.

Milesi, V.P., Debure, M., Marty, N.C.M., Capano, M., Jézéquel, D., Steefel, C., Rouchon, V., Albéric, P., Bard, E., Sarazin, G., Guyot, F., Virgone, A., Gaucher, É.C., Ader, M.: Early Diagenesis of Lacustrine Carbonates in Volcanic Settings: The Role of Magmatic CO_2 (Lake Dziani Dzaha, Mayotte, Indian Ocean). ACS Earth Space Chem. 4, 363–378. https://doi.org/10.1021/acsearthspacechem.9b00279 , 2020.

Mook, W.G., Bommerson, J.C., Staverman, W.H.: Carbon isotope fractionation between dissolved bicarbonate and gaseous carbon dioxide. Earth Planet. Sci. Lett. 22, 169–176. https://doi.org/10.1016/0012-821X(74)90078-8 , 1974.

Morana, C., Sarmento, H., Descy, J.-P., Gasol, J.M., Borges, A.V., Bouillon, S., Darchambeau, F.: Production of dissolved organic matter by phytoplankton and its uptake by heterotrophic prokaryotes in large tropical lakes. Limnol. Oceanogr. 59, 1364–1375. https://doi.org/10.4319/lo.2014.59.4.1364 , 2014.

Núñez Useche, F., Barragán, R., Moreno Bedmar, J.A., Canet, C.: Mexican archives for the major Cretaceous Oceanic Anoxic Events. Bol. Soc. Geológica Mex. 66, 491–505. https://doi.org/10.18268/BSGM2014v66n3a7 , 2014.

Ogawa, H., Amagai, Y., Koike, I., Kaiser, K., Benner, R.: Production of Refractory Dissolved Organic Matter by Bacteria. Science 292, 917–920. https://doi.org/10.1126/science.1057627 , 2001.

O'Leary, M.H.: Carbon Isotopes in Photosynthesis. BioScience 38, 328–336. https://doi.org/10.2307/1310735 , 1988.

Paneth, P., O'Leary, M.H.: Carbon isotope effect on dehydration of bicarbonate ion catalyzed by carbonic anhydrase. Biochemistry 24, 5143–5147. https://doi.org/10.1021/bi00340a028 , 1985.

Pardue, J.W., Scalan, R.S., Van Baalen, C., Parker, P.L.: Maximum carbon isotope fractionation in photosynthesis by blue-green algae and a green alga. Geochim. Cosmochim. Acta 40, 309–312. https://doi.org/10.1016/0016-7037(76)90208-8 , 1976.

Pecoraino, G., D'Alessandro, W., Inguaggiato, S.: The Other Side of the Coin: Geochemistry of Alkaline Lakes in Volcanic Areas. In Volcanic Lakes, Advances in Volcanology. Springer, Berlin, Heidelberg, pp. 219–237. https://doi.org/10.1007/978-3-642-36833-2_9 , 2015.

Petrash, D.A., Steenbergen, I.M., Valero, A., Meador, T.B., Pačes, T., Thomazo, C.: Aqueous system-level processes and prokaryote assemblages in the ferruginous and sulfate-rich bottom waters of a post-mining lake. Biogeosciences 19, 1723–1751. https://doi.org/10.5194/bg-19-1723-2022 , 2022.

Pimenov, N.V., Lunina, O.N., Prusakova, T.S., Rusanov, I.I., Ivanov, M.V.: Biological fractionation of stable carbon isotopes at the aerobic/anaerobic water interface of meromictic water bodies. Microbiology 77, 751–759. https://doi.org/10.1134/S0026261708060131 , 2008.

Posth, N.R., Bristow, L.A., Cox, R.P., Habicht, K.S., Danza, F., Tonolla, M., Frigaard, N. - U., Canfield, D.E.: Carbon isotope fractionation by anoxygenic phototrophic bacteria in euxinic Lake Cadagno. Geobiology 15, 798–816. https://doi.org/10.1111/gbi.12254 , 2017.

Rendon-Lopez, M.J.: Limnologia fisica del lago crater los Espinos, Municipio de Jiménez Michoacan. 2008.

Ridgwell, A. and Arndt, S.: Why dissolved organics matter: DOC in ancient oceans and past climate change. In Biogeochemistry of marine dissolved organic matter (pp. 1-20). Academic Press. https://doi.org/10.1016/B978-0-12-405940-5.00001-7, 2015.

Riebesell, U., Burkhardt, S., Dauelsberg, A., Kroon, B.: Carbon isotope fractionation by a marine diatom:dependence on the growth-rate-limiting resource. Mar. Ecol. Prog. Ser. 193, 295–303. https://doi.org/10.3354/meps193295 , 2000.

Rothman, D.H., Hayes, J.M., Summons, R.E.: Dynamics of the Neoproterozoic carbon cycle. Proc. Natl. Acad. Sci. 100, 8124–8129. https://doi.org/10.1073/pnas.0832439100 , 2003.

Sackett, W.M., Eckelmann, W.R., Bender, M.L., Bé, A.W.H.: Temperature Dependence of Carbon Isotope Composition in Marine Plankton and Sediments. Science 148, 235–237. https://doi.org/10.1126/science.148.3667.235 , 1965.

Saghaï, A., Zivanovic, Y., Moreira, D., Benzerara, K., Bertolino, P., Ragon, M., Tavera, R., López- Archilla, A.I. and López- García, P.: Comparative metagenomics unveils functions and genome features of microbialite-associated communities along a depth gradient. Environmental microbiology, 18, 4990-5004. https://doi.org/10.1111/1462-2920.13456 , 2016.

Saini, J.S., Hassler, C., Cable, R.N., Fourquez, M., Danza, F., Roman, S., Tonolla, M., Storelli, N., Jacquet, S., Zdobnov, E.M. and Duhaime, M.B.: Bacterial, phytoplankton, and viral dynamics of meromictic Lake Cadagno offer insights into the Proterozoic ocean microbial loop. bioRxiv. https://doi.org/10.1101/2021.10.13.464336 , 2021.

Satkoski, A.M., Beukes, N.J., Li, W., Beard, B.L., Johnson, C.M.: A redox-stratified ocean 3.2 billion years ago. Earth Planet. Sci. Lett. 430, 43–53. https://doi.org/10.1016/j.epsl.2015.08.007 , 2015.

Schidlowski, M.: Carbon isotopes as biogeochemical recorders of life over 3.8 Ga of Earth history: evolution of a concept. Precambrian Res. 106, 117–134. https://doi.org/10.1016/S0301-9268(00)00128-5 , 2001.

Schiff, S.L., Tsuji, J.M., Wu, L., Venkiteswaran, J.J., Molot, L.A., Elgood, R.J., Paterson, M.J., Neufeld, J.D.: Millions of Boreal Shield Lakes can be used to Probe Archaean Ocean Biogeochemistry. Sci. Rep. 7, 46708. https://doi.org/10.1038/srep46708 , 2017.

Sexton, P.F., Norris, R.D., Wilson, P.A., Pälike, H., Westerhold, T., Röhl, U., Bolton, C.T., Gibbs, S.: Eocene global warming events driven by ventilation of oceanic dissolved organic carbon. Nature 471, 349–352. https://doi.org/10.1038/nature09826 , 2011.

Shi, W., Li, C. and Algeo, T.J.: Quantitative model evaluation of organic carbon oxidation hypotheses for the Ediacaran Shuram carbon isotopic excursion. Science China Earth Sciences, 60, 2118-2127. https://doi.org/10.1007/s11430-017-9137-1 , 2017.

Siebe, C., Guilbaud, M.-N., Salinas, S., Chédeville-Monzo, C.: Eruption of Alberca de los Espinos tuff cone causes transgression of Zacapu lake ca. 25,000 yr BP in Michoacán, México. Presented at the IAS 4IMC Conference, Auckland, New Zeland, pp. 74–75. 2012.

Siebe, C., Guilbaud, M.-N., Salinas, S., Kshirsagar, P., Chevrel, M.O., Jiménez, A.H., Godínez, L.: Monogenetic volcanism of the Michoacán-Guanajuato Volcanic Field: Maar craters of the Zacapu basin and domes, shields, and scoria cones of the Tarascan highlands (Paracho-Paricutin region). Presented at the Pre-meeting field guide for the 5th international Maar Conference, Querétaro, México, pp. 1–37. 2014.

Sigala, I., Caballero, M., Correa-Metrio, A., Lozano-García, S., Vázquez, G., Pérez, L., Zawisza, E.: Basic limnology of 30 continental waterbodies of the Transmexican Volcanic Belt across climatic and environmental gradients. Bol. Soc. Geológica Mex. 69, 313–370. https://doi.org/10.18268/BSGM2017v69n2a3 , 2017.

Silva Aguilera, R.A.: Analisis del descenso del nivel de agua del lago Alchichica, Puebla, México 120. 2019.

Sirevag, R., Buchanan, B.B., Berry, J.A., Troughton, J.H.: Mechanisms of $C0_2$ Fixation in Bacterial Photosynthesis Studied by the Carbon Isotope Fractionation Technique. Arch Microbiol 112, 35-38. https://doi.org/10.1007/BF00446651 , 1977.

Soetaert, K., Hofmann, A.F., Middelburg, J.J., Meysman, F.J.R., Greenwood, J.: The effect of biogeochemical processes on pH. Mar. Chem. 105, 30–51. https://doi.org/10.1016/j.marchem.2006.12.012 , 2007.

Swanson-Hysell, N.L., Rose, C.V., Calmet, C.C., Halverson, G.P., Hurtgen, M.T. and Maloof, A.C.: Cryogenian glaciation and the onset of carbon-isotope decoupling. Science, 328, 608-611. DOI: 10.1126/science.1184508, 2010.

Talbot, M.R.: A review of the palaeohydrological interpretation of carbon and oxygen isotopic ratios in primary lacustrine carbonates. Chem. Geol. Isot. Geosci. Sect. 80, 261–279. https://doi.org/10.1016/0168-9622(90)90009-2 , 1990.

Thomas, P.J., Boller, A.J., Satagopan, S., Tabita, F.R., Cavanaugh, C.M., Scott, K.M.: Isotope discrimination by form IC RubisCO from *Ralstonia eutropha* and *Rhodobacter sphaeroides* , metabolically versatile members of ' *Proteobacteria* ' from aquatic and soil habitats. Environ. Microbiol. 21, 72–80. https://doi.org/10.1111/1462-2920.14423 , 2019.

Thornton, D.C.O.: Dissolved organic matter (DOM) release by phytoplankton in the contemporary and future ocean. Eur. J. Phycol. 49, 20–46. https://doi.org/10.1080/09670262.2013.875596 , 2014.

Tziperman, E., Halevy, I., Johnston, D.T., Knoll, A.H. and Schrag, D.P.: Biologically induced initiation of Neoproterozoic snowball-Earth events. PNAS, 108, 15091-15096. www.pnas.org/cgi/doi/10.1073/pnas.1016361108 , 2011.

Ussiri, D.A.N., Lal, R.: Carbon Sequestration for Climate Change Mitigation and Adaptation. Springer International Publishing, Cham. https://doi.org/10.1007/978-3-319-53845-7 , 2017.

van Mooy, B.A.S., Keil, R.G., Devol, A.H.: Impact of suboxia on sinking particulate organic carbon: Enhanced carbon flux and preferential degradation of amino acids via denitrification. Geochim. Cosmochim. Acta 66, 457–465. https://doi.org/10.1016/S0016-7037(01)00787-6 , 2002.

Vilaclara, G., Chávez, M., Lugo, A., González, H., Gaytán, M.: Comparative description of crater-lakes basic chemistry in Puebla State, Mexico. SIL Proc. 1922-2010 25, 435–440. https://doi.org/10.1080/03680770.1992.11900158 , 1993.

van Vliet, D.M., Meijenfeldt, F.A.B., Dutilh, B.E., Villanueva, L., Sinninghe Damsté, J.S., Stams, A.J.M., Sánchez- Andrea, I.: The bacterial sulfur cycle in expanding dysoxic and euxinic marine waters. Environ. Microbiol. 23, 2834–2857. https://doi.org/10.1111/1462-2920.15265 , 2021.

Wang, S., Yeager, K.M., Lu, W.: Carbon isotope fractionation in phytoplankton as a potential proxy for pH rather than for $[CO_{2(aq)}]$: Observations from a carbonate lake. Limnol. Oceanogr. 61, 1259–1270. https://doi.org/10.1002/lno.10289 , 2016.

Werne, J.P., Hollander, D.J.: Balancing supply and demand: controls on carbon isotope fractionation in the Cariaco Basin (Venezuela) Younger Dryas to present. Mar. Chem. 92, 275–293. https://doi.org/10.1016/j.marchem.2004.06.031 , 2004.

Wetz, M.S., Wheeler, P.A.: Release of dissolved organic matter by coastal diatoms. Limnol. Oceanogr. 52, 798–807. https://doi.org/10.4319/lo.2007.52.2.0798 , 2007.

Whiticar, M.J., Faber, E., Schoell, M.: Biogenic methane formation in marine and freshwater environments: CO2 reduction vs. acetate fermentation—Isotope evidence. Geochim. Cosmochim. Acta 50, 693–709. https://doi.org/10.1016/0016-7037(86)90346-7 , 1986.

Williams, P.M., Gordon, L.I.: Carbon-13: carbon-12 ratios in dissolved and particulate organic matter in the sea. Deep Sea Res. Oceanogr. Abstr. 17, 19–27. https://doi.org/10.1016/0011-7471(70)90085-9 , 1970.

Wittkop, C., Teranes, J., Lubenow, B., Dean, W.E.: Carbon- and oxygen-stable isotopic signatures of methanogenesis, temperature, and water column stratification in Holocene siderite varves. Chem. Geol. 389, 153–166. https://doi.org/10.1016/j.chemgeo.2014.09.016 , 2014.

Zeyen, N., Benzerara, K., Beyssac, O., Daval, D., Muller, E., Thomazo, C., Tavera, R., López-García, P., Moreira, D., Duprat, E.: Integrative analysis of the mineralogical and chemical composition of modern microbialites from ten Mexican lakes: What do we learn about their formation? Geochim. Cosmochim. Acta 305, 148–184. https://doi.org/10.1016/j.gca.2021.04.030 , 2021.

Zohary, T., Erez, J., Gophen, M., Berman-Frank, I., Stiller, M.: Seasonality of stable carbon isotopes within the pelagic food web of Lake Kinneret. Limnol. Oceanogr. 39, 1030–1043. https://doi.org/10.4319/lo.1994.39.5.1030 , 1994.

Zyakun, A.M., Lunina, O.N., Prusakova, T.S., Pimenov, N.V., Ivanov, M.V.: Fractionation of stable carbon isotopes by photoautotrophically growing anoxygenic purple and green sulfur bacteria. Microbiology 78, 757–768. https://doi.org/10.1134/S0026261709060137 , 2009.